JAMES COOK UNIVERSITY

COLLEGE OF SCIENCE AND ENGINEERING

The Structural Response and Progressive Failure of Batten to Rafter Connections under Wind Loads

Korah Ipeson Parackal BE Civil (Hons)

DOCTORAL THESIS

Thesis submitted to the College of Science and Engineering for the degree of

Doctor of Philosophy

(Structural Engineering)

December 2018

For my Grandfather, who taught me the way things work.
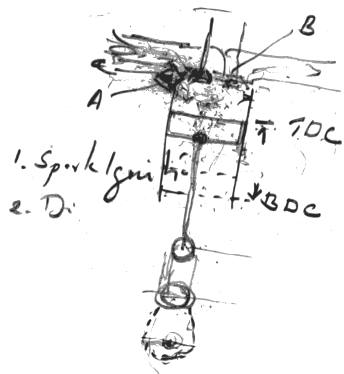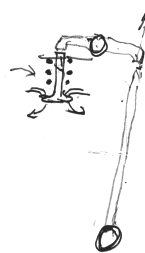
DECLARATION

I declare that this thesis is my work and has not been submitted for another degree or diploma at any university or other institution of tertiary education. Information derived from published or unpublished work of others has been acknowledged in the text and a list of references given.

Signed:_____

Date:_____

Korah Ipeson Parackal

STATEMENT OF ACCESS

I, the author of this thesis, understand that James Cook University will make it available for use within the University Library and via the Australian Digital Theses network for use elsewhere.

I understand that as an unpublished work a thesis has significant protection under the Copyright act and I do not wish to place restrictions on access to this work.

Signed:_____

Date:_____

Korah Ipeson Parackal

STATEMENT ON THE CONTRIBUTION OF OTHERS

ACKNOWLEDGEMENTS

ABSTRACT

Batten to rafter connections in light framed timber housing are vulnerable to wind loading and failures of these connections are one of the more common failure modes seen in post windstorm damage surveys. Such failures often occur in a progressive or cascading manner resulting in the loss of a large section of the building envelope. These progressive failures of batten to rafter connections are a complex process influenced by the pressure fluctuations on the roof surface, the response of individual connections and the behaviour of the structural system as a whole.

This study presents a method of examining load redistribution and progressive failure behaviour of batten to rafter connections in light framed structures. Nonlinear time history analysis was performed using a finite element model using fluctuating pressures determined from a wind tunnel study and connection properties determined from laboratory testing of connections under dynamic loads.

Flow separation and building-induced turbulence cause intermittent 'peak-events' where negative pressures on the roof surface are especially high. These 'peak-events' can move across the roof causing high loads occurring at different connections with slight lead or lag times. Damage to connections occur during the 'peak events' as nails are incrementally withdrawn. Loads are redistributed and load paths change during nail slips, causing damage to spread from an initial location. Load redistribution continues until a few connections fail completely, upon which a cascading failure occurs where almost all connections on the roof fail in rapid succession.

As an application of this research, the analyses performed were used to assess the fragility of batten-rafter failures, and the most vulnerable parts of the roof identified. Cost effective retrofitting measures can be justified and designed with this information.

CONTENTS

LIST OF TABLES

LIST OF FIGURES

LIST OF APPENDICES

1 INTRODUCTION

Progressive failures in light framed structures to wind loads are a complex and little understood failure mode. Batten to rafter connections in these types of structures can be vulnerable to wind loading, and failures of these connections are one of the more common failure modes seen in post windstorm damage surveys. Such failures often occur in a progressive or cascading manner resulting in the loss of a large section of the building envelope. These progressive failures of batten to rafter connections are influenced by the pressure fluctuations across the roof surface, the response of individual connections, and the behaviour of the structural system as a whole.

This study presents a method of examining load redistribution and progressive failure behaviour of nailed batten to rafter connections in light framed structures. Nonlinear time history analysis was performed with a finite element model using fluctuating pressures determined from a wind tunnel study and connection properties determined from laboratory testing of connections under dynamic loads.

This introductory Chapter describes the progressive failure of batten to rafter connections, defines the structural system that will be studied in this thesis and discusses the complexities of the structural response to wind loads. The aims and objectives of the thesis are then presented. A general overview of this thesis concludes this Chapter.

1.1 Failures in Windstorms

Due to their low self-weight, light framed timber houses are vulnerable to damage in windstorms, where building-induced turbulence can generate large uplift forces on the roof, which in some cases can overcome the roof's self-weight.

Damage surveys after wind events such as and Cyclone Tracy (1974) and Hurricane Andrew (1992) showed deficiencies in the performance of light framed structures compared to engineered commercial and industrial buildings. Such events were often catalysts for research in light framed timber structures and subsequent changes in building codes. In the case of Cyclones Tracy and Althea, these events prompted the founding of the Cyclone Testing Station at James Cook University where wind tunnel studies and structural testing are conducted to improve building codes and standards in Australia.

Damage surveys by the Cyclone Testing Station have shown that houses built after the 1980s, when newer building codes were introduced, show a marked improvement in performance (Boughton et al. 2011). Despite these improvements, extreme wind events continue to cause damage in Australia and other parts of the world, especially for older houses. There are social and economic reasons for this, and the perception of low risk for rare events to homeowners and governments leads to little action and less money spent on home maintenance or retrofitting. Additionally, the building industry is based on traditional practices and is often less receptive to change, especially if such changes add to the building cost.

1.1.1 Batten-Rafter Failures

Observations from damage surveys have shown that failures of batten to rafter connections often result in the removal of large sections of the roof envelope as shown in Figure 1.1. It is most likely that these failures occur in a progressive or cascading manner as loads are redistributed upon connection failure. These progressive failures are of concern as the failure of a small number, or even a single connection can result in the failure of a disproportionately larger area of the roof structure.

Figure 1.1 Typical batten-rafter connection failure: a large section of the roof envelope removed (right) with cladding still attached to battens and rafters left intact (left). Adapted from Boughton et al. (2017)

Failures in the roof structure will occur whenever there is a break in the vertical load path or the 'hold down chain'. With the weakest link in the chain being the source of the failure. Damage surveys have also indicated that major failures of the roof structure are often due to the failure of only one link in the hold down chain. When cladding fasteners fail: large sections of the cladding are removed with the rest of the roof structure remaining intact. When batten to rafter connections lack resistance, large sections of cladding and battens are removed. Finally, when roof to wall connections are at fault it is often the rafters, battens as well as cladding that are removed. It is therefore reasonable to examine the failure modes of the roof structure in isolation, as is done in the current study.

1.2 Complex Structural Response

Understanding progressive failures are difficult due to the nature of the fluctuating wind loads on the surface, nonlinear behaviour of connections due to the load fluctuations and the complexity of the structural system as a whole. Progressive failures of batten to rafter connections are governed by four main factors:

1) The timing and correlations of peak pressures on the roof surface.
2) The response of individual connections to these dynamic fluctuating loads.
3) The behaviour of the structural system as connections fail and load is redistributed.
4) The change in aerodynamics and internal pressurisation due to failure of the building envelope.

The scope of this study is limited to the first three controlling factors. The change in aerodynamics as the roof is peeled away and the resulting fluid-structure interaction may greatly affect the path that failure propagates. However, it is more pertinent to study the load redistribution process at the initiation of failure, which is the main subject of this thesis.

1.2.1 Wind Pressure Fluctuations

Wind loading on a low-rise building is a complex process influenced by several factors such as terrain and topography that affect the velocity and turbulence characteristics of the wind. The shape of the building and approach wind direction leads to flow separation and building-induced turbulence causing vortices and eddies that in turn cause spatial and temporal fluctuations in surface pressures. Thus, large negative pressures can occur on the roof surface, with an overall suction mean pressure distribution in addition to intermittent peak pressures caused by the formation of eddies and vortices. Additionally, the movement of eddies and vortices cause different connections to receive peak loads at different times during a windstorm due to the pressure fluctuations on the roof.

1.2.2 Individual Connections

Connections such as batten to rafter connections are subject to rapidly fluctuating uplift loads due to wind pressures on the roof cladding. In the case of nailed connections that were examined in the current study, effects of drying of timbers and corrosion of nails influence the performance of connections. A further complication is that there is significant variability in connection strengths within the roof of a single house and the wider building stock. This variability is especially the case with timber connections due to the variations in timber material properties amongst different timber species, amongst different trees within the same species and different timber sections taken even from the same tree. The probabilistic nature of wind loading combined with the probabilistic nature of connection resistances creates a complex reliability problem, making estimates of vulnerability of light framed structures especially difficult.

1.2.3 Load Sharing and Redistribution

The load path for wind pressures on the roof surface begins at the roof cladding, loads must then be transferred to the battens, then rafters, and finally to the walls through under-purlins and struts, or the roof to wall connections. Other structural members such as collar ties and ceiling joists also contribute to the load sharing that occurs within the roof structure. In addition to these structural elements, internal linings such as the ceiling, and wall linings act as structural diaphragms (Boughton 1983). Another layer of complexity arises with the non-linear behaviour of connections and load redistribution under the wind loading. Any damage to a single connection due to uplift loads will cause load to be redistributed to neighbouring connections, potentially overloading them and causing damage to spread.

1.3 Light Framed Timber Houses

Light framed timber construction is described as the use of small cross section members to create structural elements such as floors, walls, and roof framing with mechanical fasteners such as nails, plates, or straps. Light framed houses are complex structural systems due to the large number of members, and connections and fasteners. This leads to behaviour such as load sharing, partial composite action and, during extreme loading: the nonlinear behaviour of connections and load redistribution. Previous studies by Wolfe and LaBissoniere (1991a), Morrison et al. (2012a) and most recently Satheeskumar et al. (2016) have quantified the load sharing mechanisms in these types of structures.

Light framed timber houses are the predominant form of residential construction in Australia and in North America (Carson 1995). This is due to a number of factors such as high labour costs, a mature timber industry and cultural reasons. This form of construction developed during the 1830's in Australia with the advent of industrial sawmills and the availability of machine made nails. Light framed timber construction also became popular in North America around the same time, known there as 'Chicago' or 'balloon framing' construction. Light framed timber construction evolved from traditional mortice and tenon construction with hardwood timbers to that of softwood during the post war era, which saw a high demand for new housing in both Australia and the United States (Irving 1985). With the advent of industrial sawmills, small cross section timbers could be mass-produced, providing a relatively cheap building material that is easily handled on site with minimal use of heavy machinery.

This type of construction evolved from builders' traditions and has far less engineering input than most building types. Because of this, traditional light framed construction is designed predominantly for gravity loads. However, due to their low self-weight light framed structures are vulnerable to wind uplift loads that can overcome the buildings self-weight during winds of higher than 35km/h for metal clad roofs (Reardon 1979b).

1.3.1 Australian Construction Practices

The most significant difference between Australian light framed roof construction and that of North America is the use of battens (small purlins) to support roof cladding, as opposed to plywood sheathing. Additionally, connection details and timbers species used for construction also differ.

Several wall construction techniques are used in different parts of Australia; these include brick veneer, double brick, timber framed and masonry blockwork. However, regardless of the type of wall construction the roof structure is of light framed construction.

The most common roof cladding materials include corrugated metal cladding in the northern states and tiled roofs in southern states. Corrugated iron sheeting was popular in Australia due to the nation's isolation and colonial heritage, imported iron sheeting from Britain could be transported easily to remote areas and required little labour to install. In the southern states, tiled roofs became popular when the level of industrialisation could support the manufacture of tiles within Australia. However, in states such as Queensland, corrugated sheeting continued to remain popular. Light framed timber construction was some of the earliest construction in Queensland as it was one of the later states to be colonised (Irving 1985).

Until about 50 years ago, pitched roof construction - that is roof framing using timber rafters was the primary construction technique, since then roofs with prefabricated trusses have become more common. Thus, roof structures can be classified as 'traditional' when using rafters or 'modern' when using pre-fabricated trusses.

As shown in Figure 1.2 traditional roof construction consists of rafters supported by the wall top plates and a ridge board. Ceiling joists resist horizontal reactions and a collar tie that ties rafters on both sides together limits deflections of the rafters. For larger spans, under-purlins supported by struts provide and intermediate support for the rafters.
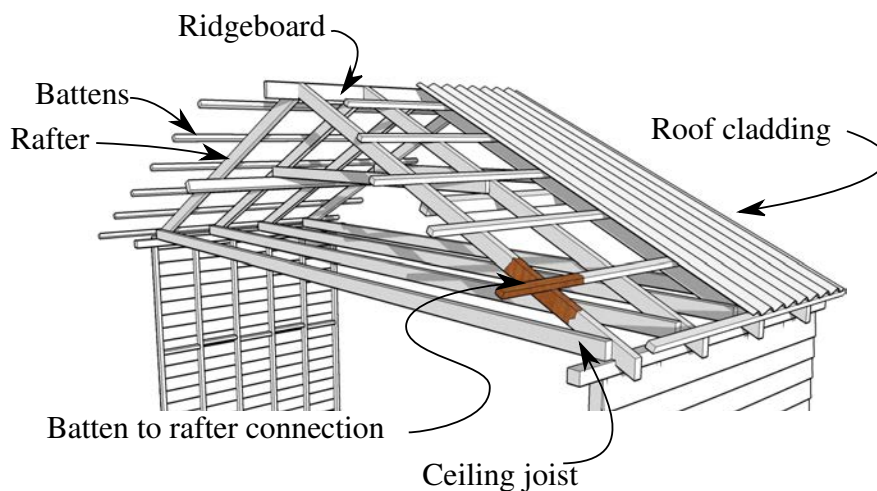
Figure 1.2 Light framed timber roof structure with corrugated metal roof cladding.

The roof structure can be described as a set of parallel primary beams (The rafters or the top chords of the trusses) that support a perpendicular set of smaller section secondary beams, the battens. Thus a grid pattern of batten to rafter/connections is formed. The battens in turn support corrugated metal cladding that acts as a structural membrane with its primary span direction being along the corrugations, from batten to batten.

The roof to wall connections are traditionally skew nailed to the top plate of the wall, contemporary construction makes use of metal plated connections such as framing anchors or hold down straps. Batten to rafter connections were traditionally single of double nailed to the rafters and newer cold formed 'top hat' battens use self-drilling batten screws. Early cladding to batten connections included lead headed nails; however, newer metal screws specifically for fixing cladding are now used.

Timbers were often Australian hardwoods sourced from local areas. Due to their hardness, these timbers were often worked while in the green condition to allow nails to be driven more easily. The drying of timbers over time has significant effects on the strength of nailed connections, which will be studied in more detail in Chapter 4.

For an older houses built before 1982, when newer building codes became legislation, connection details would have been the use of plain shank nails for skew nailed roof to wall connections, and two nails for each batten to rafter connection. These double-nailed batten to rafter connections are especially vulnerable to wind loads and are the subject of investigation in this study.

1.3.2 Selected Structural System for Study

The structural system selected for this study is a traditional pitched roof construction with corrugated metal cladding common in North Queensland, shown in Figure 1.2

- Cladding: corrugated metal sheeting
- Battens: 38 × 75mm at ~900mm centres
- Rafters: 100 × 50mm at 900mm centres
- Ceiling joists: 100 × 50mm at every rafter
- Collar ties:100 × 50mm at every second rafter
- Under-purlins: 100 × 100mm at rafter mid-span
- Struts: 100 × 100mm at ~ every 4th rafter

Batten to rafter connections, are two 75mm plain shank bullet head nails. These connections are a common detail observed in many roof failures in wind-storms, and are the subject of detailed investigation in this thesis.

Older traditionally constructed houses often have hip roofs, however this study will use a gable end roof as the focus is specifically for batten to rafter connections and it is therefore better to reduce complexity in the rest of the structural system and the aerodynamics of the roof shape.

1.4 The Current Study

Light framed construction evolved with little formal engineering input, Traditional builder's techniques focused on supporting the roof under gravity loads with the self-weight of the roof structure providing resistance to wind uplift forces.

Despite being relatively easy to construct, these houses are highly complex structures with hundreds of connections and structural members. Due to aerodynamic effects and low self-weight especially for sheet metal roofs, the roof structure is one of the most vulnerable parts of the house to wind loads. Despite the redundancy of the repetitive structural members, the failure of certain connections can result in a cascading or unzipping effect during a storm.

Reducing the vulnerability of communities is an increasing priority for governments, emergency services and the insurance industry. The research presented in this thesis is part of the Bushfire and Natural Hazards CRC project: Improving the resistance of existing housing to severe wind events. Improving codes and standards and producing guidelines for the retrofitting are the goals of wind engineering research. Additionally vulnerability modelling is an important decision making tool often used by the insurance industry and governments. Such codes and standards, and vulnerability models require the selection of valid assumptions and thus an understanding of the structural behaviour and failure modes.

Accounting for progressive failures of structures in models has been a significant challenge of existing vulnerability models. Due to the complexity of progressive failures, previous vulnerability models such as VAWS (Wehner et al. 2010) require simplifications of the load redistribution process. For example, logical statements are used to assume percentages of loads assigned to neighbouring connections upon failure of a single connection. Such assumptions must be validated as the structural behaviour of progressive failures in the roof of light framed structures has not been expressly conducted and is largely unknown.

Previous research on the aerodynamic behaviour of structures through wind tunnel studies and structural testing studies had quantified the load sharing behaviour of light framed structures. However, limited research exists that expressly studies the load sharing and redistribution within light framed structures during a progressive or cascading failure. It is this gap in knowledge that this thesis aims to address.

This thesis describes a procedure to study the load redistribution and progressive failures mechanisms of a system of batten to rafter connections in older Australian housing. This procedure involves:

1. **Wind tunnel Testing**: A 1/50 scale wind tunnel model test was used to determine fluctuating wind loads on batten to rafter connections. Simultaneous pressures signals at 98 pressures taps are recorded for multiple wind directions to provide input time-history data for dynamic connection testing and computer modelling. Using signal processing techniques, the timing and correlations of loads among neighbouring connections were also examined in detail.

2. **Connection Testing:** Static and dynamic tests of individual batten to rafter connections were performed to record force-displacement curves for use in the subsequent finite element modelling. Nail slip behaviour that occurs during realistic wind loads is also studied based on the dynamic tests.

3. **Nonlinear Time History Analysis:** A structural analysis model of a system of batten to rafter connections and cladding was used to determine the load paths, load sharing and the sequences and directions failures are likely to propagate. The implications of these system effects are discussed in relation to the connection testing results and the timing of peak loads at groups of connections.

Previous research has studied individual fasteners and structural systems, in full scale and in computer models. However only in the undamaged state using quasi-static loads. The few studies that have used spatial and temporally varying loads to cause damage to a structural system (e.g. Morrison and Kopp (2009)) have not been able to study the cascading failures where connections completely fail. The most recent research that study failure and spread of damage do so using computer models and wind pressures derived from computational fluid mechanics models, which may not capture peak loads on roof surfaces accurately. Furthermore, these studies look at the structural response of structural systems used outside Australia. As such, a study of the failure mechanisms of a system of batten to rafter connections in older Australian housing under realistic spatial and temporal wind pressures has not yet been undertaken.

The novelty of the study presented in this thesis is that the procedure developed accounts for:

1. Spatial and temporal variations in wind pressures across the roof surface.
2. Nonlinear behaviour of connections.
3. Storm duration effects and accumulated damage over time,
4. Dynamic behaviour of the structural system and load redistribution due to failed or damage connections, including the progressive or cascading failures that cause the removal of a large section of the roof envelope.

Potential outcomes of this study include improvements in codes and standards and development of engineering based codes and guidelines for economically retrofitting older houses. Additionally, the techniques developed can allow better estimates of the vulnerability of houses to progressive failures. Such techniques may also be adapted to study failures in other connections in the roof structures or other structural systems under wind loading. More importantly, this study will improve the fundamental understanding of progressive failures under wind loads that previous research has not examined in detail.

1.5 Objectives

Primary Objective:

Determine the load redistribution and progressive failure behaviour of batten to rafter connections under spatially and temporally varying wind pressures.

Why are we doing this? In order to improve the resistance of batten to rafter connections in older houses and improve their design for newer houses, we need to understand the structural response and damage progression of these types of connections under realistic wind loading conditions.

This is achieved by: Undertaking a thorough study of the wind loading mechanisms that affect batten to rafter connection response, including the nonlinear behaviour of connections and the response of the structure as a whole as loads are redistributed and connections fail.

Leading to: A better understanding of progressive failure mechanisms. This will help develop cost effective retrofitting methods for older housing and improve the design of connections for new construction.

1.6 Overview

Chapters 1 and 2 include an introduction to the research questions and a review of current and previous research on wind loading of light framed structures. The main body of this thesis is divided into 5 parts:

Chapter 3: Presents the results of a wind tunnel study performed to determine the spatially and temporally varying loads to be applied to the structural analysis model. The pressure patterns and correlations of loads across the roof are also examined. Time histories and pressure distributions during 'peak events' are selected for use in the computer analysis model.

Chapter 4: Presents the testing of batten to rafter connections performed to determine their response to fluctuating dynamic loads. Load-displacement curves and hysteresis behaviour are determined.

Chapter 5: Presents the details of a finite element method structural analysis model of an older Australian house roof structure. Batten to rafter connections are represented by non-linear links that incorporate the force displacement and hysteresis behaviour derived from the connection tests. Time history pressures derived from the wind tunnel tests are applied to the model.

Chapter 6: Presents a series of computer simulation experiments performed to study the load redistribution and progressive failure mechanisms of the modelled structural system. These include, static analyses to determine load paths in the undamaged state, 'pull up analyses' to determine load redistribution behaviour, and time history analyses under spatially and temporally varying loads to determine the system's response under realistic wind loads.

Chapter 7: Presents exploratory studies and potential applications of the techniques developed in this thesis. An assessment of fragility of batten rafter connections was made based on a small sample of randomised trials of different wind load histories and connection strengths. Survival functions that allow an assessment of vulnerability that includes storm duration effects are presented.

Chapter 8: Presents the Conclusions and Recommendations of this thesis.

2 BACKGROUND AND LITERATURE REVIEW

This Chapter introduces concepts specific to this thesis. This includes the nature of light framed structures that are being studied, their aerodynamic behaviour and the speed of load transmission within materials. Additionally, a review of previous studies on light framed houses is presented.

2.1 Codes and Standards

The desired outcome of wind and structural engineering research is often the implementation or revisions to building codes and standards or changes to legislation. In Australia, relevant codes and standards include AS/NZS 1170.2 (2011), AS4055 (2012) for the derivation of wind loads on structures. Once wind loads are estimated, standards for timber construction AS1720 (2010) and residential construction AS1684 (2010) are used for the design of structural members or the selection of connection details.

Although the design of engineered structures has been codified previously, the implementation of standards for residential construction is a relatively recent development, sparked by the damage to houses in high wind events as described earlier.

Present Codes and Standards were also developed with data from wind tunnel tests conducted during the 1970's to the 1980's. However, these tests had a limited number of simultaneous pressure measurements. Additionally, structural testing carried out at the time allowed only a limited number of measurements to be recorded and nonlinear simulations of the structural response were not feasible due to the computational capabilities of the time.

Wind engineering research conducted in the 1970's and 80's have resulted in effective building codes for newer houses. Changes to building codes in the 1980's in Australia have improved the performance of houses to high wind events, as evidenced from recent damage surveys (Boughton et al. 2011). However, standardised methods for retrofitting older structures have not been a major focus of most wind engineering research.

Pre code houses built before 1982 were not without guidelines for their construction. The Commonwealth Bank's 'Blue Book' contained construction requirements and connection details that needed to be ratified before loans could be issued. This 'Blue Book' was the precursor to the engineering and reliability based design codes such as AS1684 for residential construction.

Guidelines for retrofitting also have some precedent, in the 1980's the Insurance Council of Australia funded a study to develop retrofitting standards for houses. Outcomes were a series of handbooks - HB132 (1999) that contain alternative connection details that could be added to existing houses. However, these handbooks are not widely used for several reasons. These include: builders and certifiers simply not knowing about them, the cost of the handbooks and their availability only in hardcopy and not electronically, and several retrofits are not aesthetically acceptable for the homeowner (Smith et al. 2015). Additionally, reductions in premiums for homeowners who undertook upgrades were not satisfactorily implemented and thus there was little incentive to undertake these upgrading measures.

The retrofitting guidelines presented in HB132 were also based on the limited understanding of the failure modes at the time. The understanding of the complex failure modes produced in this thesis will allow more targeted and cost-effective retrofitting measures or devices to be designed.

2.2 Vulnerability Models

Vulnerability and catastrophe models are tools used by governments, the insurance industry, and researchers to predict the impacts of natural hazards and plan for future events. These models often determine monetary losses, but can also be used to predict disruption of critical infrastructure due to a natural disaster. Mason and Parackal (2015) and Smith et al. (2018) have reviewed a wide range of vulnerability models for wind and flood hazards. Notable vulnerability models for wind loading on residential structures from this review are presented in this section.

Wind vulnerability models have largely been developed for hurricanes and tornadoes in the United States and tropical cyclones in Australia. Walker (2011), Pita et al., (2013) and Pita et al., (2015) provide extensive reviews of vulnerability models developed for residential buildings subject to severe wind loading. These reviews detail the historical development of modelling capacity from the early empirical models developed by Friedman (1975) to the engineering-based simulation models currently used such as the HAZUS-MR4 Hurricane model.

Vulnerability models can be divided into two categories: empirical and engineering based. Empirical models use observations from past damage surveys and engineering judgment to make predictions of loss and therefore implicitly account for the effects of progressive failures. Engineering models on the other hand, use reliability and/or structural analysis computations to simulate damage occurring depending on wind speed. Accounting for progressive failures in these types of models is a challenge, as progressive failure mechanisms are still poorly understood.

The current thesis will address this limitation of current engineering based models by developing a procedure for simulating progressive failures and providing a better understanding of load sharing and redistribution between batten to rafter connections.

2.2.1 Empirical Models

Several vulnerability models have been developed for Australian residential construction. The earliest were based on observed damage to housing during Tropical Cyclone Tracy, and formulated by Leicester and Reardon (1976) based on damage survey information collected following the event. Walker (1995) studied loss data from Tropical Cyclone Althea (1971) and Winifred (1986) and derived mean vulnerability curves for Queensland housing built before and after the introduction of new building regulations in 1981 (Mason and Haynes 2010). The Walker (1995) model is still used widely throughout the insurance industry as a benchmark for wind vulnerability models.

More recently, Henderson and Harper (2003) developed a suite of probabilistic vulnerability curves for six different house types, based on assumed modes of failure and internal pressurisation. These models estimate the percentage of houses that suffer 'damage' within the population. The model was validated against damage survey information collected following Tropical Cyclones Althea, Tracy, Winifred, and Vance, with reasonable agreement. Henderson and Ginger (2007) extended this model specifically to high-set timber housing in North Queensland and the Northern Territory.

A set of vulnerability curves were also developed by Geoscience Australia through a series of expert-workshops (Ginger et al. 2010). These models were developed for a range of different housing types, considering the potential influence of different load bearing systems, wall cladding and roof types. The Geoscience Australia curves present the only publicly available set of vulnerability models for the range of housing types across Australia.

2.2.2 Engineering Models

Boughton et al. (2014) presented a reliability study of batten to truss connections for a contemporary Australian house. Fragility curves for various connection fasteners were developed for different roof areas (corner, edge and general). This study analysed the probabilities of 'first failure' of connections but did not examine what may be occurring to neighbouring connections at the time of failure.

More recently, Kothesingha (2015) performed a reliability analysis on cladding fasteners and purlin to frame connections of shed type industrial buildings. This vulnerability model is able to account for load redistribution and changes in internal pressure due to the failure of roof cladding. It was assumed that the loads were fully correlated in edge regions (correlation coefficient of 1.0) and weakly correlated in other parts of the roof (correlation coefficient of 0.5). Additionally, upon the failure of a connection, loads were redistributed to neighbours as per Henderson (2010), who examined the failure of cladding fasteners, with 90% of the load transferred along the direction of corrugations of cladding and 10% to connections to the left and right. Using similar methods and assumptions, Stewart et al. (2016) performed a reliability analysis on an industrial building to determine the effects of the presence of dominant openings in the building envelope.

Previous researchers have acknowledged that these progressive failures are a significant contributor to damage (Henderson and Ginger 2007, Vickery et al. 2006, Wehner et al. 2010). These studies have attempted to make rough approximations for these effects. However, they do not account for the complex interactions between structure, spatial and temporal pressure fluctuations and nonlinear behaviour of connections.

A feature of all these engineering-based models is that they rely on many assumptions regarding the structural response to wind loads. These models are generally specific to a certain location/region due to the construction types found there and do not reflect the change in construction through time. As such, further research into Australian light framed timber construction and the structural response of connections is required for the development of accurate vulnerability models.

2.3 Progressive/Cascading Failures

A progressive failure describes a structural failure where initial damage to a connection or structural element results in the subsequent damage of a large part of, or the total destruction of the structure. The final damaged state is often disproportionately larger than the initiating failure, therefore these failures are also called disproportionate failures.

Progressive failures have primarily been studied in the context of preventing collapse in multi-storey buildings. Such failures typically occur under gravity loads due to failures initiating due to blast, vehicle impact or seismic loads. Nair (2004) outlines the fundamentals of progressive collapse. Methods to prevent such failures include providing alternative load paths and redundancy and improving the resistance of critical structural elements that could lead to progressive failure if damaged.

El-Tawil et al. (2013) and Ellingwood et al. (2007) present literature reviews on the subject, including various methods proposed by other researchers, and methods or guidelines used by codes and standards in different countries. These techniques are more applicable to steel and concrete structures under gravity loads that are considerably different to wind uplift loads on a light framed roof. However, energy based analysis methods may provide insights on failure behaviour that can be applied to the failure of roofs during windstorms. This includes the method by Szyniszewski (2009) that interprets structural failure in terms of energy balance. In order for the collapse to be arrested, the kinetic energy of the collapsing structure must be absorbed as strain energy by the remaining structure, several 'stable energy states' might exist during the failure when the collapse of the structure may come to a stop.

Previous research on progressive failures of light framed structures mainly focus on the effects of seismic loads (Kirkham et al. 2013, Foliente 1998). This thesis will address a current gap in research by studying in detail progressive failures in roofs of light framed roofs specifically under wind loading

2.4 Observations from Past Damage Investigations

Batten to rafter connections in light framed residential structures are vulnerable to failure in wind storms. Recent damage surveys have shown that the failure of batten to truss/rafter connections is one of the more likely causes of roof damage during high wind events. These failures are especially the case when older structures are renovated and have new roof cladding placed on existing battens or have their cladding converted from tiles to metal sheeting (Boughton et al. 2017, Boughton et al. 2011, Ginger et al. 2007, Henderson et al. 2010b, Parackal et al. 2015).

Tropical cyclones are a major natural hazard in the northern coasts of Australia. Since the 1970's institutes such as the Cyclone Testing Station at James Cook University have conducted extensive research into the damage caused by these severe weather events. Damage surveys from the 1980s to present have shown that batten to rafter failures continue to be a common failure mode under wind loading. Figure 2.1 to Figure 2.4 show examples of such batten to rafter failures. In many damage surveys, batten to rafter failures were noted as the most common structural failures for houses.

Cyclone Tracy, 1975:

(Landfall – Darwin, Northern Territory)

This event was the catalyst for the improvements in building codes in Australia. Total destruction of houses due to racking failure and internal pressurization from debris damage were common. At the time there was no allowance made for internal pressures in light framed houses. Metal cladding was often pulled over the heads of cladding fasteners due to fatigue failure (Walker 1975, Leicester and Reardon 1976).

Cyclone Kathy 1984:

(Port McArthur Northern Territory)

A case study showed a batten to rafter connection failure that resulted in the removal of most of the roof envelope with the battens still attached to cladding. It was thought that the failure may have occurred early in the storm. The failure resulted in severe water damage and reduction in lateral resistance due to the removal of the battens and cladding that act as a structural diaphragm. In this case, the ceiling diaphragm remained in-tact and thus prevented additional structural damage due to lateral loads. Failure resulted as the connections had only single nails instead of two nails per connection (Boughton and Reardon 1984).

Figure 2.1 Batten to rafter failure observed during cyclone Kathy (Boughton and Reardon 1984).

Cyclone Winifred 1986:

(Far North Queensland)

This damage survey also noted that batten to rafter connection failures were one of the most common structural failures during the event. This survey noted a shift from failures of cladding fasteners to the failure of batten to rafter connections being more common. This shift was due to the uptake of using power driven screws for cladding fasteners with no change to the nailed batten to rafter connections below. These failures were predominantly for older houses built before 1982 (Reardon et al. 1986).
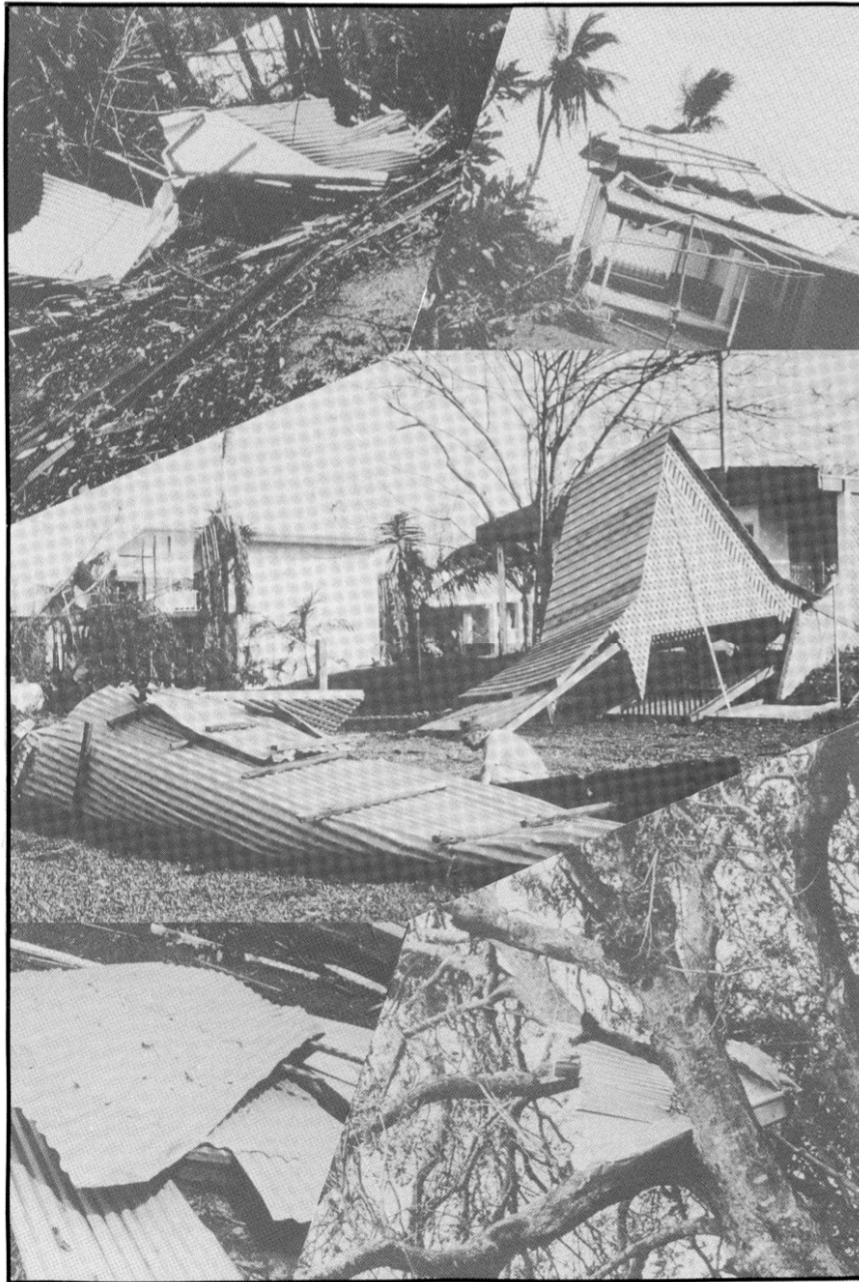
Figure 2.2 Several batten to rafter failures during cyclone Winnifred (Reardon et al. 1986) .

Cyclone Vance 1999:

(Exmouth Western Australia)

This damage survey again noted a shift in the types of failures observed from cladding fastener failures seen in Cyclone Tracy. Failures were observed in older houses that had cladding fasteners upgraded without upgrading batten to rafter connections. Failures were also observed in new housing. Failures of single nailed batten to rafter connections were also noted.

The report notes that batten to rafter connections had become the weak link in construction in cyclonic regions, and recommends changes in regulation for when houses are repaired or renovated such that batten to rafter connections are also upgraded whenever cladding and fasteners are replaced (Reardon et al. 1999).

19

Figure 2.3 Loss of roof cladding and battens during cyclone Vance (Reardon et al. 1999)

Cyclone Larry 2006:

(Far North Queensland)

Cyclone Larry crossed the Queensland coast at a similar location to cyclone Winifred. Batten to rafter connection failures of single and double nailed connections were once again a common failure mode. This survey found that houses that had their cladding fasteners upgraded since TC Winifred suffered batten to rafter failures, as those connections were not upgraded.

This damage survey was the first to report the occurrence of 'hidden damage' due to the partial withdrawal of nails in batten to rafter connections. Discussions with builders and certifiers involved in the reconstruction after TC Larry noted a significant proportion (20 to 70%) of houses suffering from hidden damage, making these structures vulnerable to future events (Henderson et al. 2006). Such hidden damage of batten rafter connections may cause to roof to feel 'springy' to walk on (Henderson et al. 2010a).

Cyclone Yasi 2011

(Far North Queensland)

This damage survey also noted several batten to rafter connections failures. Including a case of batten rafter failure on a roof repaired after a previous failure during Cyclone Larry. In this case, the nailed connections of a portion of the roof that had failed were replaced with framing anchors. However, the part that did not suffer damage during Larry was not upgraded and then failed during Yasi. This case highlights the requirements for thorough repair and renovation work following a severe wind event (Boughton et al. 2011). 'Hidden damage' may have played a role in this failure, Figure 2.4 shows an example of hidden damage in a roof during TC Yasi.

Figure 2.4 Hidden damage of batten to rafter connections caused by TC Yasi (Boughton et al. 2011)

Cyclone Debbie 2017:

(*Whitsunday region, Queensland*)

In this most recent damage survey that the author was involved in, batten to rafter connections were again noted as the most common structural failure in older housing. However, batten to rafter connection failures were also observed in contemporary code compliant housing, as shown in Figure 2.5 (Boughton et al. 2017).

Figure 2.5 Batten to truss connection failure in a contemporary apartment building (Boughton et al. 2017)

Summary of past damage surveys

Damage surveys have noted that batten to rafter connection failures are some of the most common structural failures in housing during severe wind events, predominantly in older houses built before newer codes and standards took effect in 1982. There is also a change in the types of failure through time:

1) Failures due to inadequate strength, often due to the use of one instead of two nails per connection.
2) Failures due to the upgrading of roof sheeting and connections without upgrading the batten to rafter connections
3) Failures due to damage from previous events (i.e. hidden damage) as evidenced by damage surveys performed after cyclones that affected the same area.
4) Failures that occur in modern construction with incorrect connection details.

It is also noted that such failures occur in isolation, that is, when batten to rafter connections are weaker than other connections, the corrugated roof cladding with the battens attached is removed with little effect on other connections such as the cladding fasteners and roof to wall connections. Similarly, If the cladding fasteners are the weak link in the vertical load path, the corrugated roof cladding is removed leaving the battens and rafters behind. After the cladding has been removed the batten to rafter connections are then unlikely to fail, as they are no longer subject to uplift loads from the building envelope.

2.5 Wind Loads on Low Rise Buildings

2.5.1 Wind Tunnel Studies

Wind tunnel model studies have been the primary technique of wind engineers to obtain wind loads on buildings. These studies simulate atmospheric wind flow and measure the aerodynamic behaviour of the building. Pressure measurements on the surface of the wind tunnel models are taken at high sampling rates to capture the spatial and temporal variations of pressure.

Wind engineering has been studied formally since the start of the 20th Century. Holmes (2001) in his text 'Wind Loading on Structures' provides a history of the earliest wind tunnel experiments performed on low rise buildings. Researchers such as Stanton (1925) and Sherlock (1947) were some of the earliest published works on the subject. However, it was only after Jensen (1958) who studied the similitude requirements and fundamentals of simulating the atmospheric boundary layer that wind tunnel studies became an effective tool used by wind engineers. Following this, pioneering studies by Davenport (1960), (Davenport 1961b) Davenport (1961a) developed our current probabilistic understanding of wind pressures and the effects of gusts on building structures.

Later, measurements on full scale buildings by Eaton and Mayne (1975) at the UK Building Research Station and Levitan et al. (1990) at the Texas Tech University showed that these earlier wind tunnel studies could adequately predict peak pressures on the roof and established the credibility of wind tunnel tests for low rise buildings.

In lieu of studies on boundary layer fundamentals, wind pressures specific to low rise structures were studied by Davenport et al. (1977), Davenport et al. (1978) and Holmes (1982), (1994). Researchers such as Holmes (1985) and Pham et al. (1984) then developed probabilistic models further and these studies assisted in codifying wind pressures as pressure coefficients used for structural design in Australia.

2.5.2 Spatial and Temporal Pressure Fluctuations

The movement of wind over bluff bodies, such as a low rise building results in high suction pressures over the building envelope due to the turbulence from the atmospheric boundary layer as well as unsteady flow caused by the shape of the building itself, such as flow separation at roof edges and discontinuities at ridge lines, hips and valleys. This flow separation and sometimes reattachment created by the building can occur regardless of the turbulence of the upstream flow.

Building-induced turbulence cause high negative pressures on certain parts of the roof for different wind directions. These high load areas are transient and move across the roof rapidly due to the formation of eddies and vortices. The size, location and duration of these high load areas, as well as the correlation of loads among neighbouring connections may affect the likelihood of a failure initiating and propagating and a cascading manner.

Flow separation causes the formation of localised eddies and vortices that apply high suction pressures to the underlying roof surface (Kawai 2002, Cermak 1970, Ostrowski et al. 1967). Vortices form in separation regions where the shear layer 'rolls up' near the leading edge. High loads at individual connections can occur in different locations and at different times. However, the overall distributions of pressures are dependent on wind direction.

Saathoff and Melbourne (1997) conducted a detailed investigation on the formation and behaviour of vortices in separation regions of a bluff body in turbulent flow. They found that vortices formed in the separation region intermittently 'roll-up' due to perturbations in the free stream flow. This causes the vortices to be convected along the surface of the body, thus inducing high negative pressures on the surface that it passes over. The vortices can also move closer to, or away from the surface of the body, with much higher negative pressures being applied when the vortex is closest to the surface.

Two-dimensional flow separation regions occur when flow is perpendicular or near perpendicular to the roof edge or discontinuity. Here, flow separation results in the formation of vortices that periodically roll up and are forced along the roof surface - creating a moving zone of high suction pressure.

Cornering winds can also result in three-dimensional flow separation that can create especially high suction pressures at roof corners. Three-dimensional flow separation can occur for cornering winds where the airflow is incident on the corner of the roof. Conical vortices form in these cases, similar to those formed over an aircraft delta wing. Such vortices produce especially high suction pressures intermittently as they form and dissipate.

The large intermittent negative pressures, created by the movement of eddies and vortices, cause damage to cladding elements and the underlying roof structure. Accurately measuring these intermittent peak pressures is the challenge of wind tunnel studies and full-scale measurements. Wind tunnel testing to capture spatial and temporal pressure fluctuations is therefore an important requirement of this study to model the behaviour of batten to rafter connections during a windstorm.

2.5.3 Internal Pressures

Internal pressures can be small negative values in a nominally sealed house, thus reducing the net uplift pressure on the roof and loads on connections. However, the presence of a large opening on a windward wall will result in large positive internal pressures and make the roof more vulnerable to failure. These positive internal pressures vary with time but are generally uniform throughout the building's internal volume and can be reasonably approximated if required.

2.6 Structural Response under Fluctuating Wind Loads

2.6.1 Correlations of Wind Pressures

Wind loads on roof surfaces are highly fluctuating spatially as well as through time. These fluctuations can result in peak loads occurring at different batten to rafter connections at different times. If certain connections weaken or begin to fail, load is transferred to adjacent connections rapidly.

Whether neighbouring connections also experience high loads at the 'same time' determines whether they will be overloaded if a neighbouring connection fails; potentially causing a progressive failure to initiate. Determining how these high loads across the roof surface are correlated is necessary to identify when and where cascading failures begin and which approach wind directions are critical.

Saathoff and Melbourne (1989) examined the formation and correlation of high negative pressures on the leading edge of rectangular bluff bodies for flow perpendicular to the edge of the body. Ginger and Letchford (1993) examined the correlation of wind pressure on a flat-roofed rectangular shaped building for two flow separation mechanisms: two-dimensional flow separation when the wind is perpendicular to a leading edge and the three-dimensional conical vortex formed for cornering wind directions. These studies found that pressures were correlated within these flow separation areas. However, it is unknown what kind of behaviour will be experienced for a typical sloped roof house.

Additionally, information on the response of batten to rafter connections under fluctuating loads, the timing and correlation of high uplift loads experienced by these connections and the implications to progressive or cascading failures are unavailable.

2.6.2 Speed of Load Transmission

If certain connections weaken or begin to fail, load is transferred to adjacent connections rapidly. Loads are transmitted through a material via stress waves, thus the time it takes for a load or change in load on a structural element such as roof cladding to reach a particular connection or support is related to the speed of these stress waves.

Solid materials such as steel or timber, unlike fluids, are also capable of resisting shear deformation and wave propagation is more complex than longitudinal waves (such as sound) in air or water. Such solid materials transmit loads as compressional, shear and bending waves. For beams, the speed of these waves depends on the Young's Modulus (E) of the material for compressional waves, the shear modulus (G) for Shear waves and the flexural rigidity (EI) for bending waves as shown in Equations 2.1 to 2.3. Flexural waves are dispersive, and the wave speed depends also on the frequency of the change in loads (ω) (Hambric 2006).

Compressional (beams):
$$C_c = \sqrt{\frac{E}{\rho}}$$
Eq. 2.1

Shear (beams):
$$C_s = \sqrt{\frac{G}{\rho}}$$
Eq. 2.2

Flexural (thin beams):
$$C_{B_{Bernoulli-Euler}} = \sqrt[4]{\frac{EI}{\rho A}\omega^2}$$
Eq. 2.3

The acoustic wave speeds for structural materials such as timber are orders of magnitude faster than the load fluctuations due to wind pressures. For example, for the Australian hardwood 'Spotted Gum' $\left(E \approx 26\ GPa,\ \rho \approx 1060 \frac{kg}{m^3},\ G \approx 1.9 GPa\right)$, a compression wave would have a speed of $7.2 \times 10^4\ m/s$, a shear wave speed: $1.3 \times 10^3\ m/s$ and a bending wave speed in a 38×75mm batten with a loading frequency of 1Hz is $1.4 \times 10^2 m/s$. The time it would take for such a waves to travel a 1m length of a 38×75mm batten would be between 1.4×10^{-5} and 7×10^{-3} s. The majority of fluctuating energy in wind pressures is due to frequencies less than 10 Hz with a period of 0.1s. Thus, peak loads at batten to rafter or even rafter to wall connections would be effectively experienced instantly due to pressure fluctuations on the roof surface.

Although loads may arrive at connections effectively instantly, the time it takes for a connection itself to 'respond' to the load would be influenced by the mass, stiffness and damping of the connection and structural system. The dynamic and static friction of the nails will also affect how nails behave as they withdraw.

2.6.3 Response of Nailed Timber Connections

Timber battens are often connected to rafters with nails, typically a single plain shank nail for tiled roofs and two plain shank nails for metal clad roofs. The battens that are of a small cross section are most often hardwood with rafters being either softwood or hardwood.

Nailed connections that act in tension such as batten to rafter connections are influenced by the magnitude of load and loading history. Morrison and Kopp (2011), found that loading rate does not affect nailed connection performance significantly.

Such connections are highly variable in their performance due to several parameters such as the timber species, moisture content, angle of nails, embedment depth of the nail, size and orientation of the rings of rafter timber.

One of the most significant influences of the performance of nailed timber connections is the moisture content of the timber members. Additionally, the moisture content at the time when the connection was made and the subsequent change will also affect the performance. For typical hardwood construction, timbers are fastened together whilst still in the 'green' condition (moisture content ~$30 - 40$ %) and can then dry out during their service life to about $8 - 12\%$ moisture content depending on the climate of the site.

As the timber fibers lose moisture, they contract in diameter and the overall volume of the material decreases. This reduces the grip on the shank of the nail –decreasing the strength of the connection. Depending on the type of nail used the capacity of a nailed batten-truss connection can decrease by more than 50% (Reardon 1979).

2.7 Testing and Analysis of Light Framed Timber Construction

Studies of light framed construction have sought to define the complex load sharing mechanisms and system behaviour present in light framed structures, and to quantify the non-linear response of connections. Gupta (2005) presents a review of research into system behaviour of light framed trussed roofs and outlines the complexities and the nature of load sharing and 'system' behaviour in light framed timber roofs.

These studies have taken many approaches including the testing of individual connections and fasteners, full scale testing of house assemblies, scale model tests and analytical models often based on the Finite Element Method (FEM). Each of these approaches faces their own challenges: full-scale studies are costly and have often been limited by the instrumentation to measure loads within the system. Model scale studies have difficulties meeting accurate similitude requirements. Validating computer models with full scale testing is also a challenge.

2.7.1 Full Scale Testing

Full scale testing is the most thorough method available to study structural behaviour. Early studies by Boughton (1983) and Wolfe and LaBissoniere (1991b) used full-scale tests on roof assemblies and entire houses to determine load-sharing behaviour. Notable full-scale studies are outlined in the following section.

Boughton and Reardon (1982) and Boughton (1982),(1983) conducted extensive full scale testing on two complete houses. These studies examined load sharing of lateral and uplift loads, load redistribution and the effect of non-structural elements to the load-path. For the houses studied, large displacements at roof to wall connections were required for load to be redistributed to neighbouring trusses.

Under uplift loading, the redistributed load was carried to elements surrounding elements that had failed. This caused overloading of neighbouring connections and a spread of failure. This was observed in the case of batten to rafter connections that span continuously across rafters: The loss of one connection significantly increased the load on adjacent connections resulting in a propagation of failures along the batten.

Different behaviour was observed for lateral loading, where failure of connections occurred in a more ductile manner. Additionally, the mechanisms of transmitting uplift loads are different from transmitting lateral loads. Lateral loads were found to be transmitted through walls and floor and ceiling diaphragms. Upon the failure of one bracing structure, the large in-plane stiffness of the roof diaphragms enabled the redistribution of lateral loads to other components.

Probabilities of failure and resulting progressive failures are then related to reliability theory. The probability of failure of a large section of roof is related to the probability of a defect occurring in a critical location. For a roof structure, the probability of failure is a function of the connections' resistances, the number of connections, the location of the connections on the roof and the quality of construction.

Non-structural elements such as wall and ceiling linings as well as ceiling cornices were found to attract load and contribute to the overall structural response of the house. This was primarily for lateral loads. Some diaphragms such as the ceiling were found to stiffen with increased load by reducing slack and closing gaps. The effects of these non-structural elements were summarized to have three main effects:

1. They can render actual structural systems redundant due to the unintended load paths.
2. Loads attracted by non-structural elements can cause the premature failure of these elements, reducing the overall strength of the structure.
3. Non-structural elements can give post failure strength by carrying loads that were previously carried by elements that have failed. However this feature is less applicable for uplift loads on the roof surface.

Wolfe and LaBissoniere (1991b) and Wolfe and McCarthy (1989) conducted tests on an assembly of roof trusses for the Forest Products Testing Laboratory (FLP) to study load-sharing behaviour. The process of load sharing was through two-way action and partial composite action and occurred only when a connection deflects relative to its neighbours. Additionally, it was found that when individual trusses are subjected to their design loads along the top cord: 40 to 70% of the load can be distributed to adjacent trusses. A limitation of this study from a wind loading perspective is that uniform gravity loads were applied. Shivarudrappa and Nielson (2012) showed that load transferred to connections for gravity vs. uplift loads could differ by 30 to 40%. Indicating that influence coefficients would differ significantly depending on the direction of loading.

Paevere (2002) conducted testing for lateral loads on light framed structures. This study was focused on seismic loads and not wind uplift. Additionally, this study, although conducted in Australia, examined a North American type structural system and presents a detailed review of the many types of hysteresis models available and various techniques for nonlinear analysis.

Doudak (2006) conducted field tests on an instrumented building subjected to wind and snow loads. Additionally, point loads were applied and displacements were measured at several locations. The study found that 73% of load applied at the mid-span of a roof joist was redistributed to adjacent joists. This was determined from displacement readings, as actual loads were not measured. Another limitation of this study was that limited conclusions could be drawn for behaviour due to wind loading due to the variability in wind speeds and directions.

Zisis and Stathopoulos (2009) conducted tests on an instrumented gable roof house to determine the attenuation of wind loads as they are transferred from the roof to wall connections due to dynamic effects (energy absorption). Wind pressures on the roof surface were measured and actual reaction loads measured using 2D and 3D load cells. The measured loads were compared to those determined from an idealized structural model with the same applied wind pressures. They found that the reaction forces from the idealized model were 26-46% higher than those measured by load cells, they attributed this to the effect of structural attenuation. However, as commented by Datin (2010), this is likely due to the simplifications of the structural model and not entirely from attenuation effects. Further tests on this setup were performed by Zisis and Stathopoulos (2012), this more recent study included a dynamic analysis using a Finite Element Method (FEM) model.

Morrison et al. (2012b) and Henderson et al. (2013) conducted full scale tests at the University of Western Ontario as part of the 'Three Little Pigs' project. These studies have best represented the complex nature of wind loads on roofs and the structural response of connections due to spatial and temporally varying pressures. Pressures scaled from wind tunnel studies are applied to the roof surface using 'Pressure Load Actuators' (PLAs). These specialized devices are able to follow a specific pressure trace accurately and apply this to a section of roof surface.

Morrison and Kopp (2009) used 58 PLAs to apply realistic wind pressures to a two-storey Canadian gable roof house and examine the response of toe-nailed roof to wall connections. The study found that roof trusses behaved as rigid members and that simple tributary area methods overestimate reaction forces, indicating load-sharing behaviour. Additionally, the amount of load sharing was found to change throughout the time history due to incremental nail pull out. Hysteresis was also observed during the failure of connections. Ultimate roof failures were observed to occur when multiple connections fail simultaneously

Henderson et al. (2013) later conducted similar experiments on a hip roof. Load cells were installed under the top-plates of selected roof to wall connections. A series of patch loads were applied sequentially to determine influence coefficients at roof to wall connections. Time-history loading was applied to the roof surface and the influence coefficients re-measured at the end of the simulated windstorm. These studies found that influence coefficients for roof to wall connections change only during damaging peak loads, reinforcing previous findings by Morrison and Kopp (2009). Changes to these influence coefficients occur almost continuously during high wind events due to multiple peak loads occurring at different locations throughout time. The change in influence coefficients for roof to wall connection reactions could be used to determine the redistribution of loads and load sharing that occurred in the roof structure

2.7.2 Model Scale Testing

Some researchers have made use of scale models to study light framed timber construction. However, these are fewer in number than full-scale experiments. Scale model tests allow instrumentation to be set up more easily but can face challenges when meeting accurate similitude requirements (Datin and Prevatt 2007).

Mani (1997) showed that scale model testing could be used as a tool for studying light framed timber construction. This study used a 1/8 scale model of a gable roof house to determine influence coefficients across the roof surface for truss hold down loads. Although unable to address proper similitude requirements the results showed a reasonable agreement to results of full scale tests by Wolfe and LaBissoniere (1991b).

Morrison and Kopp (2011) Mensah et. Al (2011) also used 1/3 scale models to develop a database assisted design approach. Influence coefficients for uplift loads determined from this model that used hold down straps instead of toe nails, which showed lower levels of load sharing than observed by Wolfe and LaBissoniere (1991b) for toe-nailed connections.

2.7.3 Computer Analysis Models

Analytical models have been used alongside full scale testing and model scale experiments from the early studies on light framed timber construction (Cramer and Wolfe 1989). The roof structure under wind loading and walls under lateral (usually seismic) loads have been the subject of most of these studies. Similar to full scale testing, many of these analytical studies have aimed to quantify load sharing and other system effects of light framed timber. The majority of analysis models are based on the Finite Element Method (FEM).

Li (1996) and Li et al. (1998), Analysed system effects of a wood truss assembly using the analysis and design software ETABS. The model showed good agreement when compared to full scale tests by Wolfe and McCarthy (1989) and Wolfe and LaBissoniere (1991b).

Cramer et al. (2000) used a non-linear matrix displacement based analysis model to study truss assemblies. To evaluate failure loads a 'combined stress index' CSI was defined, accounting for the effects of compression and bending; CSI values greater than 1 indicate failure occurring. Load sharing due to sheathing was measured by computing the ratios of CSI for the system with the sheathing vs. the system without sheathing. It was found that the level of load sharing increased with increasing applied loads due to the non-linear behaviour of connections. It was also found that partial composite action through the sheathing did not contribute to load sharing significantly. The main limitation of this study was that only uniform gravity loads were applied to the analysis models.

Gupta et al. (2004) performed a similar study using SAP2000 with similar findings. This study on a T-shaped roof system showed that accounting for system effects resulted in CSI values greater than 1 indicating that failures would occur. Here, design by using 3D structural analysis can be used to identify weak points that would be inadequately designed using traditional methods.

Gupta and Limkatanyoo (2008) also used SAP2000 to study system behaviour of trusses for complex roof geometries. The study also compared the design of the truss assemblies designed by traditional tributary area methods to design accounting for system effects. It was found that the trusses designed accounting for system effects sustained loads up to 10% less than traditional methods as the system based procedure accounts for the real tributary area of the truss. Additionally, stiffer trusses such as gable end trusses, 2 ply trusses and girder trusses attract more load and reduce the demand on adjacent trusses. Maximum CSI values could be reduced by up to 60% when accounting for system effects. However, in some cases CSI values were increased when accounting for system effects, such as for gable end trusses with a large tributary area. A limitation of this study is that the roof alone was modelled and realistic support conditions from stud walls were not modelled.

Shivarudrappa and Nielson (2012) used a FEM model with connections modelled as Non-linear link elements to study the load sharing effects of varying roof to wall connection stiffness. Similar to earlier findings by Wolfe and LaBissoniere (1991b); Increasing the stiffness of roof to wall connections decreased the amount of load sharing, and increasing the stiffness of sheathing increased the amount of load sharing.

Judd and Fonseca (2005), (2012) developed finite element models for fasteners in wood diaphragms under earthquake loading. Details of hysteresis behaviour of the nails were studied in depth. However, the structural system studied and the type of loading is not applicable to batten rafter connections under uplift wind loads.

Jacklin (2013) developed a FEM model, using SAP2000 for North American construction and validated it against displacement data from full-scale experiments by Morrison et al. (2012b). The model was used to aid the design of a retrofitting strategy involving running cables anchored to the ground on both sides of the house across the roof surface. Jacklin's thesis provides a good literature review on various retrofitting strategies or devices. However, only static loads are applied to the model.

Stevenson et al. (2017) conducted a damage survey of failures in trussed hip roof houses. Selected truss shapes are modelled using SAP2000 and demand capacity ratios for various members are calculated. However, nonlinear behaviour is not considered in this study.

The above-mentioned studies have shown that structural analysis models can be used to model complex load sharing behaviour in light framed timber structures. However, the complexity and the rigor to develop accurate models can be similar to conducting full-scale tests in some cases. Additionally, it is important that results are still validated using full scale testing.

One of the weaknesses of most FEM models is that the analysis mesh must generally remain a continuum. To model the failure and separation of elements and collision with other elements requires additional techniques such 'element erosion'. A newer method known as the 'Applied Element Method' (AEM) has been designed to model the separation and collision of elements (Meguro and Tagel-Din, 2002, Salem et al., 2011). The AEM has been used successfully in progressive collapse analysis of buildings and demolition planning as well as in several research applications.

2.7.4 Studies on Individual Connections and Fasteners

Connection failures, as opposed to member failures, are the critical failure mode in light framed timber construction. A considerable amount of research has examined the behaviour of individual connections to wind uplift loads. These include cladding to batten connections, batten to truss connections and truss to wall connections, i.e. the main connections in the vertical load path of a house.

Cladding Fasteners:

Research on metal cladding has primarily focused on its fatigue response to fluctuating wind loads. Studies by, Mahendran (1990),(1993),(2001) and Xu (1993) have examined this behaviour in detail. More recent studies by Henderson (2010) and Henderson and Ginger (2011) examine low cycle fatigue behaviour. Additionally, Henderson et al. (2009) compared standard fatigue tests to simulated fluctuated loading of a design cyclone. Recent studies have used innovative photogrammetry techniques for measuring the deformation of metal cladding and have used numerical modelling to analyse crack propagation from fastener locations.(Lovisa, Henderson, et al. 2013, Lovisa, Wang, et al. 2013).

Truss to wall connections:

Truss to wall connections are the most studied of roofing connections. These have taken place predominantly in the United States and for traditional toe-nailed connections. These types of studies have been more relevant to the current investigation as they often consider system effects of the roof structure as well.

Reed et al. (1997) studied both individual and system behaviour of toe nailed roof to wall connections. It was found that average failure capacity of connections within the system was higher than individual capacity of connections –indicating the level of load sharing.

Riley and Sadek (2003) compared the performance of toe-nailed roof to wall connections and hurricane clips for North American construction. Ellingwood et al. (2004) also compared toe-nailed connections and hurricane clips by performing a fragility analysis. This study also involved a sensitivity analysis of factors that influence the failure of roof to wall connections and wind speed was found to be the most significant.

Shanmugam et al. (2009) applied cyclic loads to toe nailed roof to wall connections and derived tri-linear load displacement models for these connections. An aim of the study was to quantify the energy dissipated through hysteresis by roof to wall connections. An FEM model of a toe-nail connection was also presented that was able to model strength and stiffness degradation. Energy dissipation behaviour of the analytical model was also able to predict the behaviour from the physical tests. However, this model used a cyclic loading sequence from ASTM D1761 (2006) and not time varying wind loads, thus energy dissipated during a wind storm could not be calculated.

Morrison and Kopp (2011) Applied realistic fluctuating wind loads to toe nailed connections using Pressure Load Actuators (PLAs). They observed that failure of connections occurred incrementally due to 'damaging peaks'. It was also found that the number of 'damaging peaks' a connection experienced was more significant than the magnitude of peaks. Additionally, mean failure capacity was not dependent on the loading rate. Similar findings were found by Rosowsky and Reinhold (1999).

Khan (2012) studied load sharing between roof to wall connections with fluctuating wind loads applied with a PLA and a customised bellows system. Bilinear and curvilinear models were fitted and various failure modes were observed and recorded. Noticeable hysteresis was observed in connections. The study also found that stronger connections (4 nails) could be subject to 33% higher loads redistributed from neighbouring connections. Weaker connections (2 nails) can shed up to 50% of load applied to it.

Additionally, the duration of wind loading was found to be significant, as a larger number of damaging peaks are required to cause failure in a stiffer roof system. A generally stiffer roof structure (interpreted to be stiffer cladding, battens and smaller truss spacing) results in more load sharing

Guha and Kopp (2014) also examined load sharing between toe nailed roof to wall connections subjected to realistic fluctuating wind loads. Loads were applied to individual connections using PLAs and bi-linear stress-strain curves defined for connections. An analytical procedure was used to evaluate the load sharing behaviour of a row of roof to wall connections. Similar to Khan (2012), The system behaviour of the roof was idealized as two steel beams that had the equivalent stiffness of the rest of the roof structure. The model is one of the few that is able to account for progressive failures of connections.

Batten to rafter connections:

Studies on batten to truss connections are less common, which may be because battens are not used in North American Construction. The Cyclone Testing Station conducted early research on capacities of timber batten to rafter connections; providing connection capacity data and recommendations for high wind areas in Australia (Reardon 1979b, a).

With the increased use of metal top hat battens, studies have examined the fatigue response of batten to truss connections. Ginger (2001), studied fluctuating loads on cladding fasteners and batten to truss connections based on full scale measurements from the Texas Tech building. Load cycles were examined using the rain flow counting method (Amzallag et al. 1994). It was found that similar fluctuations were experienced on both types of connections. Mahendran and Mahaarachchi (2002) and Fowler (2003) studied modern metal top hat battens under cyclic loading for fatigue effects.

Jayasinghe (2012) studied the behaviour of batten to truss connections and the effects of load redistribution upon localized failures in contemporary Australian construction. The structural elements studied were metal top hat battens connected to softwood trusses that supported a metal corrugated cladding. This study examined the load paths and load sharing between batten to rafter connections in the undamaged state, as well as when connections partly fail. However, progressive failure were not specifically examined.

The study showed that the traditional 'tributary areas' used for design of batten to rafter connections are un-conservative and proposed a larger area to be used. Influence coefficients for reactions of batten to rafter connections within this larger area are presented. Using the more accurate area of influence that was determined in the study it was found that different points in time and a different pressure distribution caused the maximum loads at connections. The effects of connection failure were also studied by the removal of screws of a connection and the new load paths created were noted.

Fragility curves of a grid of individual batten to rafter connections were presented. An alternate set of fragility curves were also presented that account for the failure of a neighbouring connection. There are some limitations in the curves presented as they do not account for load redistribution due to partial failure of connections. Additionally, the fragilities of individual connections cannot be presented in isolation, especially at higher wind speeds where the probability of failure of a connection would be dependent on the failure of other neighbouring connections. Another limitation of the study was that only quasi static loads were applied.

More recently, Boughton et al. (2014) presents a reliability study of batten to truss connections for a contemporary Australian house. Fragility curves for various connection fasteners were developed for different roof areas (corner, edge and general). This study analysed the probabilities of 'first failure' of connections but did not examine what may be occurring to neighbouring connections at the time of failure.

2.8 Combination Studies

Recent research on light framed construction has used a combination of methods including physical testing, finite element analyses, computational fluid dynamics (CFD) or wind tunnel testing. Often results from one analysis type are used as inputs for another. For example, wind pressures from CFD models are applied to a finite element structural analysis models.

Satheeskumar (2016) preformed full scale testing on s section of a contemporary Australian house to assess load sharing and load paths at different stages in construction, similar to earlier studies by Reardon and Henderson (1996). These construction stages were a bare frame, the addition of roof battens, the addition of cladding and finally with internal linings. Additionally, a detailed finite element model of a "triple-grip" connection was created as well as a separate finite element model of the same roof structure that was tested in full scale. Further to this, a detailed finite element model, incorporating behaviour of the first detailed connection model was created that showed good agreement with the full-scale test.

Connection tests found that gun nails were significantly weaker than hand nailed connections. Common construction defects change the uplift resistance between 10 and 40% compared to 'ideal' connections. Effects of such construction defects were studied using a finite element model of the house structure that was validated using the full scale testing data.

The study found that load sharing increases with additional structural elements throughout construction. More importantly, performance of triple grip connections are influenced by prying forces and reactions in three-dimensions that result from wind uplift pressures. However, the results of this model were also examined only in the undamaged or partially damaged state of the house i.e. without any complete failures of the connections.

Woldeyes et al. (2017) performed a study on progressive damage of cold formed light framed walls to spatially and temporally varying wind loads. Wind loads are determined using a CFD model and a detailed finite element model of the wall structure and sheathing is used to determine the structural response. The analysis software ABACUS was used. Connections were modelled with linear or nonlinear springs. A special emphasis was placed on analysing the buckling and post buckling behaviour of the cold formed wall studs. The CFD model may not have captured the temporal variations of the pressure, especially for peak loads.

He, Pan, Cai, Habte, et al. (2018) and He, Pan, Cai, Chowdhury, et al. (2018) studied nonlinear structural response to spatial and temporally varying wind loads. A 1/4 scale mode of a building was tested at the 'Wall of Wind' testing facility at Florida International University under severe wind speeds and wind pressures across the roof recorded. Instrumentation also recorded structural response such as deflections and lateral movements of the structure.

The scale model study was used to validate a detailed finite element model of the same building that was able to successfully represent load sharing behaviour in the linear and non-linear ranges. Although this model is perhaps capable of examining progressive failures, these failure modes are not studied in detail. The structural system studied is a North American style structural system, with the use of sheathing panels instead of battens and corrugated cladding typically used in Australia.

Tan and Hernandez (2017) present a study on progressive failures of several roofing connections for a Philippine school building. A CFD model is used to determine spatial and temporally pressures, these are applied to a SAP2000 model. Regions that fail are then removed in the CFD model and pressures updated in SAP2000. This in controlled by MATLAB® using open application programming interface (OAPI) features. It is not clear if nonlinearity is modelled in SAP2000, additionally the CFD model is unlikely to model peak events as well as a wind tunnel.

2.9 Summary of Previous Research

Research in light framed timber construction has taken many forms, including full scale testing of houses, model scale tests, analytical models and detailed studies into individual connections. A large amount of research has been conducted using full-scale experiments to quantify load sharing within the structural system. However, it is only with recent advances in equipment such as PLAs that some researchers have been able to capture the highly fluctuating nature of wind loads on the roof surface. Additionally, most of these studies, apart from that of Boughton (1988) have not examined progressive failures in the roof structure by destructive testing.

Structural analysis models have been able to capture the complex behaviour of light framed timber structures; however, considerable effort is required to create accurate models. These analytical models are not a replacement for full scale testing, as they must be validated from such experiments. Most models do not account for the effects of failure and disconnection of connections – a requirement for modelling progressive failures.

Research on individual connections has largely involved testing of toe-nailed roof to wall connections in North American structural systems. Only recent studies such as those by Morrison and Kopp (2011), Khan (2012) and Guha and Kopp (2014) have considered the effect of fluctuating time history loads on the connections. None, to the author's knowledge have performed similar tests on connection products commonly used in Australia.

The response of cladding to batten and batten to truss connections has also been examined by several researchers. The majority of the recent studies have focused on the behaviour of these fasteners due to fatigue. The application of time history loads to batten to truss connections has been examined by Ginger (2001) and the effects of load redistribution due to failure have been studied by Jayasinghe (2012) using static loads. However, the combined effects of fluctuating load on load redistribution and progressive failures are yet to be addressed.

Current gaps in research include:

- Limited work on progressive or cascading failures.
- Analytical models generally do not model the complete failure of connections
- Limited work using spatial and temporally varying wind loads
- Limited work on individual connections used in Australia subject to realistic time history wind loads.

This thesis analyses progressive failures due to wind loads in Australian light framed timber houses through physical testing and structural analysis. Physical testing of connections was used to build a description of their structural response to fluctuating wind loads such that their behaviour can be modelled in analysis software. A non-linear Finite Element Model was used to simulate the strength loss and disconnection of fasteners and to study progressive failure mechanisms within the roof structure. Outcomes of this research will enable the development of vulnerability models, building standards and techniques for retrofitting older structures.

3 WIND PRESSURE FLUCTUATIONS

This Chapter presents a 1/50 scale wind tunnel model study conducted on a rectangular plan gable roof house to record spatial and temporal pressure data. A study of the correlations of pressures at neighbouring batten to rafter connections and the movement of eddies and vortices across the roof was performed to understand the loading process that batten to rafter connections are subjected to during a windstorm. The cross-correlation between load time histories was used to give a measure of synchrony between loads experienced at neighbouring connections and indicate the direction that fluctuations move across the roof.

An additional output of the wind tunnel study includes the determination of a 95th percentile 'peak event' in the pressure time history for testing connections under dynamic loads. These time history records were then used for connection testing and time-history structural analysis presented in Chapters 4 and 5.

3.1 Wind Tunnel Tests

A wind tunnel study to determine simultaneous loads at batten to rafter connections of a typical roof system was conducted. Tests were carried out in the 2.0m high × 2.5m wide × 22m long boundary layer wind tunnel at the James Cook University Cyclone Testing Station, in Townsville Australia.

The approach wind flow simulated at a length scale (L_r) of 1/50 was that of a suburban environment using an array of 50mm tall blocks on the upstream fetch of the wind tunnel. A Turbulent Flow Instruments (TFI) 'Cobra Probe' was used to measure the approach wind velocity and turbulence intensity at various heights (z) above the floor of the tunnel. The measured profiles and those specified in the Australian wind loading standard (AS/NZS 1170.2 - 2011) for terrain category 3, as well as the power spectrum at mid roof height are shown in Figure 3.1. The length scale of the modelled turbulence shown in Figure 3.1c) indicates that the fluctuating velocities have energy at higher frequencies, and match an approach flow at a scale of ~1/400. This limitation of the available wind tunnel facility does not significantly influence the results and the applications of this study, as the local pressures measured on the surface of the wind tunnel model are most affected by building induced turbulence rather than the larger scale fluctuations that could not be modelled at 1:50 scale.
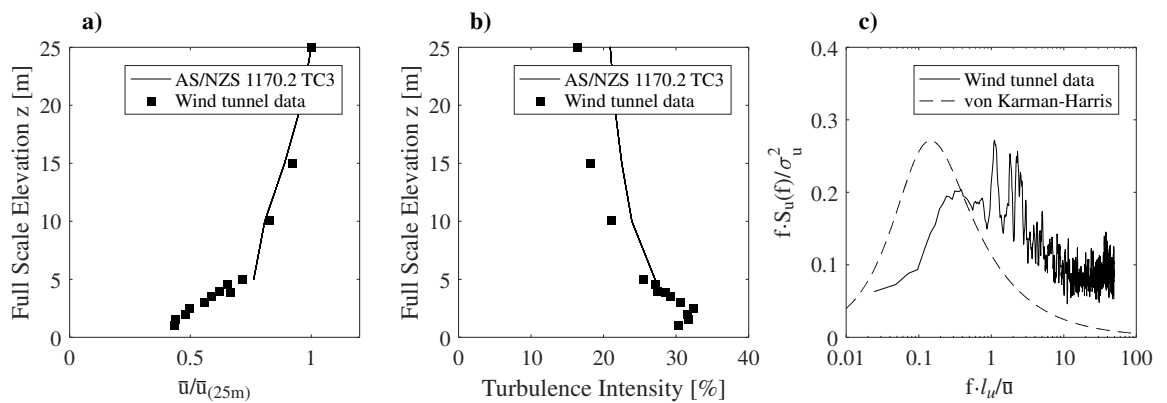
Figure 3.1: a) Mean velocity and b) turbulence intensity profiles of the atmospheric boundary layer simulated at a length scale of 1/50 in the wind tunnel. c) Power spectral density at mid roof height

A 1/50 scale model of a rectangular plan, gable roof house, represented in Figure 3.2, was used for this study. Based on survey data from Jayasinghe (2012) the model is of a 19.8m long by 10m wide house with a 22.5˚ roof pitch. Ninety-eight (98) pressure taps were installed on a study area, shown in Figure 3.3, to capture the spatial and temporally varying pressures near the gable end section of the house. Pressure taps were arranged in a 450×439mm (full-scale) grid pattern such that the 900×877mm tributary area of each batten-rafter connection would contain four pressure taps. The model was placed on a turntable in the wind tunnel and pressure time histories $p(t)$ were measured at each tap for wind directions θ in 10° increments.

Rafters and battens are spaced at 900mm and 877mm respectively, supporting metal sheet cladding. As shown in Figure 3.3, rafters and battens are labelled as T1, T2…Tn and B1, B2…Bn, respectively. Batten to rafter connections that were studied are labelled based on the batten-rafter intersection T1-B3, T3-B4, etc. within the study area.
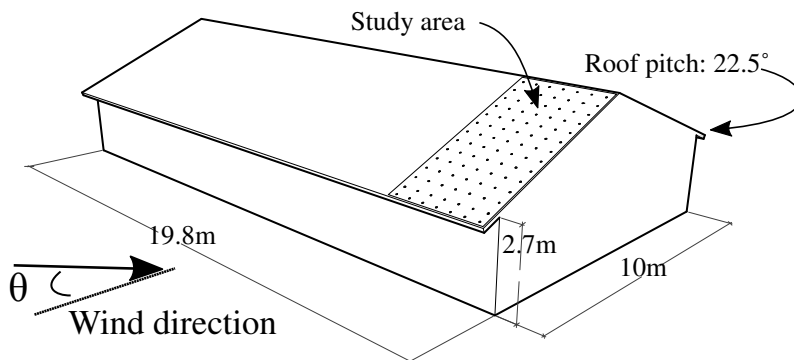
Figure 3.2 Study area on the roof of the 19.8 × 10m gable end house with roof pitch of 22.5˚ modelled in the wind tunnel.
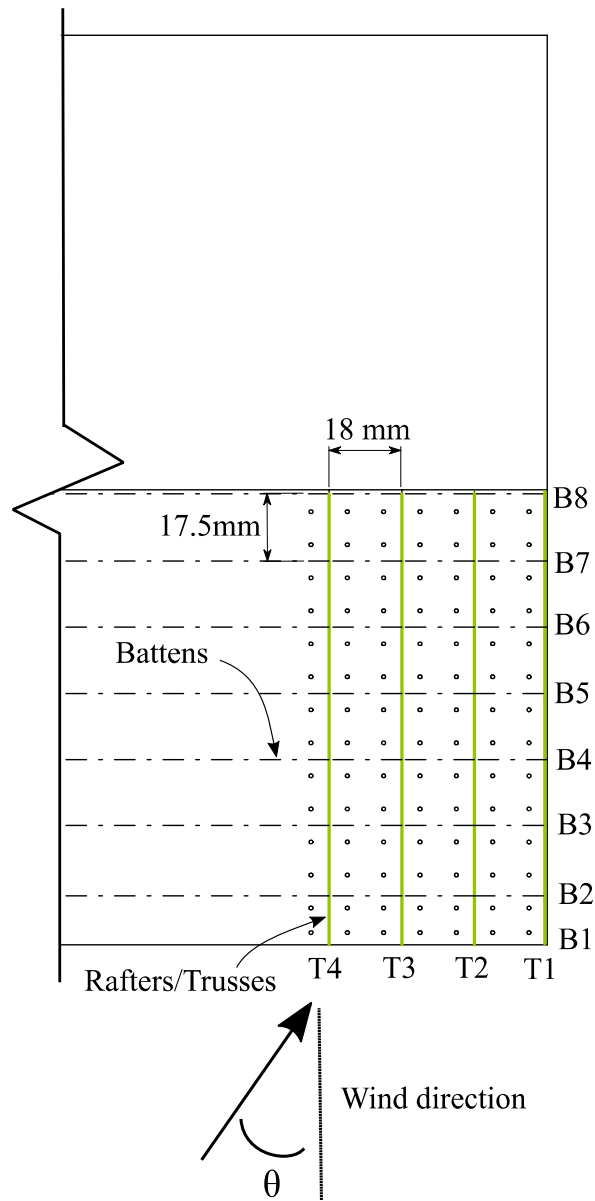
Figure 3.3 Tap layout and framing plan within the study area on the roof of the 1/50 scale wind tunnel model.

Pressure taps were connected to TFI pressure transducers and data acquisition system using a tuned tubing system. Pressure signals were low-pass filtered at 500 Hz and sampled at 1000Hz for 24 runs of 30s model scale (10 minutes full scale) for each wind direction.

Pressures measured are represented as pressure coefficients $C_p(t) = \frac{p(t)}{\frac{1}{2}\rho\overline{U_h}^2}$ referenced to the mean dynamic pressure at mid roof height of the wind tunnel model. Peak pressures are taken as the average of the maximum/minimum pressures of the 24 runs (ensemble average). The maximum, minimum, mean and standard deviation pressure coefficients are given by:

$$\widehat{C_p} = \frac{\hat{p}}{\frac{1}{2}\rho\overline{U_h}^2}, \qquad \widecheck{C_p} = \frac{\check{p}}{\frac{1}{2}\rho\overline{U_h}^2}, \qquad \overline{C_p} = \frac{\bar{p}}{\frac{1}{2}\rho\overline{U_h}^2}, \qquad C_{\sigma p} = \frac{\sigma_p}{\frac{1}{2}\rho\overline{U_h}^2} \qquad\qquad Eq.\ 3.1$$

Where,

- $\hat{p}, \check{p}, \bar{p}, \sigma_p$ are the maximum, minimum, mean and standard deviation of external pressures on the wind tunnel model.
- $\overline{U_h}$ is the mean wind speed at mid-roof height (h) of the wind tunnel model
- ρ is the density of air

Furthermore, dimensional analysis was applied to determine the relation of model scale to full scale pressures signals. Model scale pressure and load time histories were scaled to full scale using the relation between Time (*T*) Length (*L*) and velocity (U) given in Equation 3.2.

$$T_r = \frac{L_r}{U_r} \qquad\qquad Eq.\ 3.2$$

Where the subscript r denotes the ratio of model to full scale measurements. Thus, the frequency (*f*) ratio is given by:

$$f_r = \frac{1}{T_r} = \frac{U_r}{L_r} \qquad\qquad Eq.\ 3.3$$

The mean velocity in the wind tunnel was set at nominally 11m/s at z = 500mm height. For a velocity ratio (U_r) of 2.5, corresponding to about 100km/h (27.7 m/s) in full scale, the length scale (L_r) of 1/50 gives a time ratio (T_r) of 1/20. Thus, 1/500 second time steps recorded at model scale represent 0.04 s in full-scale and each 30s run is equal to 10minutes full scale.

Pressures that influence loads on batten-rafter connections could be determined by taking the average pressure of taps within the tributary area of the batten to rafter connection. For most connections, this was four pressure taps, for connections on the roof edges, two taps, and one tap for corner connections. It should be noted that the tributary areas of edge and corner connections are about 1/2 and 1/4th that of typical internal connection. As described by Jayasinghe (2012), loads at a batten to rafter connections are influenced by pressures applied to an area larger than traditionally considered as a tributary area. However, the correlation of pressures that affect the connections can still be analysed using pressures that act on a traditional tributary area.

3.2 Pressure Distributions

Plots of the mean, minimum and standard deviation of batten-rafter connection pressures coefficients (C_p) of the 24 ten-minute runs for selected wind directions (θ) are shown in Figure 3.4. Pressure distributions show that the highest negative pressures occur near roof edges and the ridgeline.

The critical connection T2-B7 experiences large uplift forces for a range of wind directions and is subject to especially high loads for wind directions 210˚ to 240˚, the critical sector. The highest uplift forces at the critical connection arise from wind direction 210˚. Connections at roof corners and the apex of the gable end experience the highest peak loads for cornering winds. High uplift loads occur in 'peak events' of load more than 3.5 standard deviations from the mean lasting for about 0.5 to 2.0 s for a mean wind speed of 100 km/h at full scale.

Wind Direction

$\breve{C}_p$

0°				90°				180°				210°				270°				300°			
-1.5	-1.4	-1.5	-2.0	-1.3	-1.2	-1.1	-0.9	-1.9	-1.9	-2.2	-2.4	-5.1	-6.5	-8.1	-11	-3.7	-4.1	-4.7	-5.3	-3.1	-3.7	-4.5	-5.9
-1.0	-1.0	-1.2	-1.7	-0.9	-0.9	-0.8	-0.7	-1.9	-2.0	-2.1	-2.3	-4.7	-4.8	-5.0	-11	-3.2	-3.8	-4.3	-4.7	-2.9	-3.4	-4.4	-5.2
-0.8	-0.9	-1.1	-1.6	-0.8	-0.8	-0.8	-0.7	-2.0	-2.1	-2.1	-2.3	-3.8	-3.6	-4.7	-7.3	-3.1	-3.8	-4.4	-4.5	-2.7	-3.4	-4.4	-5.0
-0.7	-0.8	-1.0	-1.6	-0.7	-0.8	-0.8	-0.7	-2.1	-2.1	-2.1	-2.4	-3.2	-3.2	-4.6	-5.2	-3.1	-3.8	-4.4	-4.5	-2.6	-3.6	-4.4	-4.7
-0.7	-0.8	-0.9	-1.7	-0.8	-0.8	-0.7	-0.7	-2.1	-2.1	-2.0	-2.7	-2.7	-3.2	-4.1	-4.1	-3.0	-3.8	-4.5	-4.7	-2.1	-3.5	-4.6	-4.9
-0.8	-0.9	-1.0	-1.7	-0.7	-0.8	-0.7	-0.7	-2.0	-2.0	-1.8	-2.7	-2.5	-3.1	-4.3	-3.2	-2.9	-3.6	-4.3	-5.1	-1.6	-2.8	-4.3	-5.4
-1.5	-1.6	-1.4	-1.8	-0.9	-0.9	-0.8	-0.8	-2.1	-2.0	-1.9	-2.5	-2.4	-2.8	-2.9	-2.9	-2.9	-3.2	-3.9	-5.7	-1.7	-2.2	-3.4	-5.6
-2.1	-2.6	-2.9	-3.4	-1.1	-1.3	-1.4	-1.3	-2.5	-2.7	-2.6	-3.0	-2.0	-2.2	-2.6	-3.1	-2.9	-3.4	-3.9	-4.9	-1.9	-2.3	-2.6	-4.0

$\overline{C}_p$

0°				90°				180°				210°				270°				300°			
-0.4	-0.4	-0.4	-0.3	-0.1	-0.1	-0.2	-0.2	-0.6	-0.6	-0.6	-0.7	-1.8	-2.1	-2.7	-2.8	-0.8	-1.1	-1.3	-1.3	-0.8	-1.0	-1.3	-1.6
-0.2	-0.2	-0.2	-0.2	-0.1	-0.1	-0.2	-0.2	-0.6	-0.6	-0.7	-0.7	-1.7	-1.8	-1.7	-3.3	-0.8	-1.1	-1.3	-1.3	-0.4	-0.7	-1.1	-1.4
0.0	0.0	-0.1	-0.1	-0.1	-0.1	-0.2	-0.2	-0.6	-0.7	-0.7	-0.6	-1.3	-1.2	-1.5	-2.6	-0.8	-1.1	-1.3	-1.2	-0.3	-0.5	-1.0	-1.2
0.1	0.0	0.0	-0.1	-0.1	-0.1	-0.2	-0.2	-0.6	-0.6	-0.7	-0.6	-1.0	-1.0	-1.6	-2.0	-0.8	-1.1	-1.3	-1.2	-0.1	-0.4	-0.8	-1.1
0.1	0.1	0.0	-0.1	-0.1	-0.1	-0.1	-0.2	-0.6	-0.7	-0.7	-0.6	-0.8	-0.9	-1.5	-1.6	-0.7	-1.1	-1.3	-1.3	-0.1	-0.2	-0.7	-1.1
0.2	0.1	0.0	-0.1	-0.1	-0.1	-0.2	-0.1	-0.6	-0.6	-0.6	-0.6	-0.7	-0.9	-1.7	-1.2	-0.6	-1.0	-1.4	-1.4	0.0	-0.1	-0.7	-1.1
0.1	0.1	0.1	-0.1	-0.1	-0.1	-0.1	-0.2	-0.6	-0.6	-0.6	-0.6	-0.7	-0.9	-1.1	-1.0	-0.6	-0.7	-1.1	-1.6	0.0	-0.1	-0.1	-0.8
0.0	-0.2	-0.3	-0.3	-0.1	-0.1	-0.2	-0.2	-0.6	-0.7	-0.6	-0.6	-0.7	-0.8	-0.9	-0.9	-0.6	-0.8	-0.9	-1.2	-0.1	-0.3	-0.3	-0.3

C_{σ_p}

0°				90°				180°				210°				270°				300°			
0.2	0.2	0.2	0.2	0.1	0.1	0.1	0.1	0.2	0.2	0.2	0.3	0.6	0.7	1.0	1.3	0.4	0.5	0.5	0.6	0.4	0.4	0.5	0.6
0.2	0.2	0.2	0.2	0.1	0.1	0.1	0.1	0.2	0.2	0.2	0.3	0.6	0.6	0.6	1.4	0.4	0.5	0.5	0.5	0.3	0.4	0.6	0.6
0.2	0.2	0.2	0.3	0.1	0.1	0.1	0.1	0.2	0.2	0.2	0.3	0.5	0.5	0.6	0.9	0.4	0.5	0.5	0.5	0.3	0.5	0.6	0.6
0.2	0.2	0.2	0.3	0.1	0.1	0.1	0.1	0.2	0.2	0.2	0.3	0.4	0.4	0.6	0.7	0.4	0.5	0.5	0.5	0.2	0.5	0.7	0.6
0.3	0.3	0.3	0.3	0.1	0.1	0.1	0.1	0.2	0.2	0.2	0.3	0.3	0.4	0.5	0.5	0.4	0.5	0.5	0.5	0.2	0.4	0.7	0.7
0.3	0.3	0.2	0.3	0.1	0.1	0.1	0.1	0.2	0.2	0.2	0.3	0.3	0.4	0.5	0.4	0.4	0.5	0.5	0.6	0.2	0.3	0.5	0.8
0.4	0.4	0.3	0.4	0.1	0.1	0.1	0.1	0.2	0.2	0.2	0.3	0.3	0.3	0.3	0.3	0.4	0.4	0.5	0.7	0.2	0.3	0.4	0.7
0.4	0.5	0.5	0.5	0.1	0.1	0.1	0.1	0.3	0.3	0.3	0.3	0.2	0.3	0.3	0.3	0.4	0.4	0.4	0.6	0.3	0.3	0.4	0.5

Figure 3.4 Minimum (top row) mean (middle) and standard deviation (bottom) pressure coefficients for the 32 connections in the study area for selected wind directions. The black square indicates the location of the critical connection for wind direction 210˚.

3.3 Patterns of High Suction Pressure

Wind loads on roof surfaces fluctuate rapidly in space as well as through time. These high load areas are transient and move across the roof rapidly due to the formation of eddies and vortices. These fluctuations can result in high loads occurring at different batten to rafter connections, and at different times.

Regions of high suction pressure on the roof surface occur due to different aerodynamic mechanisms such as flow separation and the formation of transient eddies and vortices. Thus, the timing, duration, location and correlation of the 'peak events' vary with wind direction. A description of the patterns of fluctuating pressures that result in 'peak events' for selected wind directions are presented in this section. Directions selected are those within the critical sector that produce high uplift loads due to different aerodynamic behaviours, wind directions 180°, 210°, 270° and 300° are analysed in detail in the following pages.

For the direction 180°, the study area lies on the leeward roof slope. Large negative pressures are experienced due to 2-dimensional flow separation as air moves over the discontinuity of the ridgeline. High negative pressures occur close to the ridgeline in the area of flow separation. However, the vortices and eddies generated periodically 'roll up' and are convected down the leeward roof slope, similar to that observed by Saathoff and Melbourne (1997). The movement of these eddies creates bands of high negative pressures that travel down the roof slope repeatedly as shown in Figure 3.5. Thus, 'peak events' at connections can occur over a large area of the leeward roof slope as shown in Figure 3.6.
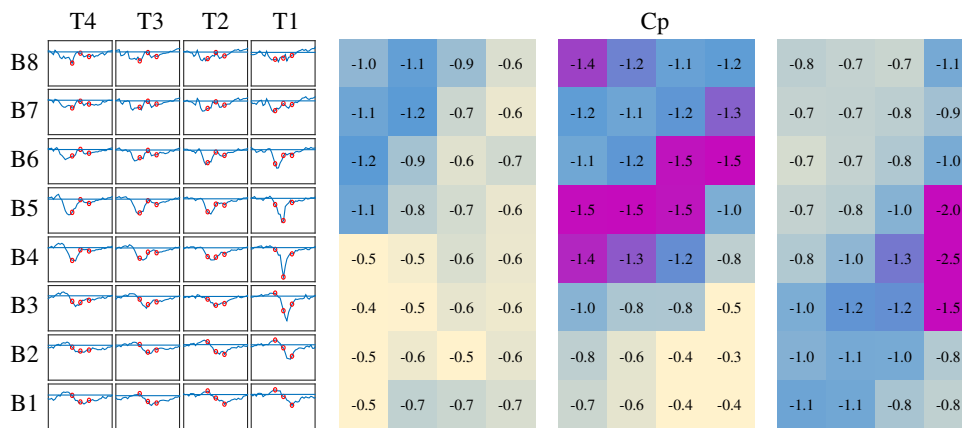
Figure 3.5 (Left): Two-second time histories of pressures at connections (arbitrary scale) for wind direction 180°. (Right): Selected time steps (encircled on left) are shown as colour scale diagrams on the right, showing the rolling peak event region on the leeward roof.
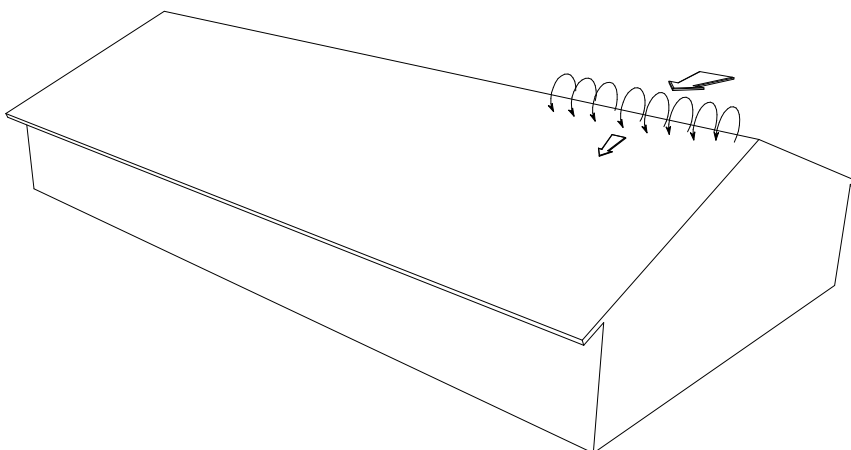
Figure 3.6 Schematic showing the moving vortex for wind direction 180°

For the critical wind direction 210°, high uplift loads are experienced at the ridgeline and near the gable end of the roof. High negative pressures are experienced here consistently throughout time. High standard deviations in the pressure signals at the apex of the roof indicate that additional building induced turbulence is being created in this area. Large suction pressures occur in a diagonal band extending from the apex of the roof diagonally down the roof slope at an angle of 10° to 30° measured from the gable end, shown in Figure 3.7. This diagonal high load area is caused by the formation of conical vortices, shown in Figure 3.8, as evidenced by its shape and angle on the roof surface. For connections in the diagonal band, high loads are experienced at similar times at connections along battens.
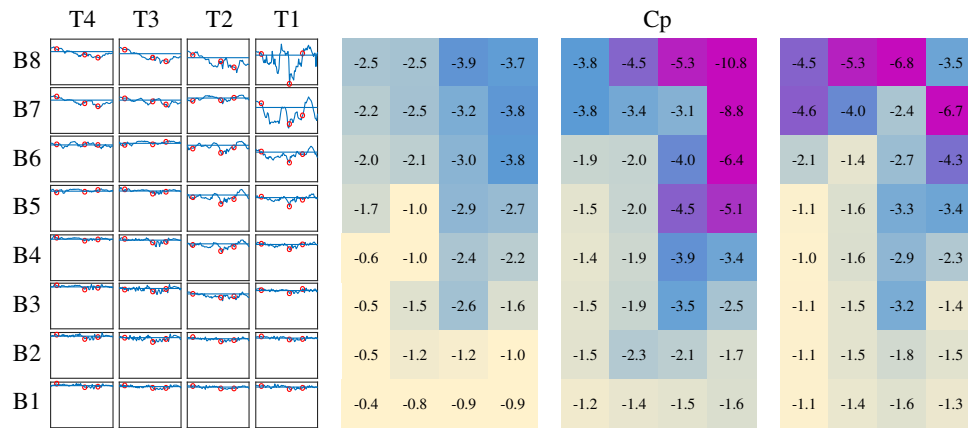
Figure 3.7 (Left): Five second time histories of pressures at connections (arbitrary scale) in the study area during a peak event for wind direction 210°. (Right): selected time steps (encircled on left) showing the evolution of a peak event on the roof surface.
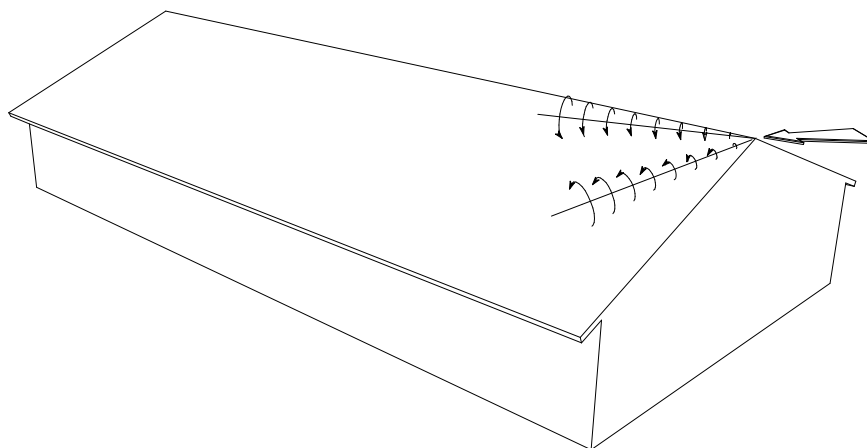
Figure 3.8 Schematic showing the conical vortices formed for wind direction 210°

For wind direction 270°, the airflow is perpendicular to the gable end of the house. Building induced turbulence is caused by the edge of the gable end where the flow is forced to separate. Additionally, due to the 22.5° roof slope, airflow travelling up the gable end must travel further up the windward wall closer to the ridgeline than when nearer to the eaves. Thus, vortices formed at this wind direction are more disrupted than those from 180° and form at different locations along the gable end at different times. At this direction, peak loads can occur over a wide range of locations, as shown in Figure 3.9. Here, high load areas occur in patches that move along the crosswind roof slopes from the windward edge as shown in Figure 3.10.

	T4	T3	T2	T1		Cp										
B8					-0.7	-0.1	-0.4	-2.3	-0.3	-0.5	-0.8	-1.6	-0.5	-0.9	-1.1	-2.9
B7					-0.4	-0.1	-1.4	-1.7	-0.3	-0.6	-1.2	-1.8	-0.4	-0.7	-1.1	-2.2
B6					-0.3	-0.7	-1.5	-1.5	-0.3	-0.7	-1.7	-1.7	-0.5	-0.8	-1.5	-1.9
B5					-0.2	-0.4	-1.2	-2.3	-0.5	-0.6	-1.8	-1.7	-0.6	-1.0	-1.6	-2.0
B4					-0.3	-0.4	-0.7	-3.0	-0.5	-0.6	-1.8	-1.8	-0.6	-0.9	-1.3	-1.3
B3					-0.5	-0.6	-0.8	-1.3	-0.5	-0.6	-1.2	-1.5	-0.6	-0.7	-1.0	-1.2
B2					-0.6	-0.7	-0.9	-0.9	-0.8	-0.6	-1.0	-1.4	-0.5	-0.6	-0.9	-1.2
B1					-0.8	-0.8	-0.8	-0.9	-0.6	-0.7	-0.7	-0.9	-0.5	-0.7	-0.7	-0.4
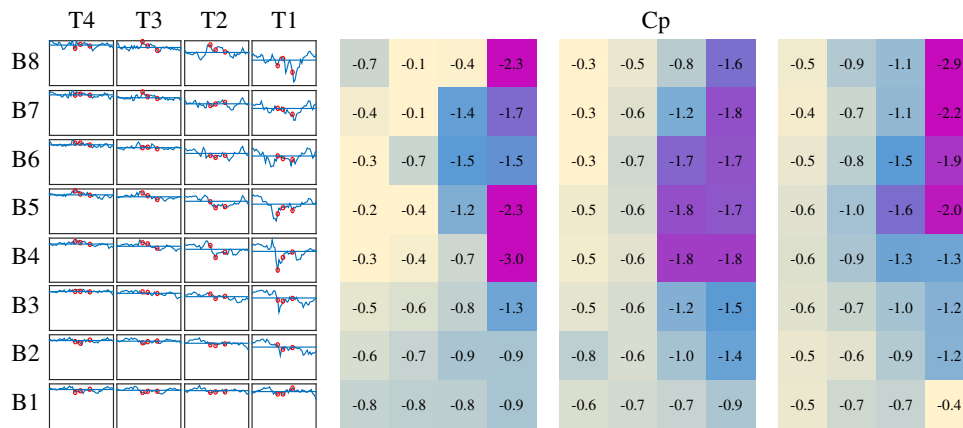
Figure 3.9 (Left): Two second time histories of pressures at connections (arbitrary scale) in the study area during a peak event for wind direction 270°. (Right): Successive time steps (encircled on left) showing movement of high load areas along the gable roof edge.
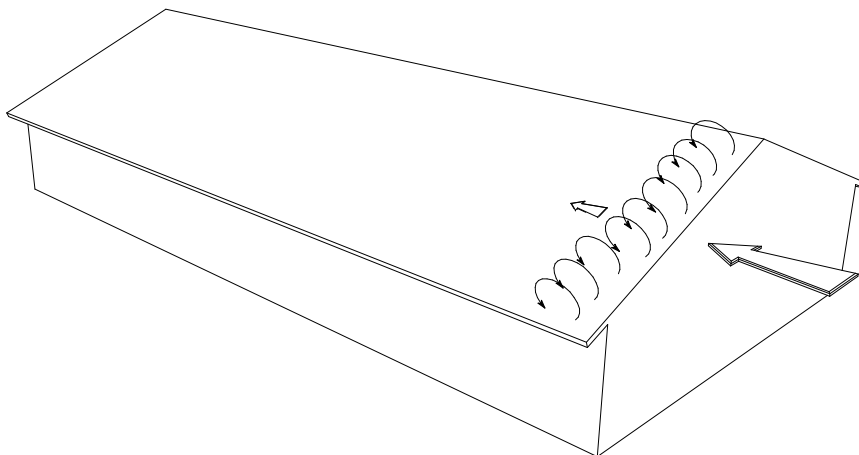
Figure 3.10 Schematic showing the disrupted, less correlated vortex at the gable end for wind direction 270°

For the cornering wind direction 300° the airflow is incident on the windward slope roof corner, high loads occur on several locations on the windward roof slope, shown in Figure 3.11. Flow separation occurs as wind moves over the gable end of the house causing high suction pressures near the gable roof edge. Additionally, a conical vortex forms at the roof corner resulting in peak load areas in a diagonal band that extend from close to the roof corner at an angle 10° to 45° measured from the gable end, shown in Figure 3.12. The interaction between this vortex and the flow separation over the gable end result in the high load area band intermittently moving upwards along the windward roof slope. To the left of the high load area with respect to the flow direction, the airflow is incident on the eaves and the windward roof slope and results in small positive pressures being applied on the roof surface.

	T4	T3	T2	T1					Cp							
B8					-0.6	-2.4	-2.0	-1.9	-1.2	-1.1	-1.6	-1.5	-0.9	-1.7	-1.9	-1.8
B7					-0.1	-1.8	-2.0	-1.6	-2.0	-1.4	-1.8	-1.7	-0.8	-1.5	-2.1	-2.0
B6					0.0	-1.4	-1.9	-1.3	-2.3	-2.0	-1.9	-1.8	-0.5	-1.1	-2.2	-1.9
B5					-0.1	-1.1	-1.3	-1.3	-1.3	-3.2	-2.5	-2.0	-0.4	-1.3	-1.9	-1.7
B4					-0.1	-0.8	-1.6	-1.3	0.2	-2.1	-3.1	-2.7	-0.2	-0.9	-2.0	-1.8
B3					-0.1	-0.1	-2.1	-2.3	0.2	-0.1	-3.4	-3.2	-0.1	-0.5	-1.9	-2.1
B2					-0.2	-0.2	-0.7	-2.3	-0.1	0.2	-1.9	-5.2	0.0	-0.2	-0.7	-1.5
B1					-0.4	-0.6	-0.5	-0.6	-0.1	-0.2	-0.4	-0.8	-0.1	-0.4	-0.5	-0.4
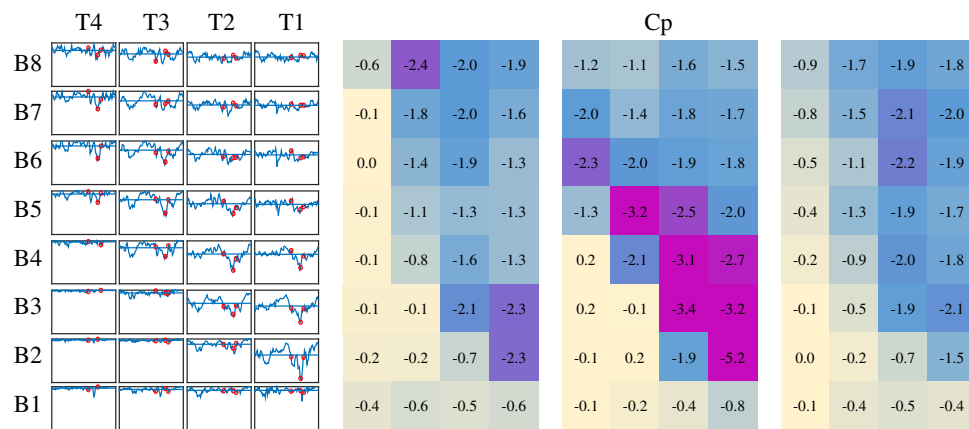
Figure 3.11 (Left): Five second time histories of pressures at connections (arbitrary scale) in the study area during a peak event for wind direction 300°. (Right): Successive time steps showing different types of high load areas for this wind direction possibly due to the formation of a conical vortex.
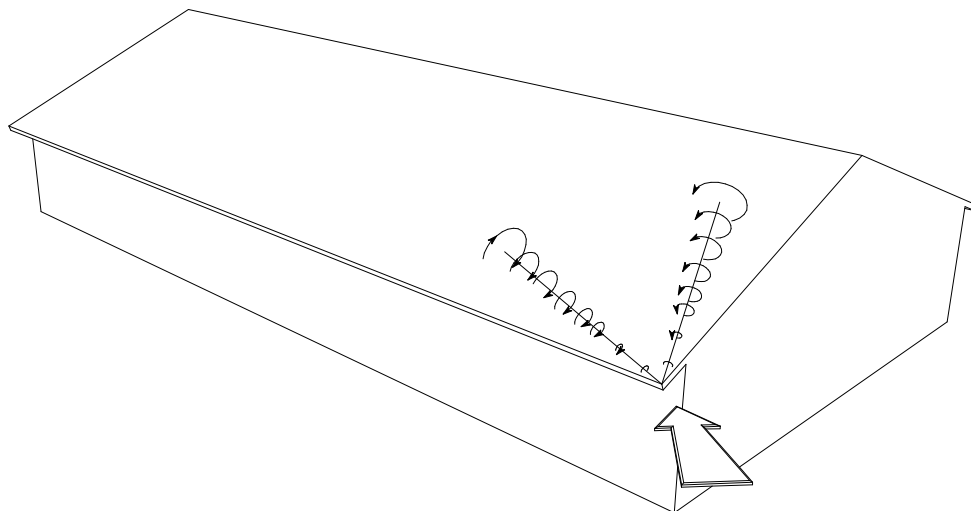
Figure 3.12 Schematic showing the conical vortices formed for wind direction 300°.

3.4 Correlation of Loads amongst Neighbouring Connections

If neighbouring connections experience high loads at the same time or near the same time, then a progressive failure is more likely to initiate as highly loaded connections may be subject to redistributed loads from adjacent connections that fail. The level of synchrony between time histories of load at neighbouring connections may influence the likelihood of a progressive failure occurring. Previous work has studied high pressures in the flow separation regions and the correlation of pressures under 2-dimensional separation bubbles and 3-dimensional conical vortices on bluff bodies, but not for assessing the initiation of failure in a light framed structure.

'Peak events' experienced at batten to rafter connections occur at different times as described in Section 3.3 . The location, size and intensity of these transient high load areas depend on wind direction. Some high load areas occur in approximately the same location for a given wind direction, others move across the roof surface due to the convection of vortices and eddies in the streamflow. The synchrony of peak events occurring at neighbouring connections can be related to the correlation coefficients of the pressures between these two connections. Correlations of temporal pressure fluctuations relative to the critical connection T2-B7 are presented in this section to illustrate different patterns of correlation amongst neighbouring connections.

3.4.1 Cross Correlation of Pressure Time-Histories

The synchrony of the signals can be related to the cross correlation of pressure time-history at two connections. The cross correlation coefficient as a function of lag time (τ) of one signal relative to the other is defined as:

$$r_{ij}(\tau) = \frac{1}{T * \sigma_{pi} * \sigma_{pj}} \int_0^T p_i'(t) * p_j'(t + \tau)\, dt \qquad \textit{Eq. 3.4}$$

Where,
- p_i' and p_j' are the fluctuating components of the pressure at locations i and j.
- σ_p is the standard deviation of fluctuating pressure
- T is the time over which the signal is analysed
- t is the time increment
- τ is the lag or lead time that the signal at j is shifted relative to i.

Pressures at connections are most correlated to that of the critical connection with small lead or lag times, indicating that pressure fluctuations arrive at connections slightly before or after they arrive at the critical connection.

Plots of correlation coefficient vs lag time show patterns of correlation among connections, indicating which connections are more correlated with loads on the critical connection and the lag or lead-time that causes the maximum correlation. Figure 3.13 shows the mean correlation coefficient of the 24 runs (T = 10 min each) vs. lag time for a 3×3 grid of connections surrounding the critical connection T2-B7 for wind directions 180°, 210° and 270°, where T2-B7 experiences large uplift loads. Additionally, this figure also shows colour scale plots for all connections in the study area of the correlation coefficient at zero lag time as well as the lead or lag time that results in the maximum correlation to T2-B7, to better represent the spatial distribution of correlation patterns on the roof surface for different wind directions.

For wind directions 180° to 200°, the connections studied are in the 2-dimensional separation region behind the ridgeline. Loads are highly correlated with connections to the left and right, along batten rows, shown in Figure 3.13a. Connections further along the downwind slope experience fluctuations at a lag time of about 0 to 0.36s full scale due to the convection of vortices along the leeward roof. However, even though correlations of peak loads at connections for wind directions 180° and 200° are the highest, the magnitude of the peak pressures are less than 50% at the critical connection T2-B7 for the critical direction 210°. Although the magnitude of peak pressures is significantly lower than for other wind directions (shown in Figure 3.14), the higher correlation along battens may make the roof more susceptible to progressive failures for these wind directions.

For the critical sector, 210° to 240°, loads are less correlated among the connections in the study area. Loads at connections diagonally downwind from the critical connection are the most correlated, shown in Figure 3.13b. Lag times of maximum correlation indicate that pressure fluctuations also move diagonally down the roof. Of note is that load time histories at connections immediately to the left and right of the critical connection are less correlated than several connections lower down the roof.

For wind directions 250° to 270°, the correlations increase. As the wind direction approaches 270°, perpendicular to the gable end, distinct bands of high correlation of loads amongst connections along each rafter/truss can be observed, shown in Figure 3.13c. Lag times of maximum correlation indicate that the fluctuations arrive at connections on each rafter slightly after each other.
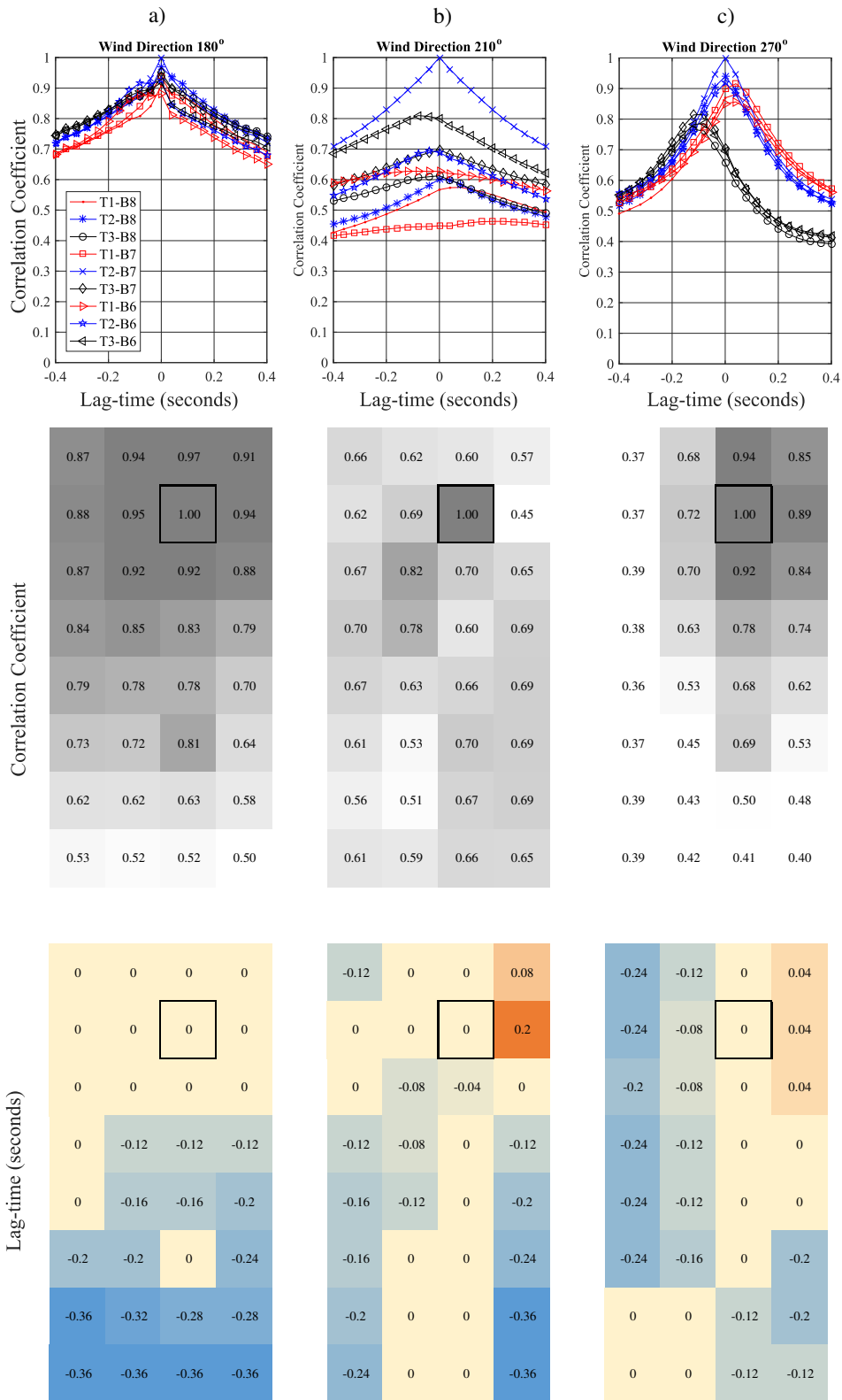
Figure 3.13: Top row: Correlation coefficient with respect to T2-B7 vs. lag time for a 3×3 grid of connections surrounding T2-B7. Middle row: Correlation coefficients with respect to T2-B7 at zero lag time for all connections in the study area. Bottom row: lag/lead time (s) that results in the maximum correlation at T2-B7.
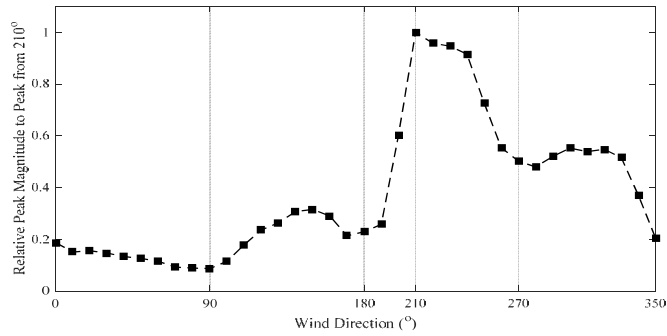
Figure 3.14 Magnitude of peaks relative to the peak caused by wind direction 210˚ for load at connection T1-B8, showing the critical sector 210˚ to 240˚.

Additionally, to examine the correlations during peak events only, local minima in the load history at the critical connection (T2-B7) were identified programmatically using an in-built MATLAB® function based on certain characteristics: peaks higher than 3.5 standard deviations from the mean with a minimum spacing of 100 time-steps. For each peak event, the signal for 1.0 s before and after the peak was selected and the cross-correlation given in Eq. 3.4 calculated for that duration. The mean values of the correlation coefficient for peaks in all 24 runs for each increment of lag/lead time were calculated. This procedure allows for the correlation of the signal slightly before and after the peak event to be examined, not simply when the signal exceeds a certain threshold. These conditional cross correlations are generally less than those calculated for the full ten-minute signal, and the magnitude of correlation drops rapidly with increasing and decreasing lag time, shown in Figure 3.15. However, similar patterns of correlations are observed for both conditionally sampled signals and full signals.
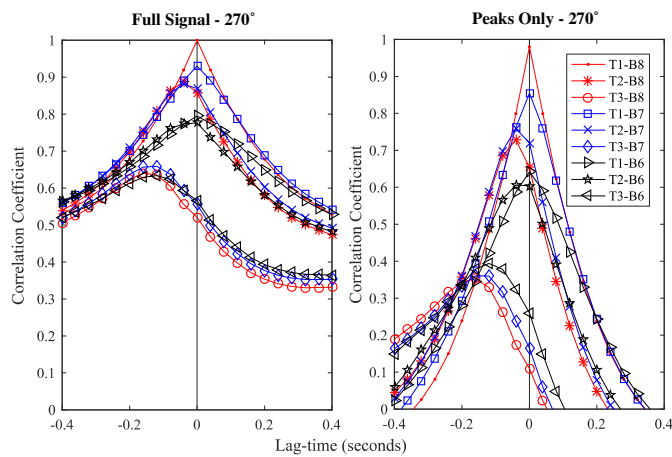
Figure 3.15 Correlation coefficient to connection T1-B8 vs. lag time for wind direction 270˚ for 10 minute runs (left) and during peak events only (right).

Lag and lead times indicate the time it takes for peak wind loads to be felt at a neighbouring connection relative to the critical connection. For immediate neighbouring connections, this lag or lead time ranges from 0.0 to 0.2 s and are of shorter duration than peak events themselves, which are between 0.5 to 2.0 s duration in full scale. Thus, neighbouring connections would still be experiencing high suction pressures even though the maximum uplift of peak events occurs at slightly different times at each connection.

Some wind directions generate loads that are more correlated along batten rows, e.g. 180°, and others correlated along trusses/rafters e.g. 270°. This may have implications on the initiation of progressive failures as they are influenced by the directions that loads are redistributed when a connection fails. Wind directions such as 270° where loads are correlated parallel to trusses/rafters may be vulnerable to progressive failures of roof cladding, as loads will be redistributed parallel to the cladding corrugations. Wind directions 270° and 180° degrees may cause batten to rafter connections to be vulnerable to progressive failures depending on the cladding and batten stiffness and their spacing.

Additionally, pressure fluctuations for wind directions that cause the highest loads at connections e.g. 210° are significantly less correlated than others. This indicates that wind directions that are conducive to the initiation of a progressive failure of batten to rafter connections may not be those that cause the highest loads at connections. Wind directions that experience high loads as well as high correlations due to two-dimensional flow separation may be the most critical. The structural response to the correlated pressures studied in this section will be studied in detail in the Chapters to follow.

3.5 Selection of Design Peak Event for Connection Testing

Flow separation and the movement of eddies and vortices result in intermittent 'peak events' where loads are more the 3.5 and up to 8 standard deviations from the mean. These peak events are of short duration and last for between 0.5 and 2.0 s, from the beginning of the ramp up to the ramp down of load.

It is during these peak events that damage to connections occurs and connections must be tested to these peak events to determine their performance. However, as load fluctuations are a random process, it is difficult to determine what magnitude of peak event should be used as an acceptable load for connection testing and structural analysis.

There are several methods of determining design pressures (Gavanski et al. 2016), previous researchers have used a range of values from 80 to 95 percentile peak pressures recorded during a wind tunnel run. ISO4354 recommends an 80% fractile peak based on the Gumbel distribution (ISO 2009). However, in this study a 95th percentile peak event will be used as the time history trace to be applied to connections during laboratory testing and also as peak pressure distributions to be applied to the roof surface in the structural analysis model.

Load time history traces were analysed to determine the frequencies and magnitude of peak events for the critical wind directions 210° at the critical connection T2-B7. A histogram of magnitude for 'peak events' 3.5 standard deviations from the mean and larger are shown in Figure 3.16. The 95th percentile value of the peak events corresponds to a peak intensity of about 6 standard deviations from the mean, as shown in Table 3.1.
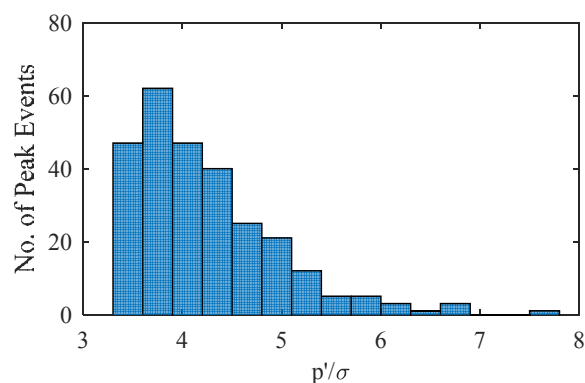
Figure 3.16 Histogram of peak event intensities at connection T2-B7 for wind direction 210°

Table 3.1 Percentile values of peak events greater than 3.5 standard deviations from the mean

Percentile	85.00%	90.00%	95.00%	98.00%	99.00%
Peak Magnitude (p'/σ_p)	4.95	5.21	5.72	6.39	6.71

During connection testing, the wind tunnel time history trace was scaled in amplitude and in time to generate a peak load similar to the connection's strength and a realistic waveform and load rate during a 'design' peak event, shown in Figure 3.17. Additionally, time steps at which 95th percentile peak events occur for a range of wind directions were recorded such that 'peak-event' pressure distributions could be used for structural analysis presented in Section 6.3.
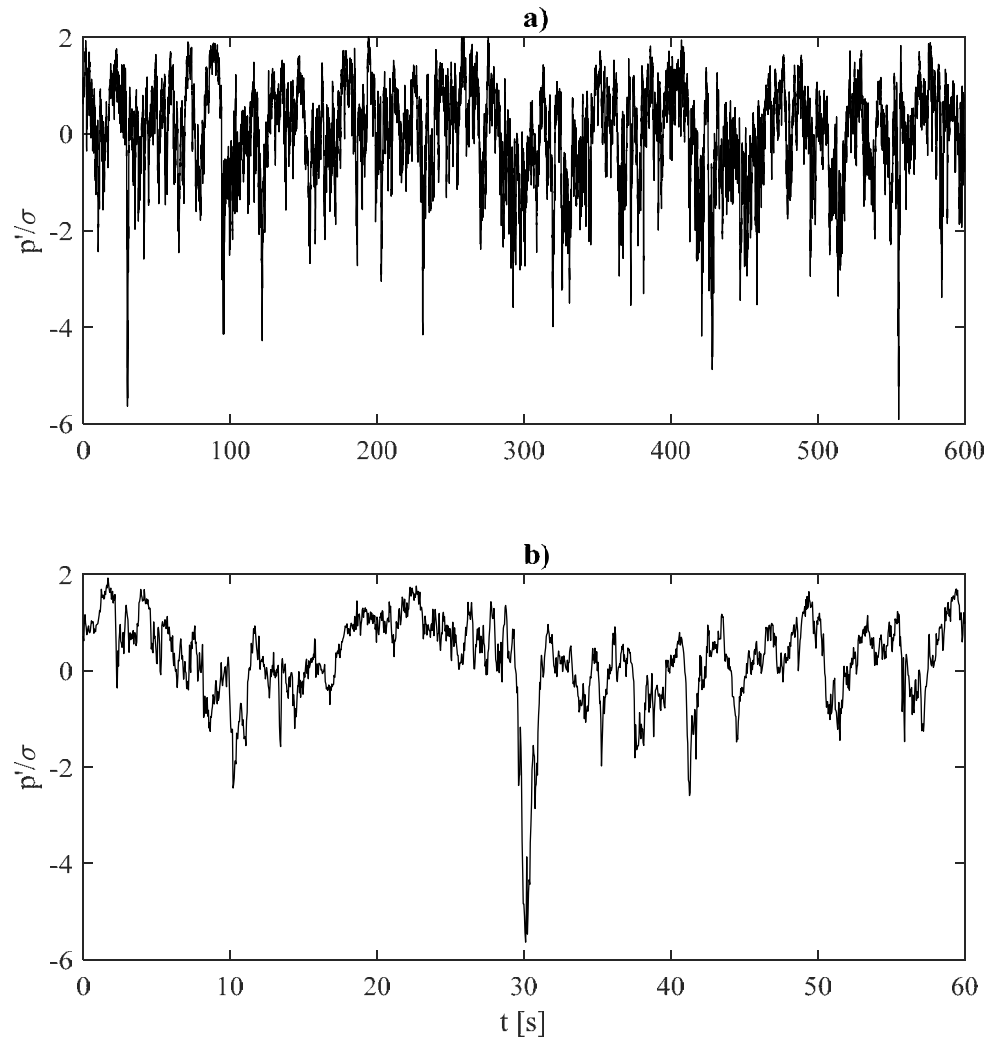
Figure 3.17 a) Ten minute time history of pressure fluctuations at connection T2-B7 for wind direction 210°. b) detail of the first 95th Percentile peak event in the same pressure signal as a).

3.6 Pressure Time History Data

Pressure data at 98 tap locations were recorded at 500Hz for 36 wind directions. Data were stored in $C_p(t)$ form to allow scaling to a desired wind speed in the structural analysis model described in Chapter 5. Pressures from all 98 pressure taps can be applied to the structural analysis model simultaneously. This dataset of time history pressures can be used for future analysis such as for the study of roof to wall connections.

Before the creation of the structural analysis model presented in Chapter 5, pressures that would influence load at a particular connection were estimated by taking the average of the pressure taps within a tributary area. These averaged pressures were used for examining pressure patterns and correlations presented in the previous sections.

Pressures at four neighbouring pressure taps above connection T2-B7 are shown for wind direction 210º. 'Peak events' and rapid pressured fluctuations can be seen in the time history data, as shown in Figure 3.18. It can be seen that these pressures are well correlated, and area averaging effects may occur that will be accounted for in the structural analysis model.
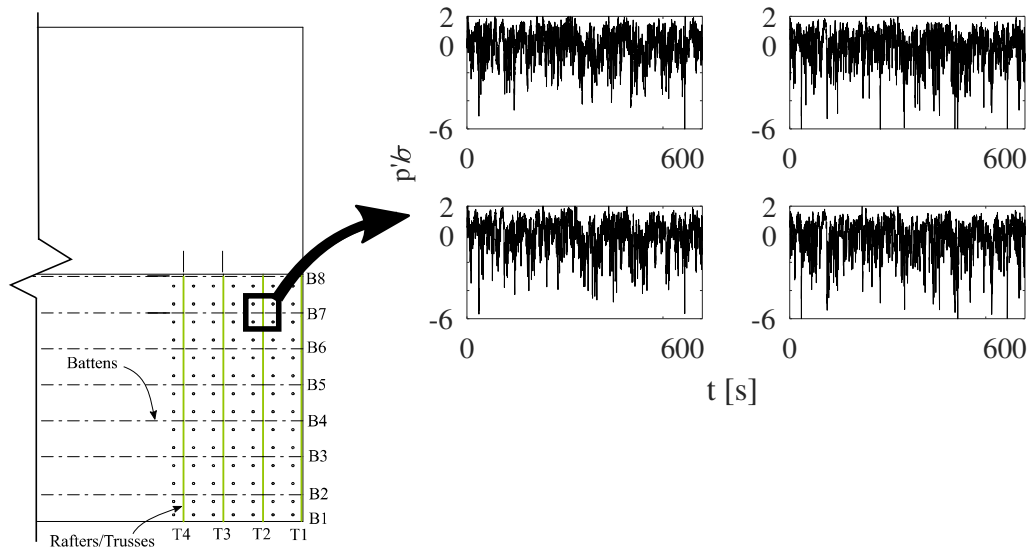
Figure 3.18 Ten minute time history of pressure fluctuations at 4 pressure taps surrounding connection T2-B7 for wind direction 210˚.

3.7 Chapter Summary

A 1/50 scale wind tunnel model study was used to determine the fluctuating wind loads on batten to rafter connections of a rectangular gable roofed house. Spatially and temporally varying loads were analyzed to determine the timing and correlation of loads among neighboring connections.

The wind tunnel study recorded 98 simultaneous pressure measurements on a study area of the gable end roof for approximately 1 hour of full-scale winds for 36 wind directions. Critical wind directions include a sector between 180 to 300 degrees, with direction 210 producing the highest loads on batten to rafter connections. Pressure patterns and the movement of eddies and vortices of four critical directions were studied in detail.

The wind tunnel study showed that high uplift loads at connections are due to 'peak events' where loads can be more than 3.5 standard deviations from the mean. Visualising the surface pressures revealed that 'peak events' are caused by the formation and movement of vortices in flow separation regions. Orthogonal wind directions, where discontinuities are perpendicular to the approach wind flow result in two-dimensional flow separation that causes the formation of vortices that are then convected along the roof surface. Cornering winds result in much higher negative pressures due to three-dimensional flow separation such as 'conical' or 'delta wing' vortices. Additionally, the size of the eddy or vortex determines the number of connections that will be subjected to high loads during a 'peak event', this influences the number of connections that could be overloaded and in turn fail when an adjacent connection fails.

Cross-correlations of load time histories show that peak loads are correlated amongst neighbouring connections for a range of wind directions. Lead/lag times of maximum correlations indicate the direction that fluctuations move across the roof. The time scales of lead and lag times between loads arriving at neighbouring connections are small compared to the durations of 'peak events'. Depending on the wind direction, loads are correlated with connections either diagonally upward, downward or across the roof slope from a given connection. It was found that highest correlations of loads occur in 2-dimensional flow separation regions for orthogonal wind directions (180° and 270°). However, the largest magnitude loads occur due to the formation of conical vortices for cornering wind directions (210° and 300°). Thus, wind directions that cause the highest peak loads are not necessarily those that have the highest correlation of peak events among neighbouring connections.

A 95th percentile 'peak event' to be used for connection testing was determined. The 'peak event' corresponds to a local maxima of wind pressures where the pressure is approximately six standard deviations from the mean and results from an approach wind direction of 210°. Time history pressure data are used in the computer analysis presented in Chapter 7 of a section of the gable roof. Connection testing of individual batten to rafter connections is presented in Chapter 4, where dynamic testing of connections was performed by applying the 95th percentile 'peak event' to the connection repeatedly.

The wind tunnel model study provides a first step in assessing the vulnerability to progressive failures of batten to rafter connections under fluctuating wind loads. Wind tunnel data have shown how various flow separation mechanisms cause pressure patterns and different synchrony of loads among neighbouring connections. These patterns give a method of identifying which parts of the roof and which approach wind directions may result in the initiation of a progressive failure. Combining information on the synchrony of loads at neighbouring connections with the structural response of individual connections and the system as a whole will provide insights on how failures initiate and propagate through the roof structure.

4 CONNECTION RESPONSE

The response of nailed batten to rafter connections under fluctuating wind loads must be quantified in order to model the overall structural behaviour using structural analysis software. Connection testing was performed to determine the structural response of double nailed timber batten to rafter connections, representative of an older Australian house with a metal clad roof, under static and dynamic loading. The effects of age and drying of timbers was simulated by oven drying the unseasoned connection samples. Force displacement behaviour of the connections is used in the subsequent structural analysis models presented in Chapter 5.

Timber connections are complex and are highly variable in performance due to several factors. Nailed connections in older housing are often nailed while the timbers are still in their 'green' conditions where moisture contents can be more than 30%. Over their service life, timbers will dry out with the nails embedded, potentially causing a decrease in strength. Furthermore, corrosion of nails and degradation of timber through rot can also adversely affect connection strength.

Previous research of connections under realistic wind loads have included cladding fasteners (Lovisa, Henderson, et al. 2013, Henderson et al. 2009), and roof to wall connections (Khan 2012). However, the response of nailed timber batten to rafter connections used in Australian housing does not appear to have been studied under dynamic wind loads.

The primary objective of the connection testing performed was to determine the structural response: i.e. force-displacement curves of nailed timber batten to rafter connections under realistic fluctuating wind loads.

Additional aspects that were explored include:

1. The effects of age and degradation of connection: Does the drying of timbers or corrosion of nails increase or decrease embedment strength over time and what is the behaviour of such aged connections under dynamic loads?
2. Any differences in performance of the connections subject to static vs. dynamic loads: For example, is a significant amount of energy dissipated during loading, or does load rate affect the strength of connections?

4.1 Connection Specimens

Samples were made to represent pre-1980's double nailed connections using a common hardwood species: Spotted Gum *(Eucalyptus maculate)*. Specimens consisted of 200mm lengths of batten and rafter material nailed together with two 75×3.37mm plain shank bullet head nails, shown in Figure 4.1. Batten dimensions were 38×75mm and rafter dimensions were 100×50mm. For a larger span roof 150×50mm rafters may be used, however this additional depth of the rafter has no impact on the embedment of the nails.

Spotted gum timbers were ordered in the unseasoned condition especially for this study, to ensure initial moisture contents were approximately 30%. Timbers were wrapped in plastic to ensure no drying occurred during transit. Samples were then prepared and wrapped in plastic again to prevent any drying in the time between and before testing.

Ten samples were tested at each stage of testing. Statistics on the variability of the connection performance with the small sample size are limited. However, pseudo replication problems would be faced if a larger number of samples from the same tree or the same timber section were used. To get a true measure of the connection variability in a population of houses, samples from many different trees must be used. Such an in-depth study of connection variability is not a focus of this study.

Figure 4.1 Batten to rafter connection Sample

4.2 Overview of Test Methods

Connection samples were tested under quasi-static loads as well as dynamic loads that were derived from wind tunnel tests. As there are no standardised methods for testing batten to rafter connections under realistic wind loads, a substantial amount of effort was spent to determine an appropriate method that would give the most information during each test.

4.2.1 Static Tests

Static pull out testing was conducted using a 100kN Instron Model 1342 servo hydraulic universal testing machine with an 8800 series controller, shown in Figure 4.2. Test specimens were subject to a displacement controlled pull out at a rate of 2.5mm/min as specified in the Australian Standard AS1649 (2001). Connections were held in place with a customised aluminium clamping system that allows the sample to be secured for loading in tension or compression. The reason for using aluminium construction was to minimise any inertia effects during dynamic loading.

Figure 4.2 Apparatus for static and dynamic connection testing

4.2.2 Dynamic tests

Testing of connections was again performed with the Instron. The machine's proportional-integral-differential (PID) controller was tuned to the initial stiffness of the nailed connections for the magnitude and rate of the load fluctuations to be applied. Initially, testing was to be performed with a customised bellows system controlled with a pressure loading actuator (PLA) similar to that used by Khan (2012). However, it was found that the Instron could apply load controlled test sequences to the samples based on wind tunnel data more reliably. Area averaged wind pressures over a tributary area of a selected connection were used to derive a fluctuating load to be applied to a connection with the appropriate time and magnitude scaling, as described in Chapter 3.

4.2.3 Preliminary Dynamic Testing

Dynamic test methods were developed during the testing of the aged connections that are presented in Appendix A., as the number of samples available for testing was limited, a considerable amount of time was spent to determine the appropriate test method and loading trace required for the dynamic tests. Several preliminary tests were carried out to determine the most suitable test method and to set the PID control gains of the universal testing machine to accurately follow a wind tunnel load trace.

As there was significant variability in connection strengths, it was not known what magnitude of peak event, i.e. what wind speed, to apply to the connections. Initial testing showed that too high a wind speed would result in the immediate failure of the connections during a 'peak event', on the other hand, for lower wind speeds, no damage would result after several peak events. In both these cases, limited information of the non-linear response of connections would be obtained.

Therefore, it was decided to apply a load trace, where the 95th percentile peak, defined in Chapter 3, was applied repeatedly to connections. Additionally, several 'stages' of peak events were applied to each connection, using the mean connection strength determined from static tests as a first estimate for the peak events to be applied. For example, several peaks could be applied at a load equal to one standard deviation below the mean connection strength, followed by several peaks at the mean connection strength followed by peaks higher than the mean connection strength if required.

4.3 Static Tests

Two sets of static tests were performed, firstly on ten control samples in the green condition and an additional ten that were oven dried. Control specimens resisted an average maximum load of 3.26 kN and an average initial elastic stiffness of 0.90 kN/mm. After reaching their maximum loads connections weakened in a near linear fashion until the disconnection of the nail from the rafter at approximately 25mm displacement. Table 4.1 provides a summary of the performance of the control specimens and Figure 4.3 shows force-displacement curves of these connections. Additionally, details of a quasi-static test on a connection under reverse cycle loading are presented in Appendix B.

Even though the testing machine maintained a constant rate of displacement, a saw tooth pattern in all the tests is apparent caused by the nails slipping incrementally, which caused the tensile load within the nail to drop rapidly during each nail slip. The force displacement curve of each sample can be defined by connecting the points of the peaks of the saw tooth pattern recorded by the load cell.

Table 4.1 Green test specimens

Test No.	MC % (Outside)	Strength [kN]	Stiffness [kN/mm]
Test 1	33.4	3.55	1.11
Test 2	25.6	3.52	0.87
Test 3	26.3	2.80	0.44
Test 4	31.3	3.00	0.86
Test 5	30.3	4.33	1.50
Test 6	27.6	4.72	0.83
Test 7	27.4	3.64	1.03
Test 8	31.1	2.49	0.77
Test 9	28.8	1.98	0.83
Test 10	28.2	2.58	0.72
Mean	29.0	3.26	0.90
Std Dev	2.5	0.85	0.28
CoV	9%	26%	31%
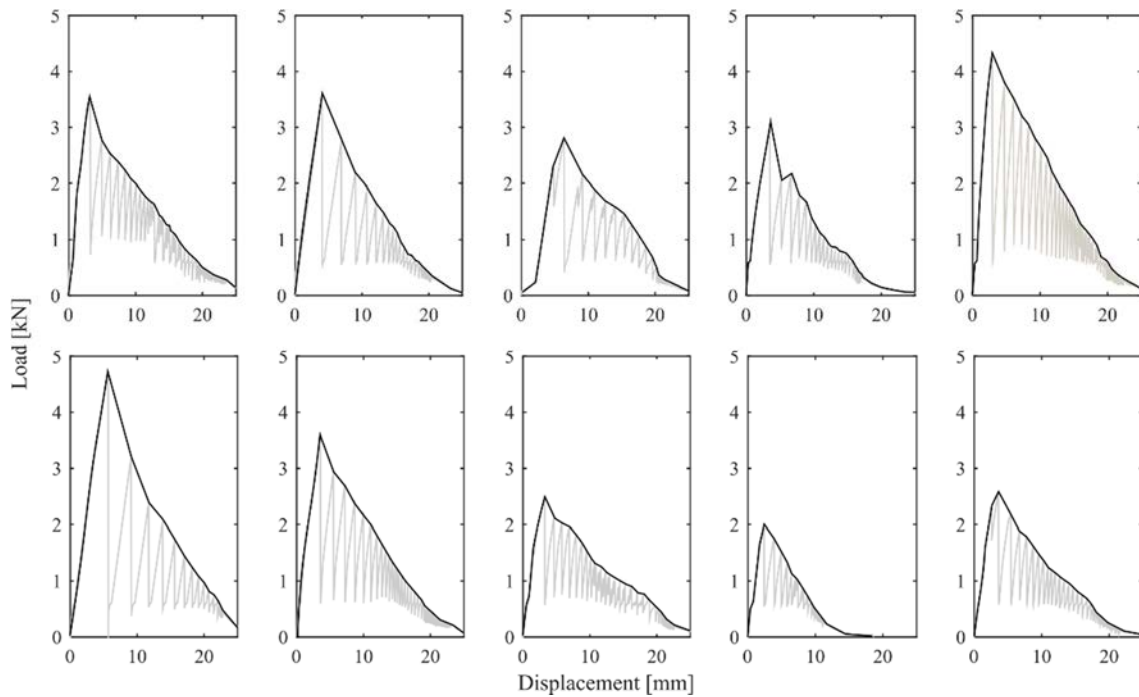
Figure 4.3 Load-displacement curves of the 'green' specimens

Ten additional samples were then placed in a ventilated drying oven at 35°C for about three weeks to reach a moisture content of about 12%. Some checking (cracking on the end grain) was observed at the ends of battens and rafters. However, these did not penetrate through the samples and did not affect the embedment of the nails. The ten oven dried samples were then tested under the same displacement controlled pull out of 2.5mm/min.

As shown in Table 4.2, maximum loads decreased with the average maximum load being 1.45 kN, a 60% decrease in strength compared to the control samples. However, the overall shape of the force-displacement curves remained similar as shown in Figure 4.4. The oven dried static tests showed that drying of timbers after connections are nailed significantly reduces connection strength.

Table 4.2 Oven dried test specimens

Test No.	MC % (Outside)	MC % (Inside)	Strength [kN]	Stiffness [kN/mm]
1	14.0	24.0	1.69	1.25
2	13.4	23.2	1.36	0.88
3	13.4	22.0	1.52	0.69
4	16.1	24.9	1.68	1.04
5	14.9	22.5	1.37	0.74
6	13.7	23.8	1.28	0.68
7	15.9	21.6	1.47	1.24
8	14.6	22.9	1.50	1.03
9	14.1	22.4	1.15	0.69
10	15.2	21.1	1.48	1.17
Mean	14.5	22.8	1.45	0.94
Std Dev	1.0	1.17	0.17	0.24
CoV	7%	5%	12%	25%
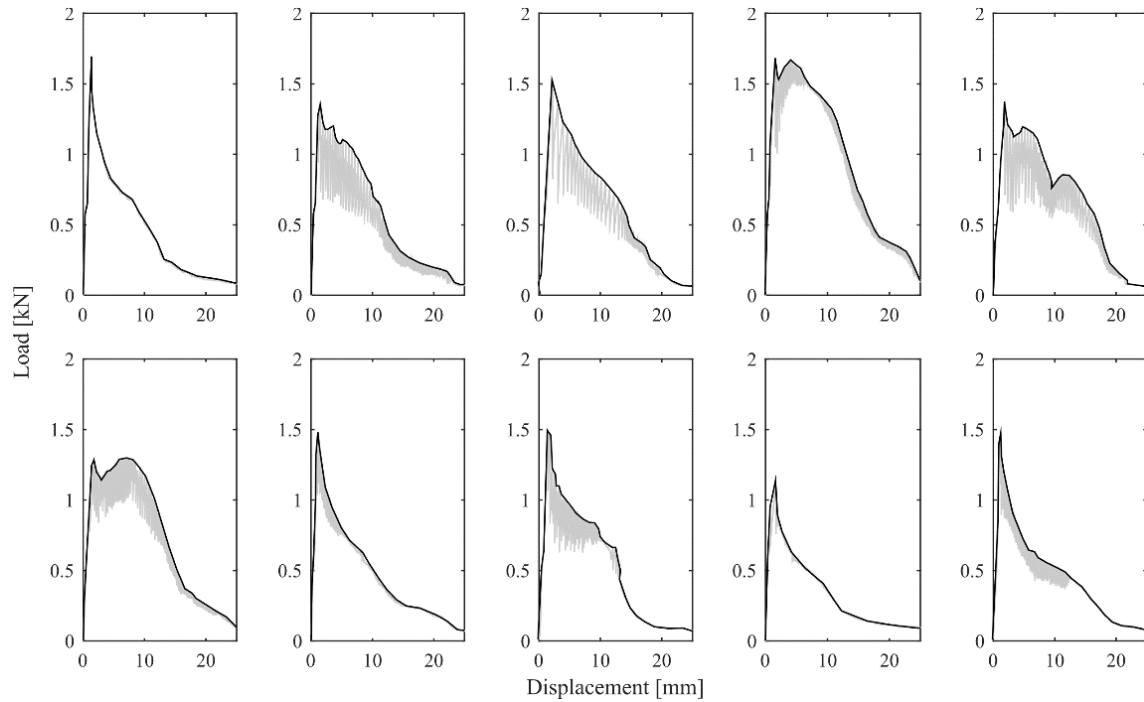
Figure 4.4 Load-displacement curves of the oven dried test specimens

After Testing, the oven-dried specimens were split perpendicular to the grain to open the samples and observe a cross section of the location of nail embedment, as shown in Figure 4.5. This cross section showed a faint drying profile, indicating that the moisture content within the middle of the sample was higher than at the boundaries. A black stain was produced as a corrosion by-product of the nail reacting with the timber or possibly the tannins within the timber. It is unclear how long it took for the stain to develop or its effect on the nail embedment strength. Some samples showed some rust left in the nail hole at the top of the nail. The timber fibres surrounding the nail were bent downwards when the nail was initially driven. It did not appear that these fibres were forced upwards during the pull-out test.

Figure 4.5 Cross section through oven dried test specimen showing deformation of fibres due to nail penetration and dark coloured corrosion bi-product.

4.3.1 Comments on the Variability of Connections

Coefficients of variation for the static tests are low compared to what would be expected in as-built connections. The tests presented in this Chapter using samples created in the laboratory will have a limited ability to capture the true strengths and variability in aged batten to rafter connections due to the level of drying that was possible within the time constraints while using the oven. Additionally, variability in strength due to factors such as nail angles and edge distances cannot be accounted for with the samples created in the lab.

However, it is the overall shape of the force displacement curves and a reasonable estimate of the strength of two nailed connections that are required as inputs for structural analysis modelling. Quantifying connection strengths and variability more accurately was not part of the scope of this thesis.

Appendix A presents testing results on as-built 50yr old batten to rafter connections. As these were single nailed tiled roof connections these data could not be used for studying the metal clad structural system selected for this study. The tests of these as-built connections provided valuable information on the effects of age and degradation of connections as well as the expected variability in connection strengths accounting for installation errors on site.

Several factors such as nail angles, timber grain size and orientation, cracking in timber were recorded. Weak relationships were found between the influence of single factors to the connection strength. However it is likely that the overall performance was due to the combined effect of these factors.

4.4 Dynamic Tests

Connections were subject to load controlled dynamic loading traces consisting of a 95th percentile peak event applied to the connection repeatedly. The peak events selected were for the critical connection (T2-B7) near the ridgeline and the critical wind direction 210˚, as described in Chapter 3.

For the static tests, the mean connection strength was 1.45kN with considerable variability. It is expected that some connections would fail below this load and some above this load. Peak events were increased in magnitude in steps (0.8, 1.0, 1.2, 1.4, 1.6, 1.8, 2.0, 2.2 kN). Nail slip behaviour during peak events could then be observed for most samples without connections failing immediately at the first peak or having no deformation at all during the test process.

The appropriate time scaling was applied to the load traces. For example, a 1.4kN peak event would be generated by a 0.2 second gust wind speed of approx. 51m/s at mid roof height in suburban terrain. With the speed of the wind tunnel at mid roof height being 6.58m/s, this corresponds to a time ratio of approx. 1/12. A ten-second segment of the synthetic 'peak event' load trace is shown in Figure 4.6. Each peak event lasts approximately 1.5s from initial ramp up to final ramp down time, with loads exceeding 1.2kN for about 0.3s. The load rate of the ramp up is approximately 5kN/s.
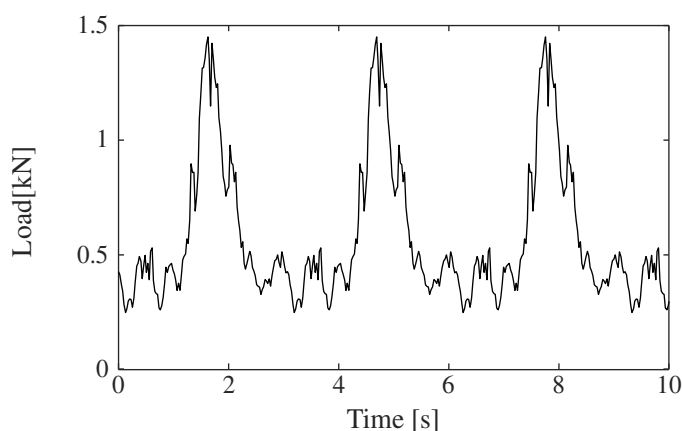
Figure 4.6 Three repeated peak events at a load of 1.45kN, i.e. the mean connection strenght of the static tests.

Connections were subject to 25 peak events at each load step. The actual load rate based on wind speed could not be applied by the machine for target loads above 1.4kN as this would cause unpredictable behaviour of the actuator. Therefore, the time scaling for load steps 1.6 and above were set to be the same used for the 1.4kN load step.

The dynamic tests were able to show qualitatively, the nail behaviour under fluctuating, dynamic loads. Figure 4.7 shows force displacement curves of the ten connection samples under the synthetic 'peak event' wind trace. Nails slip incrementally with each peak event and the elastic stiffness of the connections remainins almost constant throughout the test.
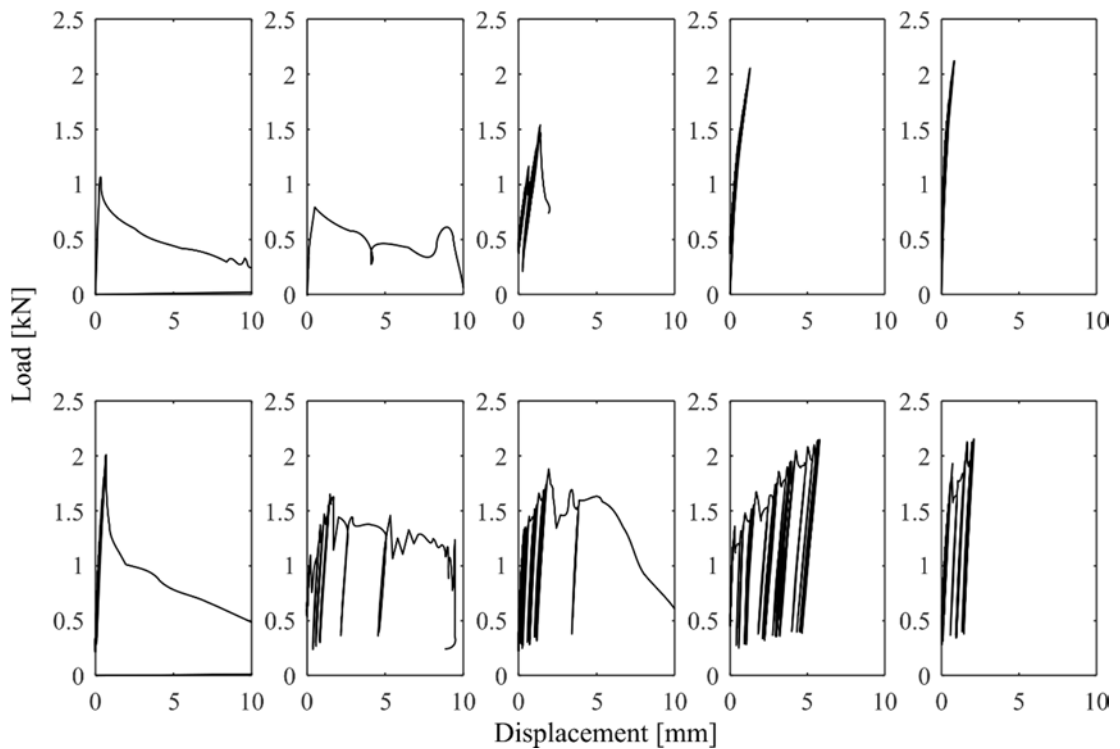
Figure 4.7 Connection response (load vs. displacement) under repeated dynamic peak events

Two connections failed on the first load step and two connections showed no nail slip at all during the test sequence. One connection failed at the second to last load step without any incremental nail slip beforehand. Another two connections failed during an intermediate load step after several nail slips and the remaining two connections showed several nail slips but still did not fail by the end of the test sequence.

In some cases, nails may slip during the first peak event and stop slipping at that load step. The nail will slip further at the next load step and then may be unaffected again. This shows that nailed connections may be subject to damage at peak events below their maximum strength and making the connection weaker for future loading

4.5 Average Connection Properties for Structural Analysis

The overall shapes of the connection force-displacement curves showed that maximum loads and reductions in load occurred at similar displacements. This is expected as all the nails were the same length. Table 4.3, shows the loads at 5, 10, 15, 20, 25mm displacement that were used to determine an 'average' force-displacement curve to be used in the structural analysis model, shown in Figure 4.8.

Table 4.3 Oven dried connection force and displacement at set displacements

	Elastic Slope			Load at displacements [kN]				
Test No.	x [mm]	y [kN]	Slope [kN/mm]	5 mm	10 mm	15 mm	20 mm	25 mm
1	1.36	1.69	1.25	0.80	0.50	0.20	0.10	0.00
2	1.14	1.28	1.12	1.08	0.70	0.30	0.20	0.00
3	2.21	1.52	0.69	1.00	0.80	0.40	0.15	0.00
4	1.61	1.68	1.04	1.60	1.30	0.60	0.40	0.00
5	1.87	1.37	0.74	1.00	0.80	0.60	0.15	0.00
6	1.55	1.23	0.80	1.20	1.10	0.50	0.20	0.00
7	1.19	1.47	1.24	0.80	0.50	0.25	0.20	0.00
8	1.45	1.50	1.03	1.00	0.70	0.20	0.10	0.00
9	1.67	1.15	0.69	0.60	0.35	0.18	0.10	0.00
10	1.26	1.48	1.17	0.70	0.50	0.38	0.10	0.00
Mean	1.53	1.44	0.98	0.98	0.73	0.36	0.17	0.00
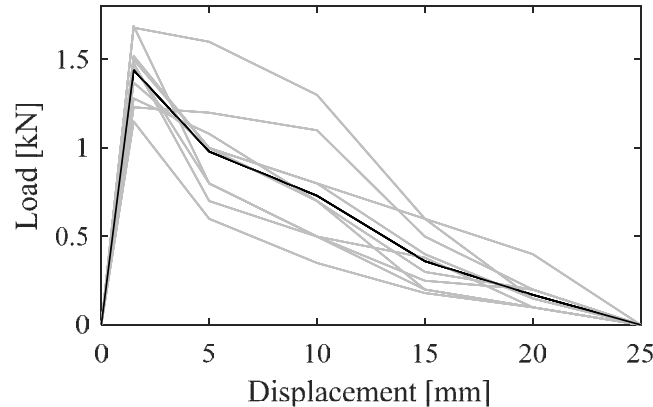
Figure 4.8 Idealised load- displacement relations for oven dried connections with average connection properties shown in black.

4.6 Discussion

Static tests showed that connections have an initial elastic slope, yield and then a loss of strength until the nails fully withdraw from the rafter. Additionally, drying of the timber after nails are installed has a significant effect on the strength of connections and the general form of the force-displacement curve. There is also significant variability in connection strengths.

Connections tested under dynamic loads show that damage occurs during 'peak events' and not during lower level load fluctuations. Depending on the loads applied, failure of a connection can occur incrementally due to the nails slipping during each 'peak event'. Additionally, the initial stiffness, indicated by the gradient of the loading and unloading paths, does not change with accumulated damage through successive peak events i.e. the elastic behaviour of the connection is similar for each peak load event. This indicates that load redistribution to adjacent connections occurs due to nail slip rather than due to a decrease in stiffness.

The stepped dynamic load trace showed that, in some cases, plastic deformation can occur at low magnitude peak load events, which causes less plastic deformation at each nail slip. A small amount of hysteresis was also observed during the low level fluctuations in between peak load events. However, it is not known whether this hysteresis is due to the movement of the sample within the apparatus or the behaviour of the connection itself.

Furthermore, the force-displacement response of a connection under dynamic loads is bounded by the force-displacement curve of the static tests. This behaviour indicates that load rates that occur during wind loading do not appear to affect the connections' strength.

4.6.1 Limitations of Individual Connection Testing

The force-displacement relationships have an initial stiffness that represents the elasticity of the timber that is gripping the nail but also that of the timber being compressed under the head of the nail.

Due to the nature of the apparatus, the slope of the loading and unloading bands may be influenced by the clamping system as well as bending of the batten. To verify the true elastic behaviour in the loading bands, the tests could be repeated with a clamp that holds the batten only immediately above the nail. Alternatively, the nail heads alone can be gripped and the load displacement behaviour compared to that of the connections tested.

4.6.2 System Behaviour Compared to Individual Connection Response

System behaviour will cause the connections to respond as a combination of the stiffness of the connection itself and the stiffness of the span between neighbouring supports and the cladding. This system would behave similarly to a set of springs in parallel. This load sharing will allow much higher loads to be applied to the tributary area of an individual connection than what could be withstood by a single connection tested with no system behaviour. Much higher wind speeds may be required to produce the low-level nail slips observed during dynamic testing of a single connection, as the nails of a given connection are held in place by the batten and neighbouring connections.

In reality, as soon as one connection displaces, load is immediately transferred to neighbouring connections, reducing the load applied to the connection further. When nails do slip, the pressure in the hydraulic ram immediately decreases causing the machine to drop some of the load for a short period. In reality, the wind pressure on cladding does not decrease at the instant that a connection slips; although it may decrease later in time. Therefore, the system effects of the other connections may be somewhat accommodated for by this limitation of the servo hydraulic testing machine.

4.7 Chapter Summary

Testing of individual batten to rafter connections was performed to determine their force-displacement behaviour under static and simulated dynamic wind loads. Under dynamic loads, batten to rafter connections exhibited nail slip behaviour during peak events when loads exceeded the load displacement curve as defined by static tests. Although there was significant variability in strength among the connections, it was found that the overall shape of the force-displacement curves were similar and could be simulated by finding the average load the connections could withstand at a particular displacement. The average force-displacement relationships of the connections are applied to non-linear link elements that represent batten to rafter connections in the finite element model presented in Chapter 5.

5 STRUCTURAL ANALYSIS MODEL

The Structural response of light framed houses is complex due to non-linear behaviour of connections, multiple load paths, load sharing and partial composite action. Full scale testing has been the preferred tool used for assessing these light framed structures. However, with improvements in computational power, time history analysis has become a viable option for assessing the structural response to wind loads.

This Chapter presents the construction of a nonlinear finite element model that was used to study the progressive failure mechanisms of batten to rafter connections. Model geometry, support conditions, material properties and simplifying assumptions are presented in detail.

5.1 Structural Analysis Model

The model was created using the Finite Element Method structural analysis program SAP2000. This particular software was selected as it has extensive documentation and includes several features for non-linear time history analysis typically used for earthquake engineering.

The model is of a traditional roof structure that would be used to frame a gable roof house. Timber sections are modelled as frame elements with orthotropic material properties. Corrugated roof cladding is modelled as shell elements with stiffness and mass modifiers used to represent the effect of corrugations. Batten to rafter connections are idealised as non-linear link elements with force-extension behaviour determined from laboratory test results presented in Chapter 4.

The computer model was created to be able to study the load sharing and redistribution of batten to rafter connections, not other roofing connections. As such, several simplifications of boundary conditions have been made for computational efficiency.

Simplifying Assumptions Include:

- Nonlinear behaviour being isolated to batten rafter connections only
- At failure, batten to rafter connections remain connected to the structure but support only a small load. This assumption allows load redistribution to take place and allows the connectivity of the model to remain constant.
- Batten to rafter connections are permitted to move in the local z direction only.
- Batten to rafter surface contact is modelled with compression only 'gap' elements.
- Damping is assumed as 5% modal damping for all modes of vibration.
- Boundary conditions representing roof to wall connections and strut supports are pinned supports.

These simplifications would not significantly affect load transfer between batten to rafter connections. However, if the model were to be used for a more detailed study of other connections e.g. roof to wall failures, additional refinements would be necessary. Further details of the model geometry and assumptions are presented in the following sections.

5.1.1 Overall Geometry

The model is of a rectangular plan gable roof house with rafters spaced at 900mm and battens at 877mm, with a 22.5° roof pitch shown in Figure 5.1 Battens are 38×75mm and rafters are 100×50mm, sections typical of older Australian houses. Roof to wall connections are not modelled in detail and the rafters are supported by pin supports as well as 100×100mm underpurlins at mid-span. The underpurlins are supported by 100×100mm struts, pin supported at their base, at every 4th rafter. Collar ties at every second rafter are located 1/3rd the vertical distance from the ridgeline to the roof to wall connection. These collar ties are assigned major axis bending releases at both ends. Joint offsets and the appropriate insertion points are used to model the effects of partial composite action in the structural system, which occurs when more than one structural element (e.g. cladding and rafters) act in bending together, shown in Figure 5.2.

Eight rafters are modelled to include four rafters in the study area and an additional four to account for any load sharing effects of elements outside the study area and to better represent the direction a failure cascade may propagate across the roof surface. Batten to rafter connections at the last and second to last internal rafter are modelled with linear springs thereby preventing the structure from becoming a mechanism if a failure cascade propagates to the end of the model.

Collar ties 100x50
(every second rafter)

8100mm

Linear links used
for last two bays

Rafters 100x50 @900 c/c

Study Area

900mm

Battens 38x75 @877 c/c

Ridgeboard 150x50

747mm

3340mm

2049mm

Moment Releases

1303mm

877mm

Struts 100x100
(every 4th rafter)

650mm

Underpurlins
100x100

Pinned Supports

9884mm
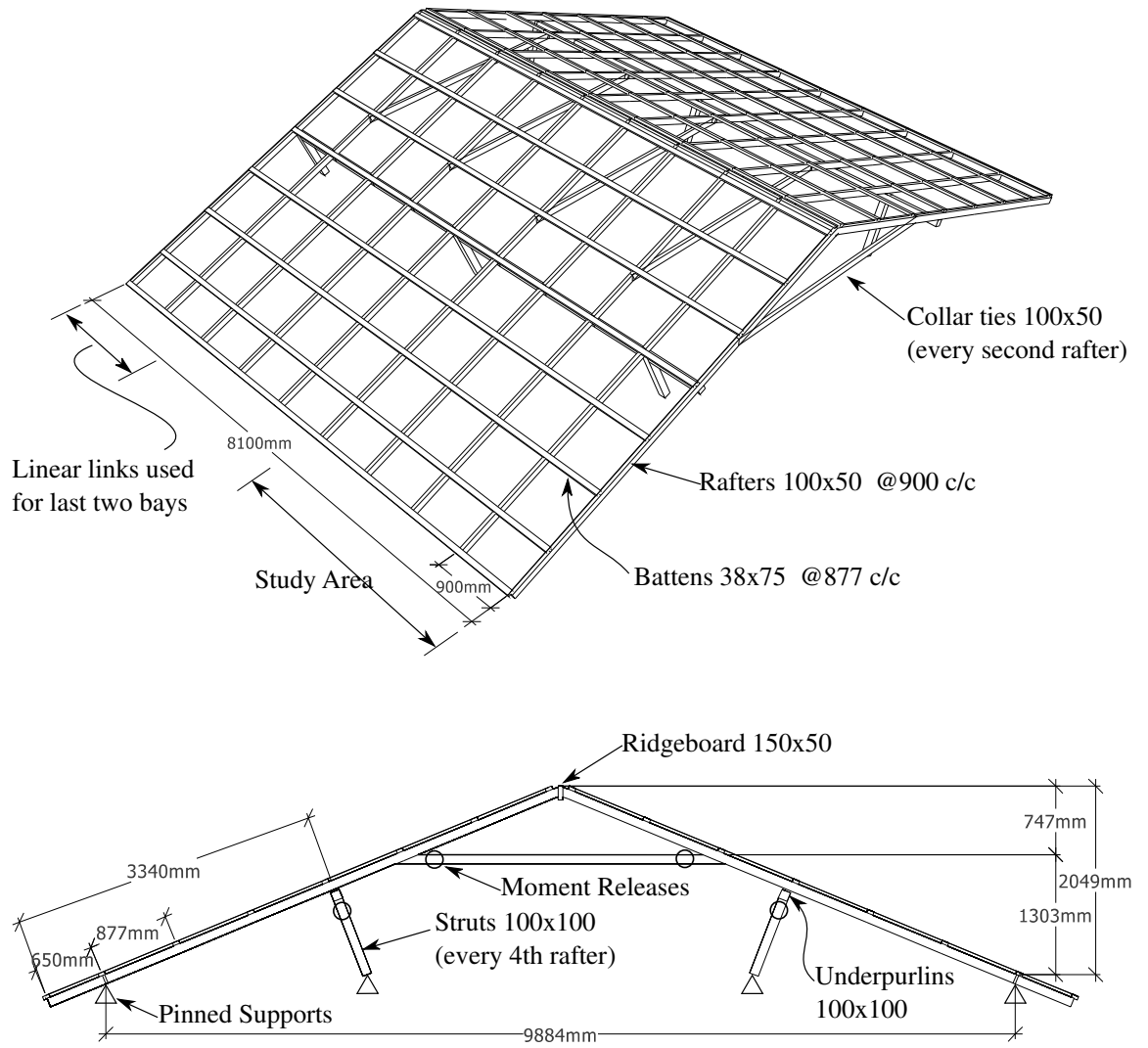
Figure 5.1 Schematic of the nonlinear structural analysis model.
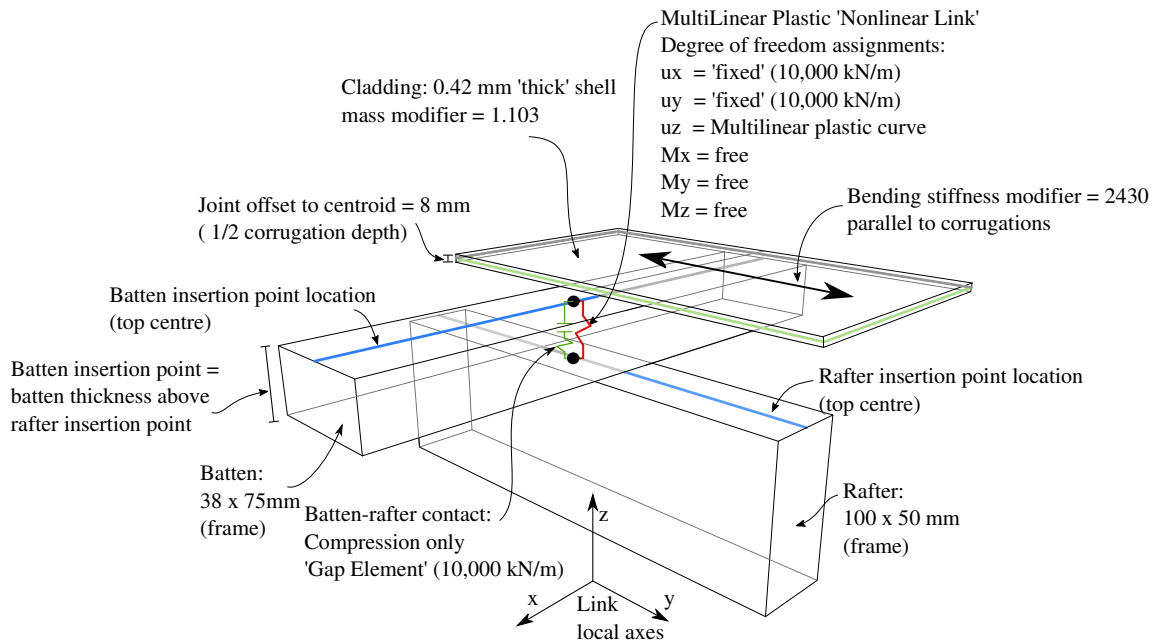
Figure 5.2 Geometry of modelled batten to rafter intersections and offsets used to account for partial composite action

5.1.2 Roof Cladding

The corrugated cladding profile that was modelled is that of a G550 grade 0.42mm BMT custom orb profile. The cladding was modelled as a flat 0.42mm 'thick shell' element in the structural analysis program and was assigned a Young's modulus of 219GPa, Rogers and Hancock (1997).

The 'thick shell' elements used are able to model both membrane and plate behaviour as well as transverse shear deformations. CSI recommends the use of the thick shell formulation even when modelling thin elements. The thick (Mindlin/Reissner) shell formulation has been found to be more accurate than the thin plate formulation. However, the thick plate formulation is more sensitive to large aspect ratios and mesh distortions.

Property and stiffness modifiers are used to model the effects of the corrugated profile by increasing the bending stiffness and membrane and shear area in the local axes direction parallel to the corrugations. The mass and weight are modified to account for the additional material within a metre width of cladding due to the presence of corrugations. A stiffness modifier used to obtain the bending stiffness required for an $I_{xx} = 0.015 \times 10^6 \; mm^4/m$, in the direction of the corrugations (Frye et al. 2012). Property modifiers for the cladding shell elements are summarised in Table 5.1. Additionally, the centroid of the cladding shell is offset from the top of the battens such that it lies half the depth of a corrugated profile (8mm) from the top of the batten.

Table 5.1 Property/stiffness modifiers for analysis

Membrane f11	1.0
Membrane f22	1.1031
Membrane f12	1.0
Bending m11	1.0
Bending m22	2430
Bending m12	1.0
Shear v13	1.0
Shear v23	1.1031
Mass	1.1031
Weight	1.1031

5.1.3 Battens and Rafters

Battens and rafters are modelled as frame elements with cross sections of 38×75mm and 100×50mm respectively. Such frame elements in SAP2000 are able to account for effects of biaxial bending, shear, torsion and axial deformation.

- Property modifiers are not used.
- Meshing of frame elements is at intermediate joints.
- Local axes of the battens are rotated by ±22.5° such that the bottom surfaces of the battens align with the roof slope.

The location of the centroids of the cladding, battens and rafters do not lie on the same plane, and are offset from each other. The battens and rafter frame elements are separated from each other by a distance equal to that of the batten thickness. The insertion points of cross section of the batten and rafter as set to be at 'top centre' creating the geometry shown in Figure 5.2.

5.1.4 Timber Material Properties

Timber is an orthotropic material with different material properties in the longitudinal, radial and tangential directions due to the nature of its grain structure. These properties include three elastic moduli, three shear moduli and six poisons ratios.

Literature on the material properties other than the longitudinal direction is scarce. However, some specialised studies on certain timber species have been performed using physical testing and ultrasonic measurements. Elsener (2014) presents a detailed study on the properties of Spotted Gum (*Eucalyptus maculata*) and Tallowwood (*Eucalyptus microrys*). Material properties of Spotted Gum are used in the current structural analysis model and are shown in Table 5.2. The subscripts L, R and T denote the longitudinal, radial and tangential grain directions respectively

Table 5.2 Material properties used in the structural analysis model

Spotted Gum	
Density	$1060 kg/m^3$
Young's Moduli	
E_L	$26512 MPa$
E_R	$2207 MPa$
E_T	$1457 MPa$
Poisson's Ratios	
v_{LR}	0.49
v_{LT}	0.55
v_{RT}	0.66
v_{TR}	0.48
v_{RL}	0.045
v_{TL}	0.047
Shear Moduli	
G_{LR}	$1895 MPa$
G_{LT}	$1306 MPa$
G_{RT}	$556 MPa$

Certain assumptions are made in order to model timber properties that are in circular coordinates into Cartesian coordinates. Depending on which part of the tree the timber section is taken from, the orientation of the radial and tangential directions will be different. In reality timber sections would be taken from a range of locations in the cross section of the tree however, it was assumed that the grain orientation of the batten and rafter sections are oriented as shown in Figure 5.3. As the analysis model is primarily used to model the behaviour of batten to rafter connections, this simplification is deemed acceptable.
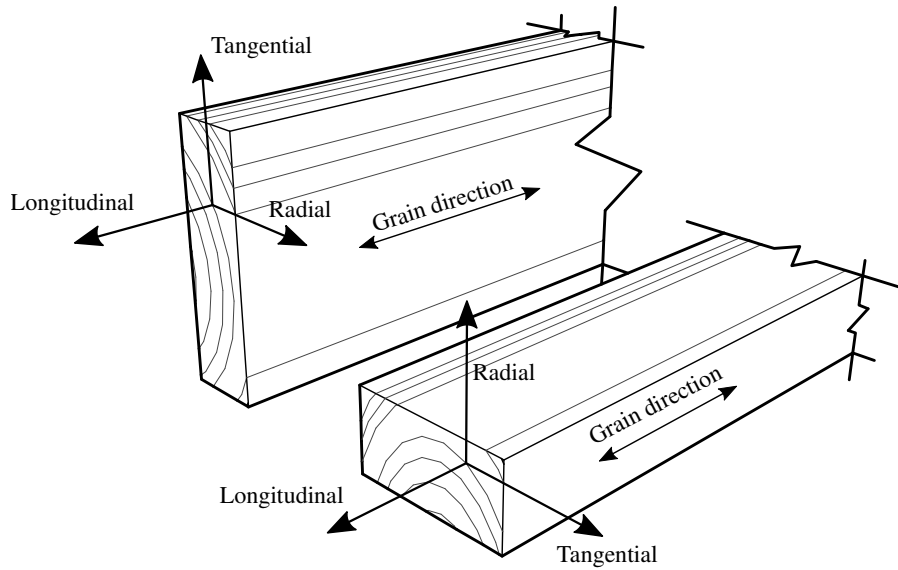
Figure 5.3 Approximate longitudinal, radial and tangential grain directions used to define material properties in the analysis model.

5.1.5 Underlying Roof Structure and Support Conditions

The structure supporting the rafters consists of a 150x50 ridge board; 100x50 collar ties located at 1/3rd the roof height below the apex of the roof; 100x100 under-purlins located at mid span of the rafters and 100x100 struts spaced at every 4 rafters (3600mm spacing) that support the under-purlins. Major axis moment releases are added to each end of the collar ties where they connect to the rafters. Additional moment releases are added to the struts where they connect to the under-purlins.

The under-purlin nodes are located at 100mm under the nodes of the rafters with the insertion points of the under-purlins set to be 'top centre'. Rigid body constraints are applied to the nodes on the rafter and the under-purlin where the two members are connected. Roof to wall connections and the supports of the struts are modelled with pin supports. Such simplified boundary conditions will give reasonable results for load sharing between the batten to rafter connections but less so for roof to wall connections.

5.1.6 Batten to Rafter Connections

Within the analysis model, connections are idealised as two node, multi-linear plastic link elements. A kinematic hysteresis model is specified for the non-linear links. Stiffness degradation does not occur in this hysteresis model and is representative of the nail slip behaviour observed during connection testing.

Each nonlinear link can be assigned six degrees of freedom, each with its own nonlinear force-displacement curve. The directions of the link local axes are shown in Figure 5.2. The force-displacement curve in the local z direction was determined from connection testing in Chapter 4 and shown in Figure 5.4. The curve has an elastic stiffness of 0.98kN/mm, a maximum strength of 1.45kN and a gradual loss of strength until 25mm displacement, when the nail has completely withdrawn.

The non-linear links are assigned the same elastic stiffness under compression loads as in tension to allow for compression forces that could be withstood when the nail is partially withdrawn. However, as a simplification, nonlinear behaviour is not modelled for the links in compression. Therefore, nails cannot be pushed back into the rafter material when nails have been partially withdrawn.
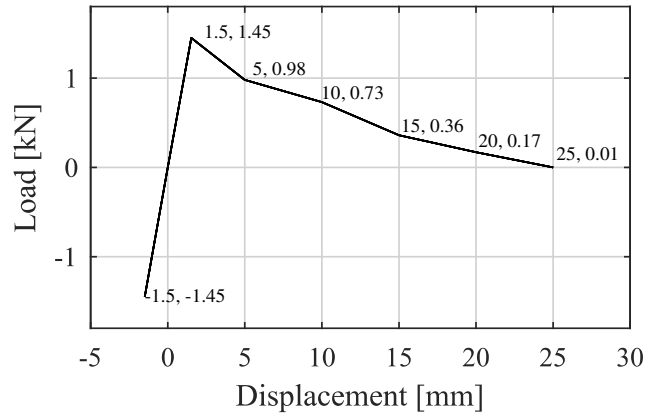
Figure 5.4 Idealised force-displacement curve of a nailed connection

Each nonlinear link is assigned a stiffness in the local x and y directions of ten times the stiffness of the local z direction. These x and y direction stiffness assignments are to model the restraint of the nail by the rafter material enabling the nail to resist shear forces. However, when the links completely fail in tension, their local x and y direction stiffness remains, and the peeling back of the battens and cladding in later stages of failure cannot be modelled accurately. The model is therefore able to simulate the onset of damage to the structure as well as its behaviour until the initiation of a cascading failure. During later stages of a failure cascade, changes in internal pressure and aerodynamics of the roof envelope will be significant driving factors of the path of a failure cascade.

All rotational degrees of freedom of the nonlinear links are free. In reality, the rotational resistance of a nailed batten to rafter connection will be greater when the nails are fully embedded in the rafter, and will decrease as the nails withdraw. Moments applied to the nailed connections would cause further withdrawal of the nails by prying actions. This process cannot be idealised by the non-linear link elements and these degrees of freedom are assumed free.

When complete failure of the connection occurs at approximately 25mm displacement, the non-linear links are not assigned zero load but a value of 0.01kN. This small value is to allow the load redistribution process to take place and maintain connectivity within the FEM mesh.

Furthermore, links on the other side of the roof to the study area are linear and are assigned only an elastic range to reduce computational demand. Additionally, batten to rafter connections of the last and second to last rafters of both sides of the roof are modelled with linear links that cannot drop load. This is to ensure that the structure does not become a mechanism when a cascading failure propagates to the end of the roof

5.1.7 Batten to rafter contact

Special considerations must be made to model the surface contact between frame elements in SAP2000. The contact between the underside of the battens and the top surface of the rafters is modelled using compression-only 'gap' elements in conjunction with the non-linear link elements representing the nails. In the undamaged state, any compressive loads, including gravity loads will engage the gap element and the compressive component of the nonlinear link as springs in parallel. However, in tension, it is only the non-linear link that is engaged.

Additionally, if any permanent deformation occurs, It is only the nonlinear link (and not the gap element) that is engaged if the connection is then subject to compression. This represents a connection in the state when a nail has been partially withdrawn and needs the nail to be pushed back into the rafter material for the battens and rafter to be in contact again.

The gap elements are assigned a compressional spring stiffness of ten times that of the non-linear links, higher values are not selected in order to avoid floating point number errors. The behaviour of the links at the same nodes as the gaps was verified using a simple multi-span beam model to ensure that no instability issues would be encountered.

Nonlinear behaviour is not assigned to the compressive segments of the non-linear links. Thus, the model cannot account for nails being pushed back into the rafter material after damage has occurred. This simplification is justified by the fact that wind pressures for critical directions are suction pressures and the roof surface is not pushed down during the time-history analyses conducted.

The software package cannot model the compressive stiffness of the links in a conditional way i.e. only when the nails are embedded in the rafter material. Therefore, even when connections fail completely the nonlinear links still retain their compressive stiffness and if a large section of the roof fails and the applied loads are removed completely, the battens and cladding cannot fall back down to the rafters as they will be held in place by the compressive stiffness of the nonlinear links. This limitation does not affect the results as the roof section only reaches large displacements after the initiation of a cascading failure. Furthermore, at this stage of the failure, other factors such as changes and aerodynamics and internal pressurisation will play a role, factors that are not studied in this thesis.

5.1.8 Geometric Non-Linearity and Fluid-Structure Interaction

Large scale geometric nonlinearities e.g. large displacement effects and p-Δ effects will be significant in the later stages of a failure cascade. However, at these later stages of failure, changes in aerodynamics will play a greater role. Fluid-structure interaction is not included, therefore the effect on the change of aerodynamics as the roof peels away cannot be modelled by this method.

Small scale geometric nonlinearities such as deformation of cladding corrugations and depression of cladding fasteners into the cladding material is not accounted for in the model. Additionally, the withdrawal of nails due to prying forces is also not modelled, these forces may be significant in later stages of damage. However, for the initial stages of damage when battens remain perpendicular to rafters, the non-linear links are a suitable approximation.

5.2 Analysis of Structural Response – Fast Nonlinear Analysis

Fast nonlinear analysis (FNA) is a method for solving time-history finite element problems developed by Wilson et al. (1982) for seismic engineering purposes and can accurately perform non-linear time history analyses with significantly less computational effort than direct integration methods. FNA is a modal superposition time-history analysis using load dependent Ritz vectors. A key requirement of FNA is that nonlinear behaviour be localised at determined points that represent dampers, base isolators or predefined plastic hinge locations. This method is ideal for seismic engineering where structures are often designed to have localised energy dissipation devices.

In the case of light framed construction under wind loading, nonlinear behaviour is usually limited to connections as evidenced by damage survey information. Failure of members does occur but this usually takes place only in advanced stages of failure, making this technique ideal for use in this study. The FNA method is used for the time-history analyses presented in Chapter 6. Results were also compared to more computational intensive direct integration methods with near identical results. Further details of the FNA method are presented in Appendix C.

5.3 Analysis Sequence and Initial Conditions

5.3.1 Initial Conditions - Dead Load

Several time-history load cases can be run in sequence to account for initial loading conditions such as dead load before the model is subject to uplift wind pressures. To account for Dead Loads, an initial FNA analysis was run that applied self-weight loads as a quasi-static ramp. The ramp duration is 10s, which is several times larger than the period of the first mode of free vibration (0.06s.) as recommended by the software documentation (CSI 2016). The time step duration is set at 0.5s and modal damping is assumed as 5% for all Ritz modes. Solution control parameters are set to their default values as no convergence problems were encountered during the analysis.

5.3.2 Starting Ritz Vectors for FNA Analysis

Dynamic response determined by the FNA method uses the superposition of the response of the dynamic modes excited by a specific loading. The Dead Load is selected for the starting load vectors such that the internal forces calculated for the initial conditions are accurate and the initial deformed shape is symmetrical. Additionally, when running multiple FNA load cases in sequence, all cases must use the same set of Ritz vectors. The dynamic modes excited by the dead load are similar to that of the uplift pressures on the roof surface and is thus an acceptable assumption.

One-hundred (100) Ritz modes are calculated with starting load vectors based on the applied loads from the dead load and the artificial link loads that account for non-linear elements in the FNA method.

5.4 Damping

Structural damping causes energy to be lost from a dynamic system resulting in the amplitudes of oscillations being reduced over time. Damping is caused by deformations of materials and surface friction between structural and non-structural elements (Chopra 2007). The combined effect of these many interactions results in a 'damping ratio' of the structure that describes the extent of the reduction in amplitude of each oscillation during free vibration. Modelling the effects of damping in a structural analysis program requires approximating the effects of the above-mentioned physical processes by artificially removing energy from the oscillating system.

Estimating the amount of damping in a structure is difficult and considerable research has gone into this field. Damping ratios can be estimated in real structures using experimental methods such as using a rotating dynamic exciter or a hammer modal analysis for smaller components. Previous research on timber structures have measured damping ratios using experimental methods to be between 2 and 5 % (Ellis and Bougard 2001, Labonnote 2012), however, not specifically for light framed house construction used in Australia.

The damping ratio of the structure in this study was assumed to be 5% in the structural analysis program. This value of 5% is also a commonly used assumption for design of many types of structures when experimental data is not available. Some preliminary sensitivity analyses showed that the structural response and damage levels were only affected when damping ratios were increased to high levels e.g. 15%. It was only at these high levels of damping that loads at batten to rafter connections were clearly attenuated resulting in the structure being more resilient to wind loading.

Damping ratios also vary with the deformation of a structure, with damaged structures subject to large deformation having higher damping ratios. Limited literature is available on this subject specific to light framed timber housing however, 'wood structures with nailed joints' have been known to have damping ratios between 5-7% in the undamaged state and 15-20% when reaching their yield point (Newmark 1982). However, assigning a damping ratio of 15% to the undamaged structure is an inconsistent assumption as such a high damping ratio would prevent initial damage from occurring, therefore giving the structure additional resistance to wind damage that it does not have.

5.5 Chapter Summary

This Chapter has provided a detailed description of the structural analysis model and the approximations used for modelling the nonlinear behaviour of batten to rafter connections. The next Chapter presents a series of computational experiments to investigate load redistribution and progressive failure behaviour of a system of batten to rafter connections.

6 ANALYSIS AND RESULTS

This Chapter presents the results from several computer experiments that examine the mechanisms of load redistribution and progressive failure in a system of batten to rafter connections. The complexity of the analyses increases from initial static analyses that examine the load paths in the undamaged state, to non-linear quasi-static analyses that determines load redistribution with increasing damage. Following this, dynamic analyses are performed to assess failure under 'peak events' derived from wind tunnel as well as synthetic data, and determines the effect of the spatial distribution of pressure on the failure location and the effects of the correlation of loads at neighbouring connections, introduced in Chapter 3. The roof surface of the model is then subject to 10 minutes of spatially and temporally varying pressures to determine its response under realistic wind loading.

The following analyses were performed:

1. Static analysis to determine influence coefficients for reactions at batten to rafter connections in the undamaged state
2. Pull up analysis with load applied over a single connection
3. Pull up analysis to investigate behaviour of brittle connections
4. Pull up analysis to investigate behaviour of ductile connections
5. Pull up analysis with a 'peak event' pressure distribution
6. Dynamic analysis with repeated 'peak events'
7. Dynamic analysis with a simulated triangular 'peak event'
8. Dynamic Analysis with ten minutes of wind tunnel pressure time histories.

6.1 Static Analyses – Influence Surfaces

The computer model roof surface was divided into 98 panels corresponding to the locations of pressure taps on the wind tunnel model where independent surface pressure loads could be applied. Pressures that resulted in 1kN of uplift load were applied to each of the panels as separate load cases to determine influence surfaces for reactions at each connection location.

Objectives:

- Determine Load paths and load sharing in the undamaged condition
- Determine extent of influence, i.e. tributary area of a connection
- Verify computer model behaviour by comparing to testing by Jayasinghe (2012) and Frye et al. (2012)
- Check the structural stability of the model using static analyses and an eigenvector modal analysis

---

Static analyses showed that the area influencing the load at a connection is larger than the traditional tributary area. This area of influence varies depending on the connection's location on the roof surface. Generally 50% of the load is due to pressures within the traditional tributary area, and 50% lie in the area bounded by the other connections, similar to that found by Jayasinghe (2012). Colour scale diagrams showing the influence surfaces for reactions at four different connections are shown in Figure 6.1.
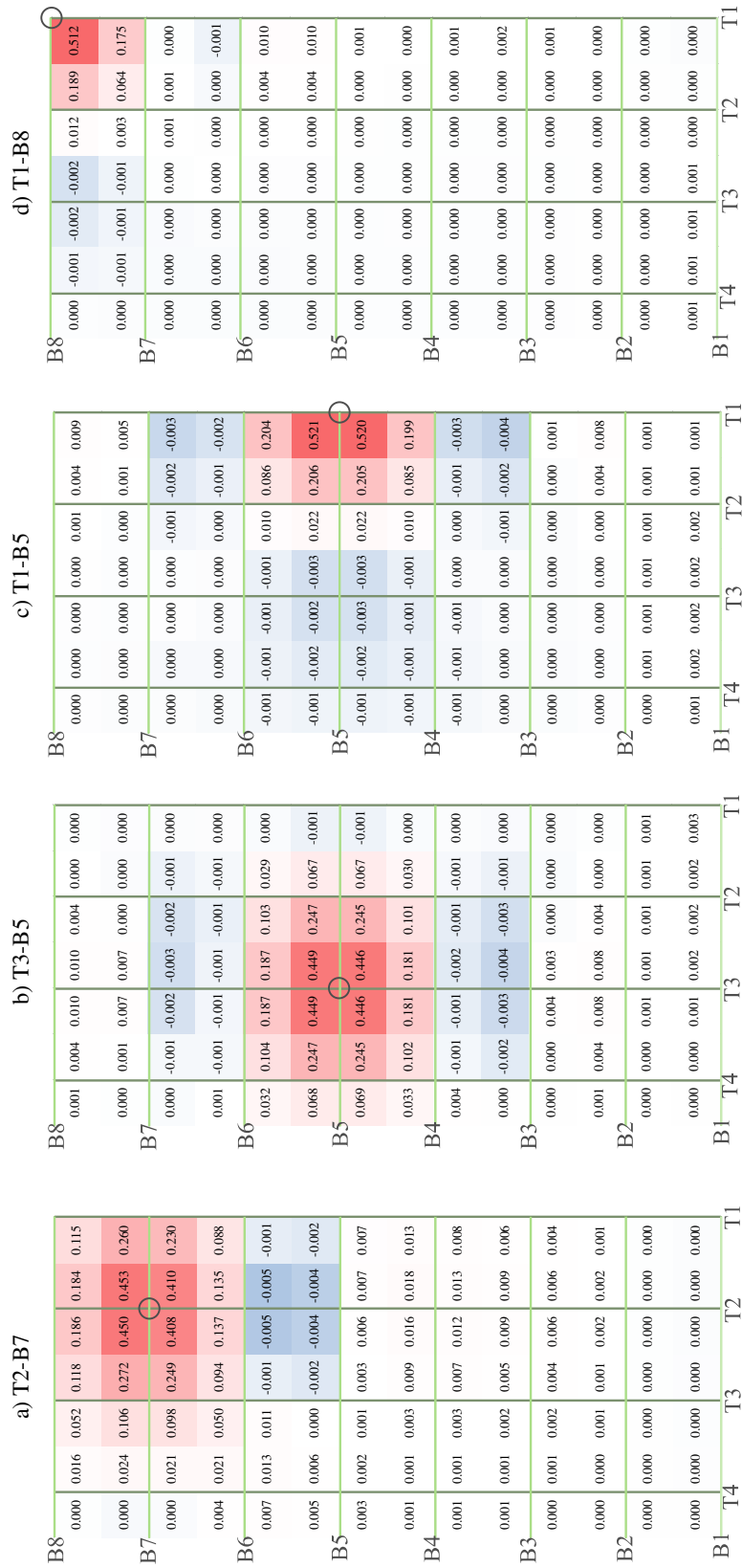
Figure 6.1 Influence coefficients for reaction forces at selected batten to rafter connections: a) T2-B7, b) T3-B5, c) T1-B5, d) T1-B8.

6.2 Patch Pull-Up Analysis

Load sharing and redistribution behaviour was studied using non-linear pull up analyses that use the FNA method. Linearly increasing uplift pressures are applied to the cladding at a quasi-static load rate and the behaviour of the structure is examined. A small patch load directly above a single batten to rafter connection (T2-B7) is applied gradually until failure to study the load sharing behaviour of one connection and its effect on its immediate neighbours.

Objectives:

1. Understand load redistribution at a basic level under quasi-static conditions
2. Explore the effects of ductility on connections
3. Reality check for the behaviour of the analysis model

Modelling Parameters:

- Analysis Method: FNA
- Timestep size: 0.001s
- Number of modes: 100
- Initial conditions: Dead Load
- Damping – Modal Damping 5%

A uniform pressure over the nominal tributary area (0.877m × 0.9), above connection T2-B7 was increased linearly at 9.5kPa/min: a load rate of approximately 7.5kN/min at the connection. This load was selected such that failure would occur within a one-minute analysis time. Figure 6.2 shows the response of a group of nine connections surrounding the loaded connection T2-B7 during the duration of the ramp load. Stages of failure are labelled showing the effects of the connections weakening and finally resulting in a cascading failure.

As load is applied above T2-B7, the system behaves as a set of springs in parallel, with part of the load being resisted by the connection T2-B7 itself and the remaining resisted by the batten and the cladding in flexure as well as extension of the neighbouring connections. Uplift loads are thus shared among neighbouring connections even when T2-B7 is undamaged and in the elastic range.

Figure 6.2 shows several plots of the connection behaviour throughout the pull up analysis. Figure 6.2 a) shows the reaction forces at all the connections in the study area, connections around T2-B7 are highlighted according to the legend showing the reaction forces of the connections close to where the load is applied. Other connections in the study area are shown in grey. Loads increase at connection T2-B7 and surrounding connections in the initial stages of the pull up. As connections fail, loads decrease at those connections and increase at others to where loads are redistributed. Some of the loads are redistributed during discrete failure events where loads are dropped by certain connections and picked up rapidly by others, indicated by the near vertical lines in the plot. About three such events occur before a cascading failure begins, where all connections fail in rapid succession.

Figure 6.2 b) shows the ratio of the load borne by each connection to the total applied load. At initial stages of the pull up, the applied loads are overcoming the self-weight of the structure after which, connection T2-B7 bears about 25% of the applied load. This percentage decreases quickly when the connection fails and loads are redistributed to neighbouring connections. Throughout the pull up analysis loads are borne by a larger number of connections as damage spreads.

Figure 6.2 c) plots the displacement of connections, i.e. the displacement of the battens relative to the rafters, throughout the pull up analysis. Displacements increase steadily at T2-B7 and surrounding connections until the yield of T2-B7. Displacement then increases rapidly at this connection and then in turn at other connections as they also yield. The connections lose most of their strength at 10mm displacement and fail completely at 25mm displacement, i.e. when the nail has withdrawn completely.

Figure 6.2 d), shows the energy balance of the structural system throughout the analysis. Potential energy in the form of strain energy in the connections increases steadily until connections begin to yield. After yield, potential energy in the form of strain energy in the battens and cladding increase rapidly as the structure beings to deform significantly. During this time, energy is also being lost through permanent deformation of the batten to rafter connections, indicated by the link hysteresis plot that also include plastic deformation of links.

During later stages of the analysis, when connections fail in rapid succession, energy dissipated by damping increases and strain energy is converted to kinetic energy as the structure moves rapidly. During the final stages of the failure cascade, the energy error increases, indicating that the computer model is not suited for modelling these final stages. Energy error is defined as: input energy – (potential energy + modal damping energy +link hysteresis + kinetic energy). This limitation is not of concern for this thesis, however, one must keep in mind that the final stages of failure are also influenced by changes in aerodynamics, internal pressure and geometric nonlinearities due to the large displacements of the structure.

Figure 6.2 e) from left to right shows a colour scale diagram indicating the reaction forces at the connection in the study area, this gives a understanding of the spread of damage across the roof surface at various stages of the pull up analysis.

Detail of the spread of damage is described as follows, with Figure 6.2 a) and e) being annotated with the corresponding stages:

1. Loads increase at connection T2-B7
2. Connection T2-B7 yields and weakens, load is redistributed to connections on either side - along the battens.
3. Connection T2-B7 weakens further and loads are redistributed along the corrugations of the cladding. The rate of increase in load at connections to the left and right reduce.
4. The first connection along a batten yields: T3-B7, which is to the left of the initial failure. Load at this connection decreases quickly followed soon after by a decrease in load at T2-B7. Loads at all other connections increase at a similar rate. Loads are now redistributed to diagonal connections at the top right and bottom right of the initial failure.
5. The first partial failure occurs: Connection T2-B7, has failed completely at this stage. Connection T1-B7 yields and fails almost immediately. Loads are redistributed to Connection T2-B6, which yields but does not fail completely. Loads are now rapidly redistributed to connections diagonally away on the top right and the bottom right.
6. The second partial failure: Diagonal Connections at the top right and bottom right yield and fail immediately. Connection T3-B7 and connection T2-B6 fail completely. Loads are redistributed to connection T2-B8 along the corrugations of the cladding and the connections diagonally away on the left - connections T3-B6 and T3-B8.
7. Connection T2-B8 yields and fails gradually. Loads have now been redistributed to connections outside the detailed study area. As connection T2-B8 fails, loads are redistributed to connections diagonally away from the initial failure at a similar rate at which T2-B8 drops the load.
8. The last of the connections in the detailed study area, T3-B6 and T3-B8 yield and fail almost immediately as there is less load sharing possible. A cascading failure commences where all connections in the study area fail in succession over the next 2 s.

In Summary, Load sharing and redistribution is a complex process and load paths change continuously as nails in connections withdraw. In this analysis, the failure of approximately three connections is required for a cascading failure to take place. Load paths and directions of load redistribution change as damage in a system increases.
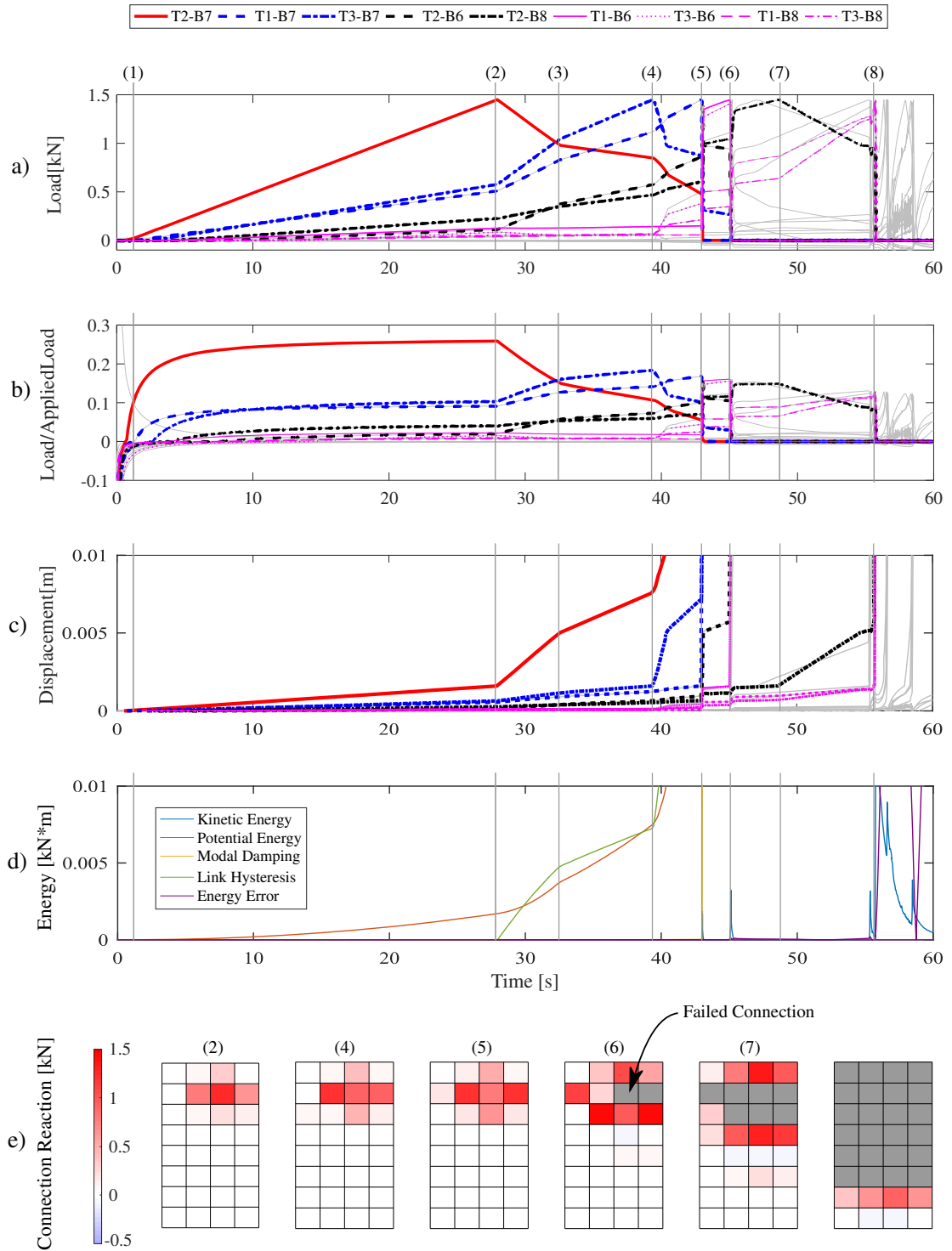
Figure 6.2 Connection response through time: a) reaction forces, b) proportions of applied load, c) connection displacement, d) energy balance, e) connection reactions showing the spread of damage

6.2.1 Mechanics of Cascading Failure – Energy Balance

During a cascading failure, connections are overloaded and fail in rapid succession causing the failure of a large section of the roof. This process can be easily imagined but is still worth careful examination using concepts of energy balance, a technique used by researchers studying progressive collapse of multistorey buildings (Szyniszewski 2009). This discussion is presented here to aid the understanding of the analyses that follow.

In a structural system, input energy from loading is balanced by strain energy of the structure. Under dynamic loads with connection non-linearity some of the input energy is also dissipated through hysteresis as well as damping. When movements of the structure occur some of the energy is also converted into kinetic energy.

During a 'pull up' analysis strain energy is 'built up' in connections until they are forced to release it - as defined by their force-displacement curve. When strain energy is released by one connection, other connections pick up this strain energy during the release. Strain energy released from initial failures causes neighbouring connections to be overloaded and fail. Strain energy released from those connections can cause additional connections to fail, and thus most connections on the roof fail in rapid succession.

During partial failures in the patch pull up analysis - the failure of one or two connections can cause loads to be suddenly redistributed to neighbours. Here, a cascading failure does not take place and the spread of failure is arrested by neighbouring connections that are able to accommodate the additional strain energy redistributed to them. Two to three of these stable 'energy states' take place before the input energy exceeds the strain energy that is able to be stored by the connections in the system - at this time a cascading failure begins.

Thus, a cascading failure begins if the strain energy released from connection failure plus the current input energy exceeds the strain energy that can be stored in neighbouring connections. When a cascading failure does occur, the strain energy released needs to exceed the resistance of the surrounding connections only and not the whole structural system. This will create a 'failure front' of batten to rafter failures that can continue to propagate, with the strain energy that cannot be accommodated within the connections is converted to kinetic energy.

6.2.2 Patch Pull-Up with Brittle Connections

The ductility of connections can have a significant impact on the resistance of the structural system. Load redistribution is a more gradual process with high ductility connections, whereas with brittle connections load redistribution occurs in discrete 'redistribution events'. For connections with realistic connection properties, the response is in between that of idealised brittle and ductile connections.

Figure 6.3 shows the same set of plots shown previously but for connections modelled with brittle properties that have the same elastic stiffness as before, but no plastic range i.e. these connections fail immediately after reaching a load of 1.45kN. Loads are redistributed at discrete events when connections fail. In this case, three such failure events occur before a cascading failure begins. With these brittle connections, the onset of cascading failure occurs at a lower applied load than for realistic connection properties.
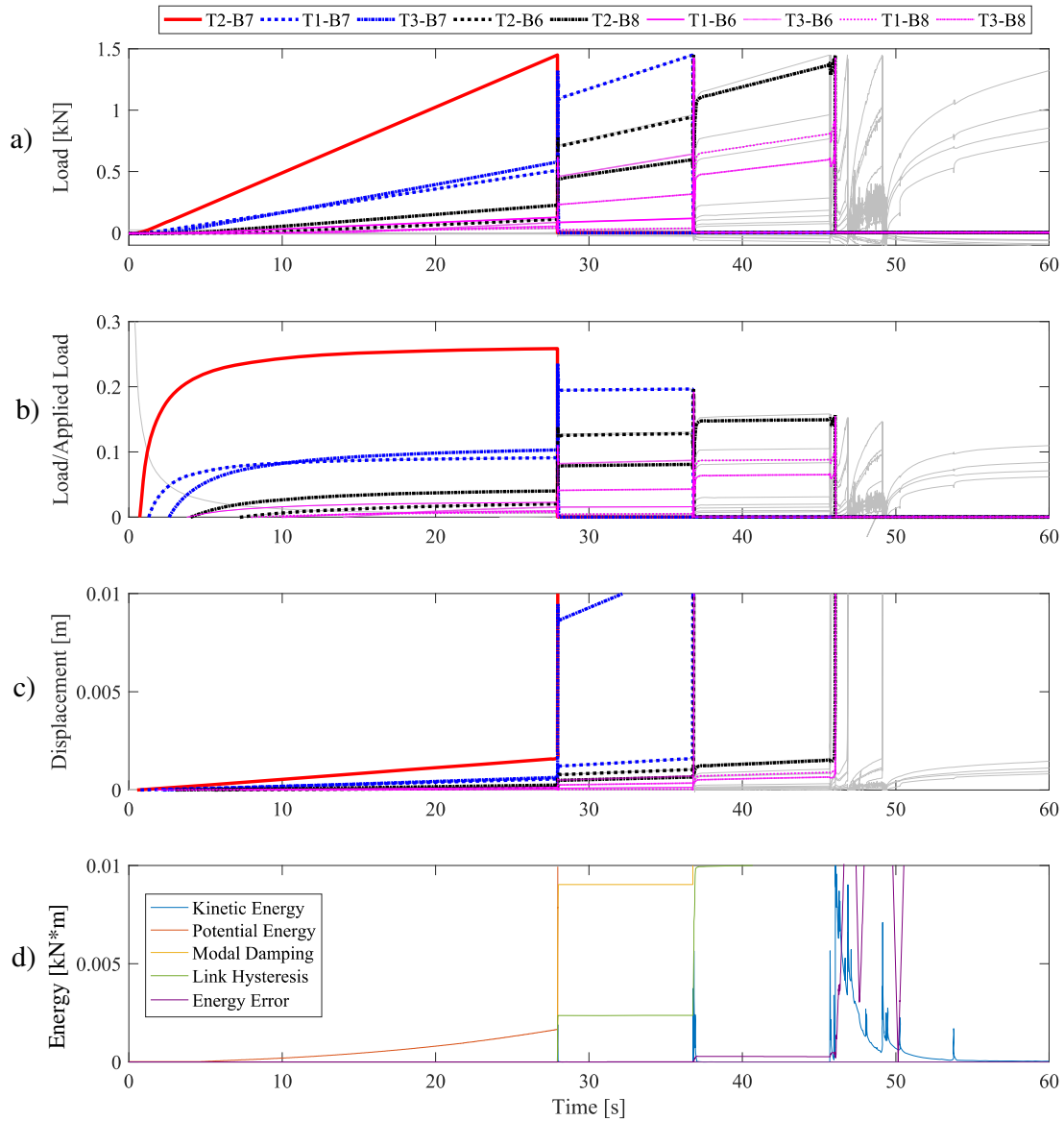
Figure 6.3 Connection response through time for brittle connections: a) reaction forces, b) proportion of applied load, c) connection displacement, d) energy balance.

6.2.3 Patch Pull-Up with Ductile Connections

The pull up analysis was repeated with ductile connections modelled with a force-displacement curve shown in Figure 6.4, with the same elastic stiffness used previously, a large plastic range at 1.45kN and then a loss of strength from 25mm to 30mm.

Figure 6.5 shows reaction forces, percentage of load, displacement and energy balance, this time for ductile connections. Connection ductility allows load redistribution to take place more gradually compared to brittle connections. Even after yield, connections can still withstand load for a considerable amount of time before failure.

Ductility also improves the resistance of the structural system, with no failure occurring during the one-minute pull up analysis. Even when running the analysis for longer than one minute the discrete redistribution events are not seen

Loads gradually increase and decrease at connections as they fail. Only upon the failure of three to four of the connections surrounding T2-B7 does a cascading failure commence. Thus connection ductility improves the resistance of structure under uplift loads allowing load sharing to take place for larger applied loads. The lack of ductility causes loads to be redistributed abruptly in distinct redistribution events.

Realistic connections properties that are semi-ductile, exhibit a mix of ductile and brittle properties with load redistribution taking place during distinct evens as well as gradually in-between these times.
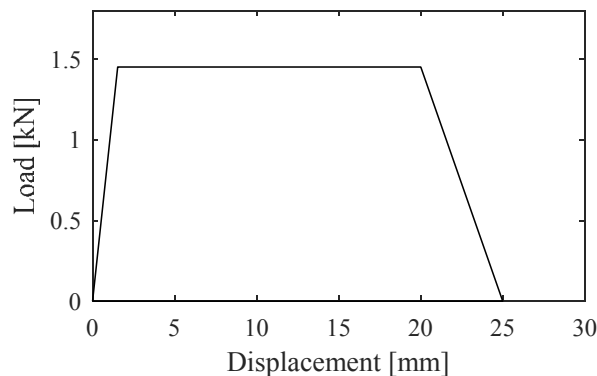
Figure 6.4 Force-displacement relation assigned to ductile connections
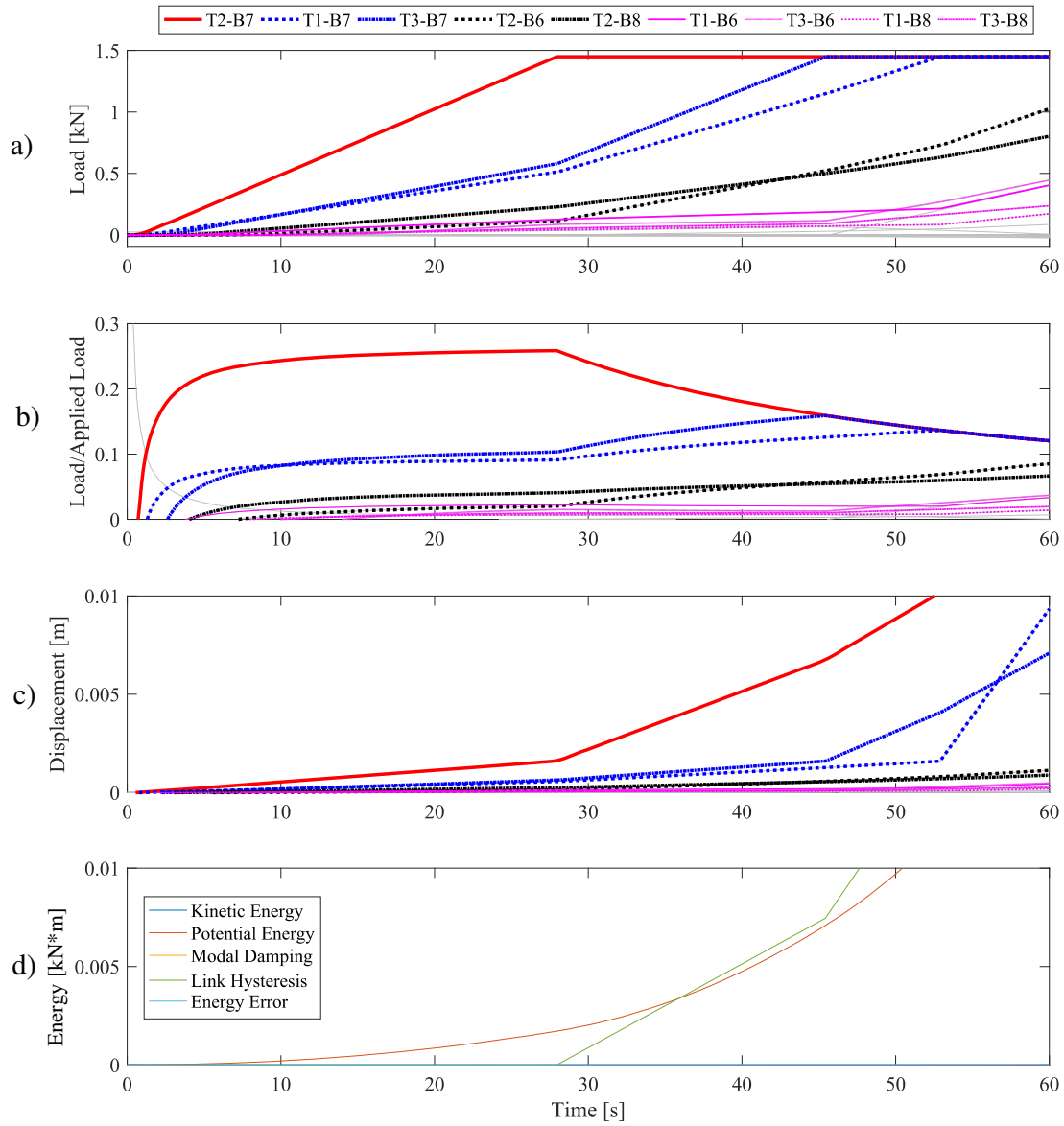
Figure 6.5 Connection response through time for ductile connections: a) reaction forces, b) % of applied load, c) connection displacement, d) energy balance.

6.3 'Peak Event' Pull Up Analysis

Spatial distributions of pressure (pressures occurring during a snapshot in time) that would occur during a 95th percentile 'peak event', such as the one described in Section 3.5 were applied, with the magnitude of the pressure increased linearly, from zero until failure. 'Peak event' pressure distributions for wind directions 180º, 210º, 270º and 300º, each with different critical connections were studied. These analyses determine where a failure cascade may begin for a certain wind direction and give an indication of how the failure would propagate while accounting for loads felt at neighbouring connections. However, any temporal variations in pressure are not considered.

Objectives:

1. Determine the direction of failure propagation for various wind directions.
2. Determine where failure initiates
3. Determine wind speeds at which damage initiates
4. Determine response to 'fully correlated' pressures
5. Determine wind speeds to be used in subsequent dynamic analyses

Modelling Parameters:

- Analysis Method: FNA
- Timestep size: 0.001s
- Number of modes: 100
- Initial conditions: Dead Load
- Damping – Modal Damping 5%

6.3.1 Definitions

The following definitions are used in the descriptions of the subsequent analyses:

Wind speeds: Unless noted otherwise, wind speeds in this analysis refer to mean wind speeds averaged over 10 minutes duration at the mid-roof height of the building (3.9m) in suburban terrain (Terrain Category 3) as modelled in the wind tunnel.

Progressive failure: Incremental failure of connections during wind loading, redistribution of loads and spread of failure resulting in a cascading failure where a large section of the roof is removed.

Onset damage wind speed: The minimum mean wind speed at mid roof height required to cause incremental damage to batten to rafter connections during peak events.

Cascading failure: The final stages of a progressive failure where almost all connections fail in rapid succession.

Cascading damage wind speed: The minimum mean wind speed at mid roof height required to cause a cascading failure of batten to rafter connections.

Onset-to-cascading damage range: The range of wind speeds in between the onset of damage and cascading damage wind speeds.

6.3.2 'Peak Event' Pressure Distributions

Under wind loading, all connections within a certain area may be subject to uplift loads, therefore when one connection weakens, loads are redistributed to connections that are already experiencing uplift loads. Figure 6.6 shows the 'peak event' pressure distributions in C_p that were applied across the roof surface for wind directions 180°, 210°, 270° and 300°. The C_p values of the pressure distributions were scaled in a linear fashion for 70s, to simulate the effect on increasing wind speed while maintaining the shape of the pressure distribution. For wind direction 210°, this results in a load rate of approx. 1.8kPa/min for pressures above the nominal tributary area of T2-B7.
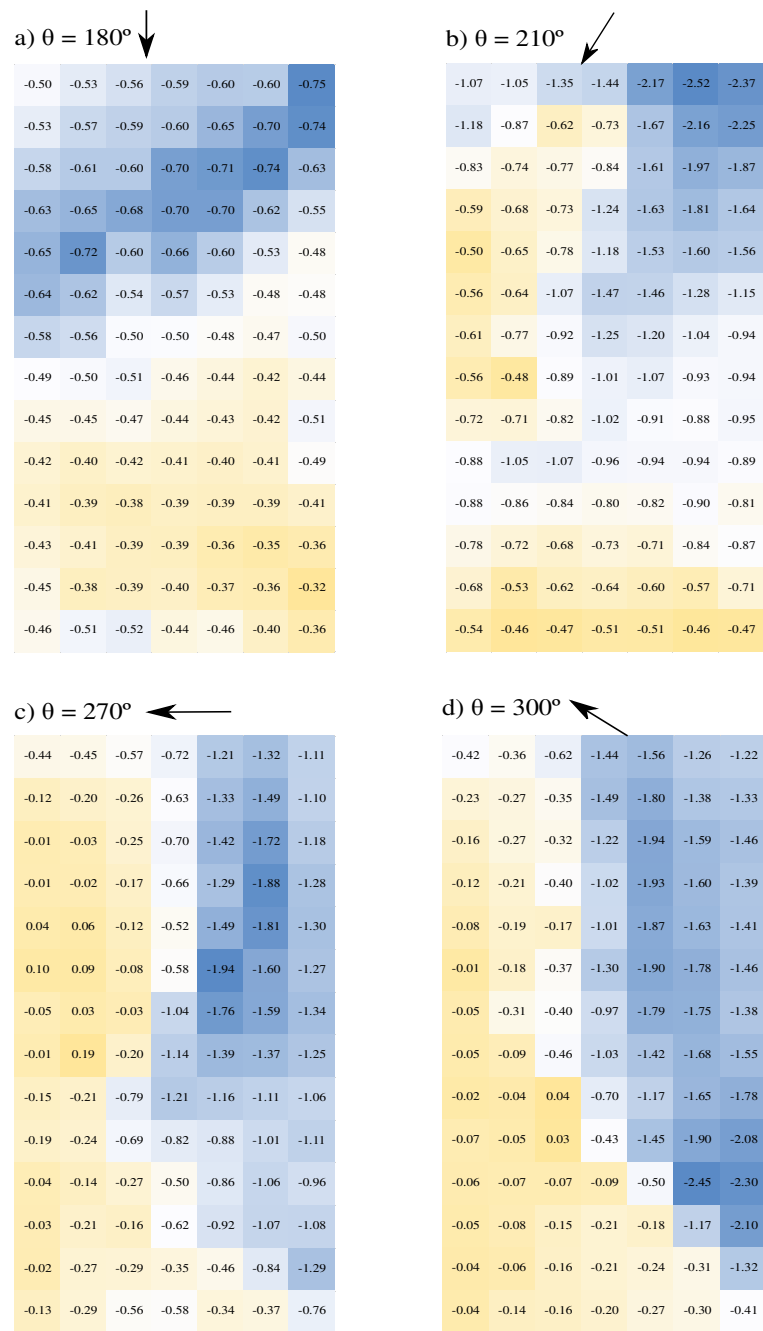
Figure 6.6 Pressure distributions (Cp) that occur during 'peak events' for selected wind directions

6.3.3 Reaction Forces and Spread of Damage

Figure 6.7 shows the reaction forces over the study area for different wind directions. As pressures are applied to the whole surface area, loads at all the connections increase at the initial stages of the pull up, instead of only the connections around T2-B7. Under a realistic pressure distribution, damage spreads further and faster than the patch pull up analysis in Section 6.2 as connections are more easily overloaded when loads are redistributed to them.

Varying behaviour can be seen during failures caused by 'peak event' pressure distributions for different wind directions. The point of initiation of the failure cascade and critical connections vary. More interestingly, the resistance of the structure also depends on the approach wind direction. For wind directions such as 270°and 300° where failure initiates closer to the middle of the study area - more load redistribution and load sharing can occur before a failure cascade begins. This is in contrast to other wind directions where damage begins closer to roof edges and corners where there are fewer neighbouring connections available for load sharing.
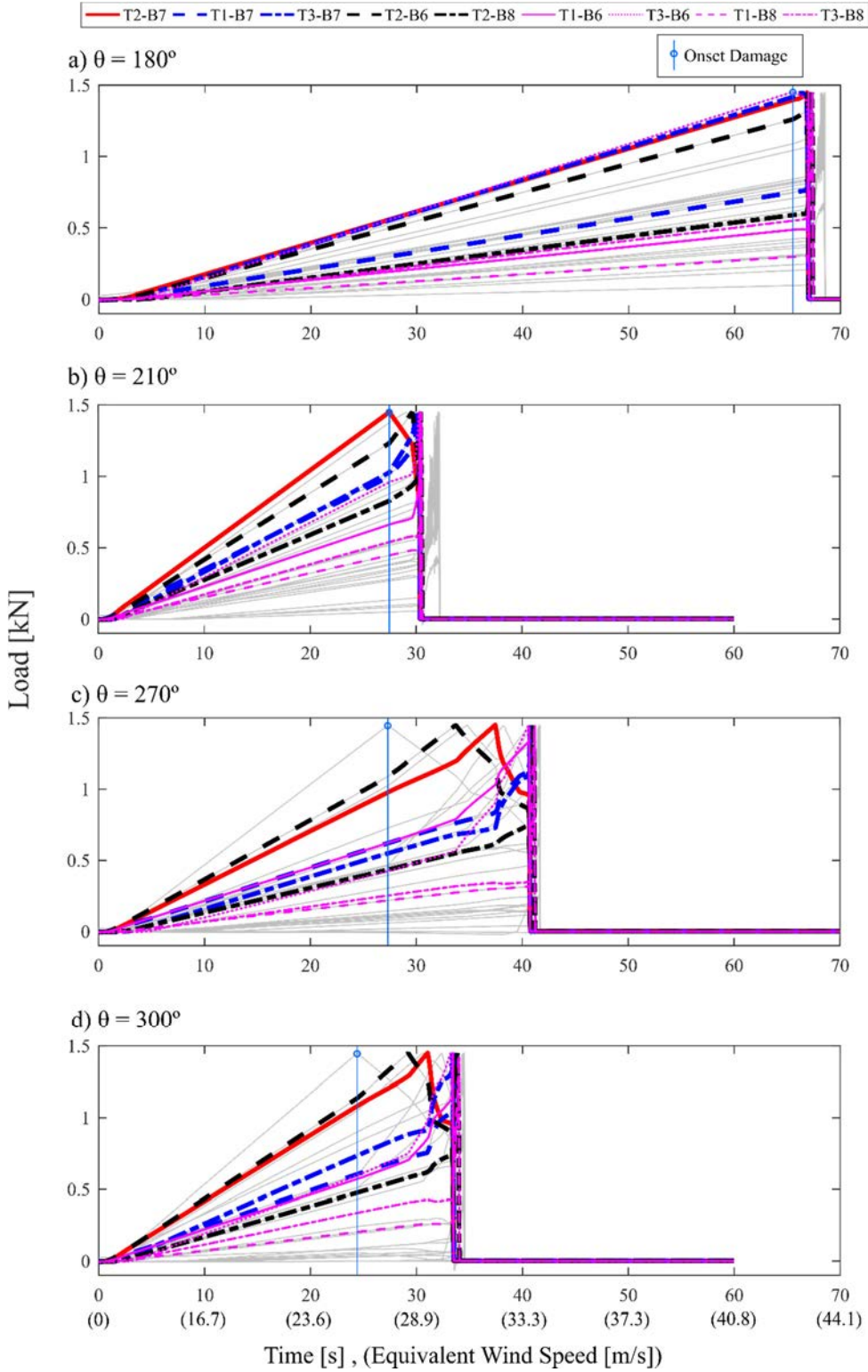
Figure 6.7 Reaction forces at connections through time during the pull up analysis for selected wind directions.

Detail of a failure cascade is shown in Figure 6.8 for a 0.7 second duration for wind direction 210°. During the cascade, loads rapidly increase to 1.45kN, then quickly decrease indicating connection failure. As loads decrease at certain connections, loads also rapidly increase at neighbouring connections, which fail in quick succession as seen between 30.4 and 30.7s.
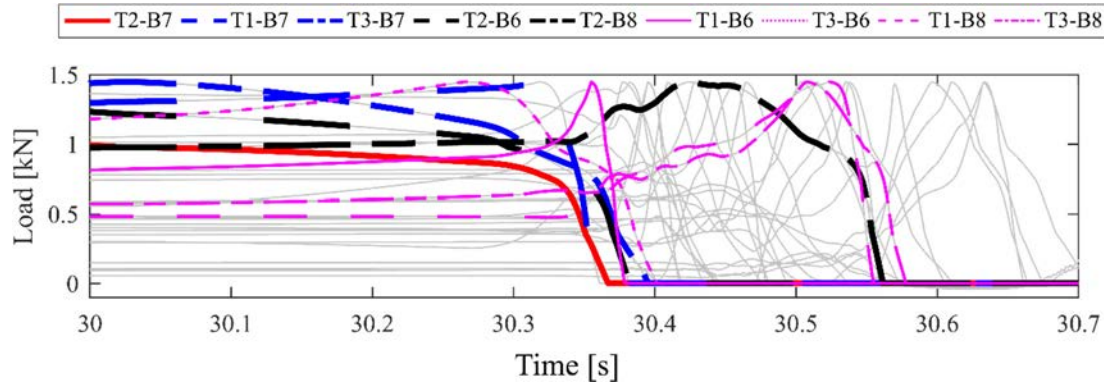
Figure 6.8 Connection reaction forces during the failure cascade for wind direction 210º

Figure 6.9 shows a colour scale diagram indicating the uplift reaction forces of the connections in the study area at several stages of damage progression for different wind directions. Each snapshot, shown from left to right, shows the reaction forces at the time a connection yields. For wind direction 210°, the spread of damage can be seen beginning at connection T2-B7 and spreading in to neighbouring connections in a similar fashion shown in the patch pull up analysis presented in Section 6.2. The path of the failure cascade can also be seen, which begins after the yielding of about six connections. Failure spreads diagonally to the left, down the roof surface towards the eaves leaving connections at the ridgeline and at the eaves intact. When these finally fail the roof is peeled away. Even for a single wind direction, each peak event is slightly different and each peak event might have its own critical connection.

 The analyses presented in this Section can give an estimate of the magnitude of wind speed required to cause damage and to identify the most vulnerable parts of the roof. Pull up analyses using peak pressure distributions showed the effect of wind direction on the location where damage initiates. Damage begins at different wind speeds for each wind direction depending on the type of flow separation mechanisms. It was found that the connection that is first damaged is usually not the one that causes a failure cascade. The amount of redistribution that can take place before a failure cascade takes place depends on where damage initiates, which in turn depends on wind direction.
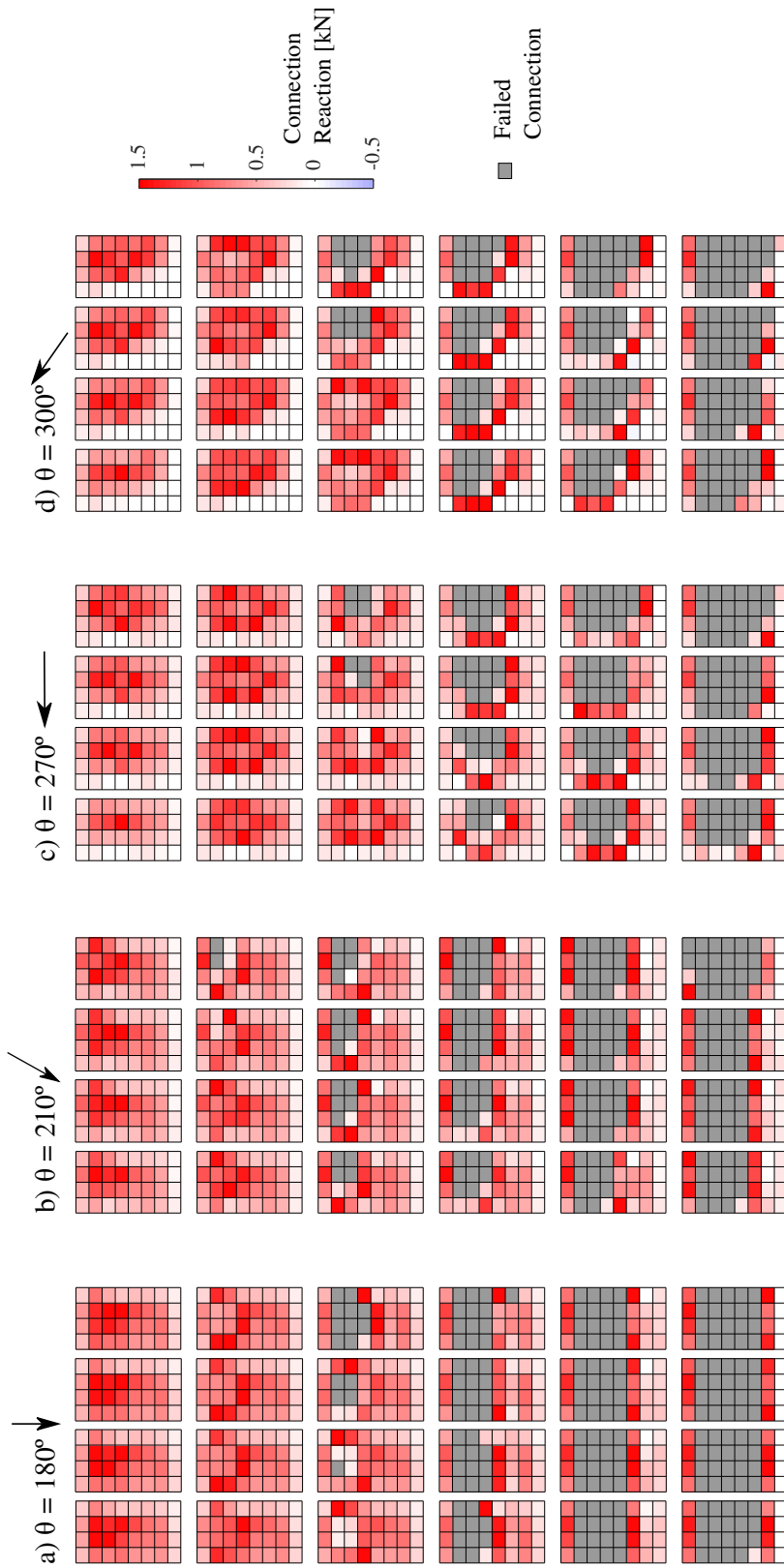
Figure 6.9 Connection reaction forces and spread of failure for selected wind directions

6.4 Summary and Discussion of Quasi Static Analyses

6.4.1 Static Analyses

Static analyses showed that the area influencing the load at a connection is larger than the traditional tributary area. The size of the tributary area varies depending on the connection's location on the roof surface.

6.4.2 Patch Pull-Up Analyses

Non-linear, quasi-static pull up analyses showed the following load sharing and redistribution behaviour of a system of batten to rafter connections:

- Load paths and directions of load redistribution change as damage in a system increases.
- The ductility of connections can have a significant impact on the overall resistance of the structural system.
- Load redistribution is a gradual process with high ductility connections, whereas with brittle connections load redistribution occurs in distinct 'redistribution events'. For connections with realistic connection properties, the response is in between that of brittle and ductile idealised connections.

6.4.3 Pull-Up Analyses with Peak Pressure Distributions

Quasi-static pull up analyses with a 'peak event' pressure distribution showed the effect of wind direction on the location where damage initiates and the directions where failure propagates during a progressive failure. This analysis ignores the effects of spatial and temporal variations in pressure.

- Wind speed thresholds for onset and cascading damage could be identified for different wind directions.
- Damage begins at different wind speeds for each wind direction depending on the flow separation mechanisms involved.
- It was found that the connection of first damage is usually not the same connection that initiates a failure cascade.
- It was also found that the amount of redundancy from neighbouring connections, i.e. the amount of load redistribution before a cascading failure begins depends on where damage first initiates, which in turn depends on wind direction. Thus, depending on wind direction there can be a varying range of wind speeds in between that which causes the onset of damage and where a cascading failure initiates.

6.4.4 Thresholds of Damage

Table 6.1 shows information on the onset of damage and the initiation of cascading failures for selected wind directions. The connection of first damage is usually not the point of the initiation of the failure cascade. Additionally, for some wind directions a larger amount of strain energy is absorbed by the structure before failure, e.g. wind direction 270°. Load redistribution can continue with successive peak events or slightly higher peak events until a threshold number of failed connections is reached. This behaviour of the structural system as a whole may be analogous to the effect that ductility of individual connection has on the resistance of the structure. Thus, the resistance of the structure is significantly affected by the location of where first damage occurs, which is in turn dependent on wind direction. The pressure distribution during a peak event can also affect how much reserve capacity the structure has between the onset of damage to a cascading failure.

Table 6.1 Critical connections and onset and cascading damage thresholds for a selected wind directions

Wind Direction [°]	Critical Connection		Mean Wind Speed [m/s]	
	Onset Damage	Cascade initiation	Onset Damage	Cascading Damage
180	T3-B6	T2-B6	42.6	43.1
210	T2-B7	T3-B7	27.6	28.9
270	T2-B5	T1-B6	27.6	33.6
300	T2-B5	T3-B7	26.0	30.4

6.4.5 Effects of Internal Pressures

The wind tunnel model study was used to measure external pressures on the roof surface. Positive Internal pressure fluctuations due to the presence of a large opening are generally uniform throughout the building volume. As such, the effect of internal pressure on the structural response would mainly be to reduce the wind speeds required for damage, i.e. reduce the onset and cascading damage thresholds. Locations of critical connections and spread of failure would be similar to the analysis presented in this thesis.

6.4.6 Fragility Relationships

The wind speeds for the onset of damage and cascading failure can be used to develop basic fragility relationships of batten to rafter failures under wind loading for a range of wind directions. A straight line was drawn from 0 to 1 from the onset to the cascading damage wind speeds, as shown in Figure 6.10.
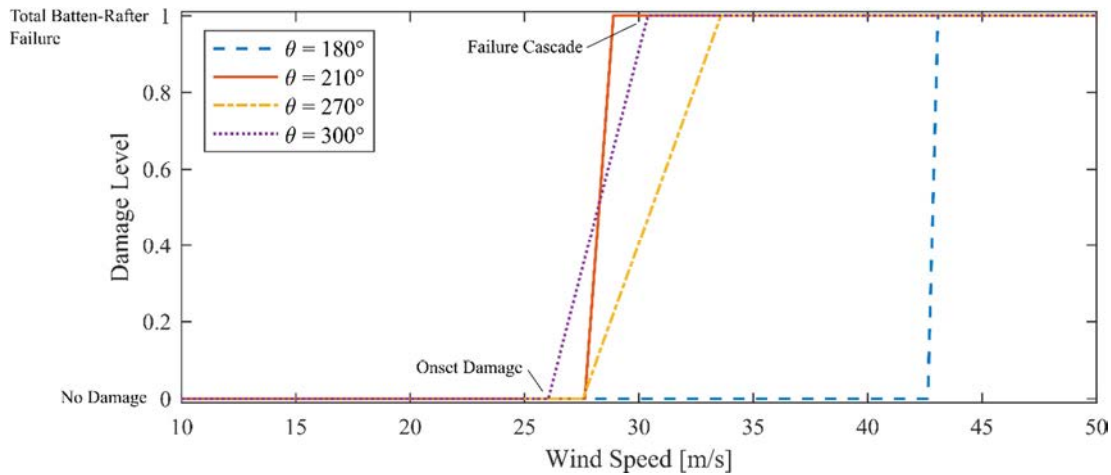
Figure 6.10 Basic fragility curves for batten-rafter failures for different wind directions

There is some overlap in the fragilities from directions 210° and 300°. In reality, batten to rafter connection fragility of the whole building for these directions is coupled as the two directions are 90° apart, thus for oblique wind directions both the windward and leeward parts of the roof are vulnerable to a batten rafter failure at similar wind speeds. However, in reality an exponential relationship may be more suitable that suggests a rapid approach to complete failure with increasing wind speed after onset of damage.

Other wind directions such as 270°and 90° may also cause some damage at wind speeds similar to the onset damage of oblique wind directions. For the orthogonal direction 180°, much higher wind speeds are required to cause the onset of damage and a failure cascade.

For wind direction 210˚ the onset-to-cascade range is only a narrow range of wind speeds. On the other hand, wind direction 270˚ has a larger onset-to-cascade range as damage initiates near the centre of the study area and allows more load redistribution to take place before a cascading failure. The redundancy/reserve capacity due to available neighbouring connections changes depending on where the first point of damage occurs.

The fragility relationships can be used to understand the many factors that influence the performance of the structural system in relation to batten rafter failures.

1. Wind direction can shift the lines to the left or right and change the slope of the lines i.e. raise or lower the onset and cascading damage wind speeds and change the onset-to-cascade range.
2. Increasing the strength of connections will increase the onset and cascading damage wind speeds, i.e. will shift lines to the right.
3. Increasing the ductility of connections will increase the onset to cascading damage range, i.e. reduce the slope of the lines.
4. The addition of positive internal pressures would reduce the onset and cascading damage wind speeds, i.e. shift the lines to the left.
5. Retrofitting certain parts of the roof will increase the onset and cascading damage wind speeds, and if retrofitting by using additional screws: the slopes of the lines may be steeper due to the brittle failure mode of screw connections.

The simplistic fragility functions shown here provide upper and lower bounds for the wind speeds where damage may occur. However, these relationships do not account for the loading history and incremental damage that could be sustained over a duration of time containing several peak events. The effects of loading history and dynamic loading will be investigated in the following sections on dynamic analysis.

6.4.7 Damaging Wind Speeds in Real Events

The onset damage (~28m/s) and cascading damage (~30m/s) mean wind speeds at mid roof height for the critical wind direction 210deg are equivalent to 0.2s gust wind speeds at 10m height of 75m/s (268km/h) and 80m/s (288km/h) in open terrain.

Damage recorded in Proserpine, Queensland during cyclone Debbie corresponded to maximum 0.2s gust wind speeds at 10m height of 44.4m/s (160km/h) in open terrain (Boughton et al. 2017). Lower wind speeds for damage compared the computer model can be mainly attributed to the effects of positive internal pressures due to windward wall openings, which are not considered in the computer model.

Other factors that contribute to lower wind speeds required for damage during real events include:

- Effects of terrain and topography
- Variability in connection strengths in a real population of houses
- Variability roof geometries and heights
- Variability in batten and rafter spacing

It is expected that with improved input data that accounts for the factors cited above the model would yield onset and cascading damage wind speeds to those recorded during cyclone events. Nevertheless, the damage thresholds determined from the model are in a similar range to those recorded during recent cyclones where batten to rafter failures occurred. This similarity is significant, as no additional calibration was required of the computer model to produce these results.

6.5 Dynamic Analyses with Repeated Peak Events

Dynamic Analyses were conducted using spatial and temporal pressure fluctuations derived from the wind tunnel tests described in Chapter 3. An approximately two second (full-scale) duration of time history with a 'peak event' was applied to the structural system repeatedly similar to the process used during dynamic connection testing. The magnitude and the time scaling of the pressure traces were modified based on the desired full-scale wind speed. Five 95th percentile peak events from wind direction 210º are applied to the analysis model over a duration of about 45 s at a constant mean wind speed of 28.4m/s, which is in between the onset and cascading damage thresholds. A small time step size of 0.0001s was used to capture the connection response.

Objectives:

1. Determine structural response under consistent spatial and temporal variations in wind pressure
2. Determine load redistribution during damage caused by individual peak events
3. Determine the effects of correlations of wind pressures across the roof surface

Modelling Parameters:

- Analysis Method: FNA
- Timestep size: 0.0001s
- Number of modes: 100
- Initial conditions: Dead Load
- Damping – Modal Damping 5%

During the analysis the structural system withstood five peak events before a cascading failure takes place. Nails are incrementally withdrawn during each peak event resulting in load redistribution and spread of damage among the batten to rafter connections beginning with the critical connection T2-B7.

Figure 6.11 shows the reaction forces and displacements of connections as well as the energy plots during five repeated peak events. The reaction force plot, Figure 6.11 a) shows the effects of load redistribution as different connections experience higher or lower reaction forces after each peak event. Connections such as T2-B7 that fail after the second peak event are subject to compressive loads while the nails are partially withdrawn.

Displacements, of connections shown in Figure 6.11 b), highlight the incremental nail slips and permanent deformation caused by each peak event. Deformation per peak event increases as damage within the structure also increases.

Figure 6.11 c) shows the energy balance of the system during the analysis. Potential energy increases and decreases during each peak event, however an overall increase in potential energy is also present as battens and cladding absorb strain energy in bending after connections yield. Energy dissipated through work done on connections in permanent deformation also increase in distinct steps during each peak event. Energy dissipated by modal damping also increases over time and finally dramatically increases during the failure cascade when rapid movements occur.

Finally, during the failure cascade, potential energy in connections and applied loads are converted into kinetic energy as the roof is peeled away. However, potential energy within the system increases overall as cladding and battens are placed under increasing flexure. Error in the energy balance increases during the later stages of the cascade indicating that the structural response during these stages of large displacements may be unreliable.
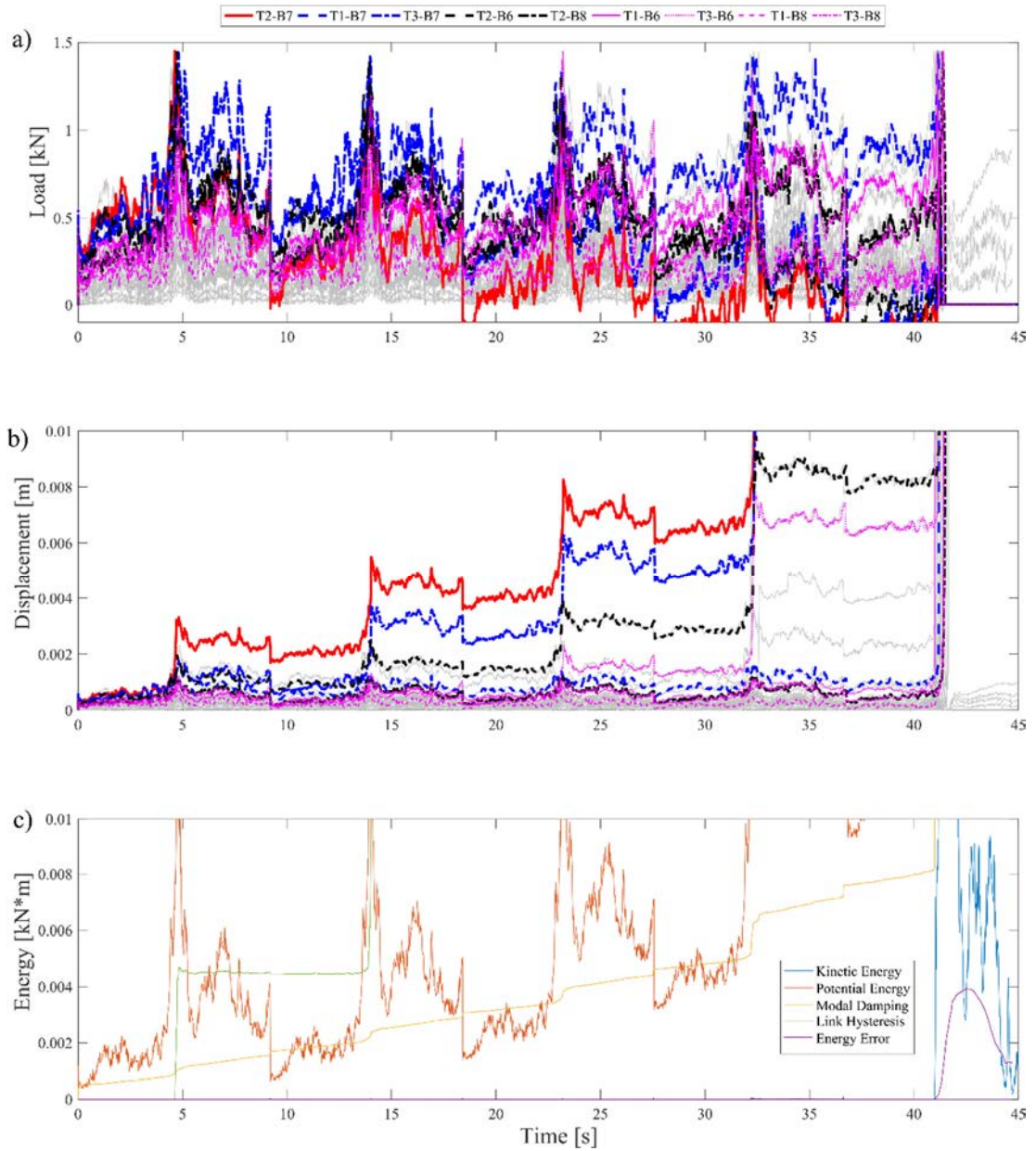
Figure 6.11 Repeated Peak Events at 28.4m/s for wind direction 210° showing incremental damage until a failure cascade at the 5th peak event.

Additional details of structural behaviour are shown in Figure 6.12 to Figure 6.14. These figures show individual sub plots of connection behaviour of the 32 connections in the study area, highlighting the spatial distribution of connection responses.

Figure 6.12 shows plots of force vs displacement for the 32 connections in the study area. Diagonal slip bands similar to those observed during connection testing can been seen in the force-displacement plots of the modelled connection response due to the repeated peak events. Before a cascading failure, nail slips occur at different times for each connection. All connections are assigned the same strength and thus the outlines of the force-displacement curves are identical. Connections near T2-B7 exhibit these diagonal nail slips, however all other connections show the force displacement behaviour of a nail withdrawal in a single motion - indicating that these connections yield and fail during the failure cascade.

Figure 6.13 shows the reaction forces at individual connections through time. Connections T2-B7 and its neighbours are seen to decrease loads they experience after each peak event. Other connections experience higher loads after each peak load, indicating loads are being redistributed *to* them from connections that are being damaged. The near vertical line at approximately 40s shows the time where the failure cascade taking place, which occurs within less than 0.5s. Load is shared and redistributed in similar directions to the pull up analysis. The structure becomes unstable after several peak events and a cascading failure then commences and propagates in a similar manner to that of the pull up analysis.

After the failure of the first connection (T2-B7), small compression loads are felt at this connection. This is because upon unloading, the stiffness of the surrounding structure attempts to push the nail back into the rafter. This is expected due to the behaviour of a connection sample under reverse cycle loading, as shown in Appendix B Figure B.1.

Figure 6.14 shows the displacements of the individual connections. Incremental nail slips and permanent deformation can be clearly seen in the step-like shape of the plots of connection T2-B7 and neighbours. Vertical lines at about 40s indicate a rapid increase in displacement due to the cascading failure.

Applying repeated peak events showed that no damage occurred for wind speeds below the onset damage threshold. Whereas for peak events at the cascade threshold, all connections would fail during the first peak event. For wind speeds in between the onset damage and cascade damage thresholds, the structure could withstand several peak events before a cascading failure begins.

These damage thresholds correspond to those noted during the quasi-static pull up analyses. This indicates that load rate and the spatial and temporal fluctuations in pressure across the study area have little effect on the wind speeds that cause damage to the structure. Quasi-static non-linear pull up analyses may be an effective yet efficient way to determine a system's resistance to wind loads.
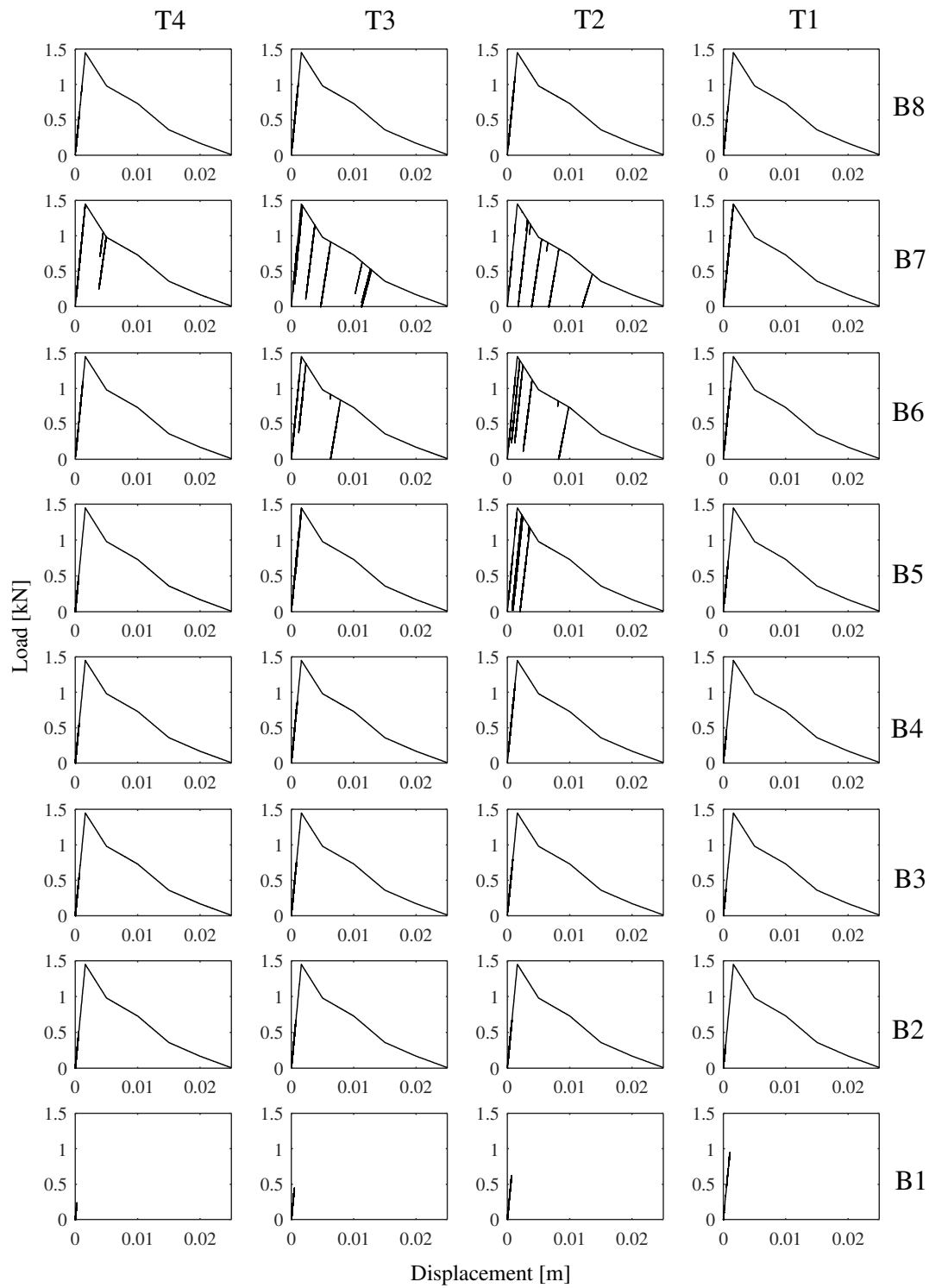
Figure 6.12 Force-displacement plots of the 32 connections in the study area showing diagonal bands from the incremental nail slips (28.4m/s at wind direction 210°).
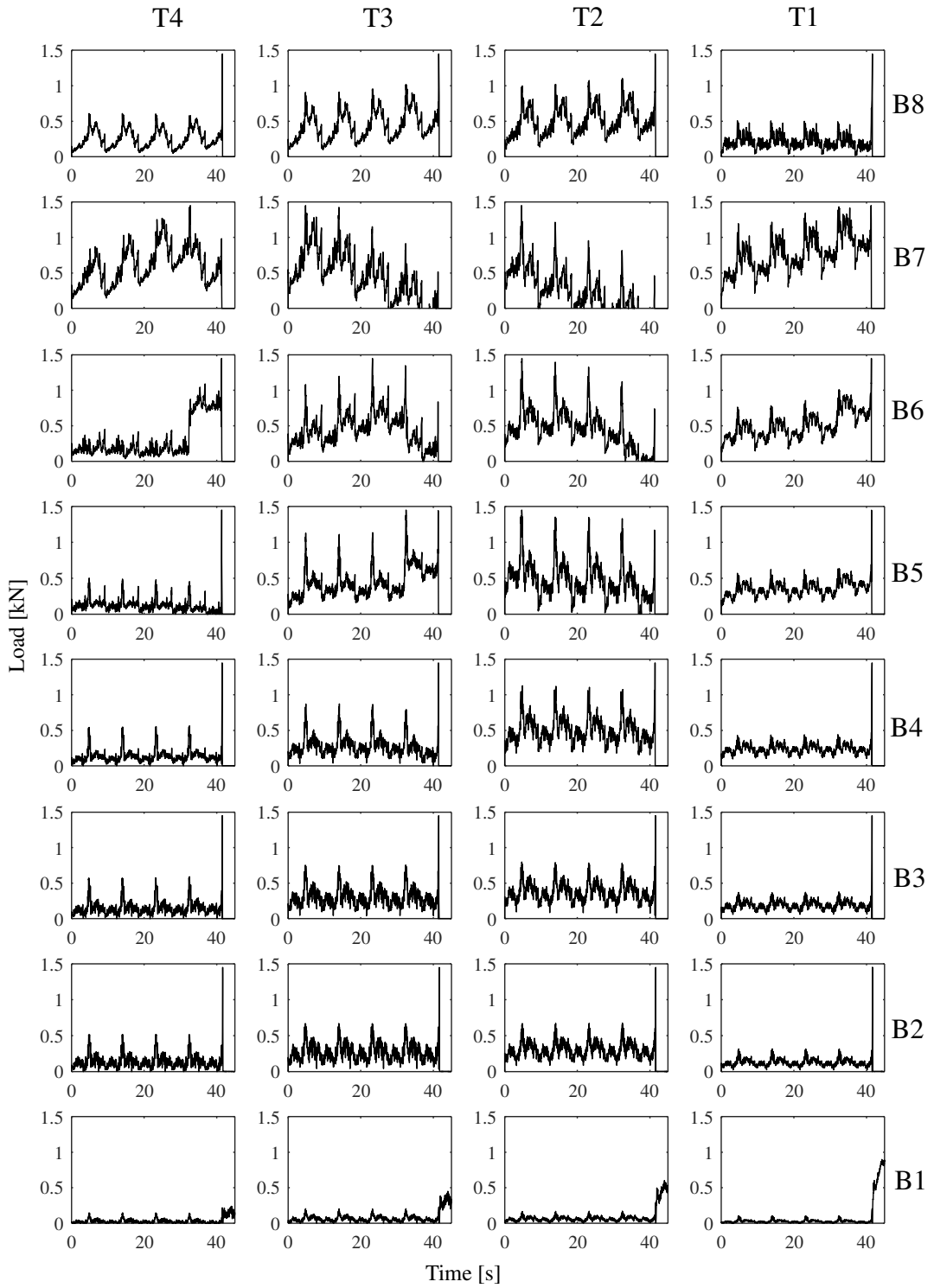
Figure 6.13 Reaction forces at connection over time showing load redistribution as loads increase and decrease at various connections as damage spreads from the critical connection (28.4m/s at wind direction 210°).
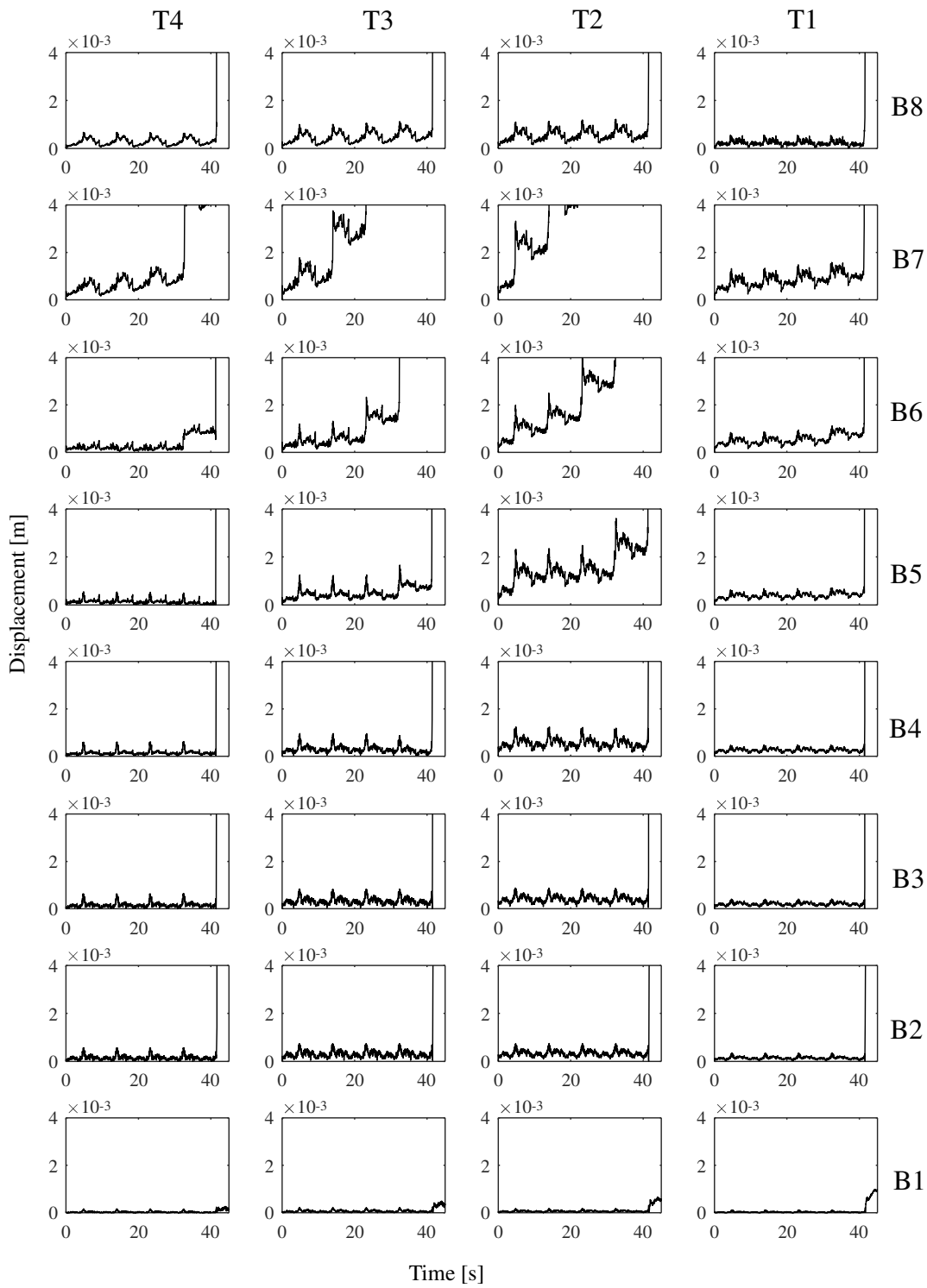
Figure 6.14 Displacement of connections over time showing jumps in displacement when nails slip (28.4m/s at wind direction 210°).

6.5.1 Load Redistribution during a Peak Event

Connection and system response was examined in detail during the first peak event at approximately 5s shown in the previous section that causes incremental damage to the structure. Structural response was compared with a case with a slightly lower wind speed where no damage occurs.

Figure 6.15 shows detail of the connection response during the first peak event, between 4 and 6s. Loads at different connections vary greatly, indicating the spatial and temporal variations of pressure across the roof surface. Different connections reach their peak load at different times and the waveforms of pressure time history at each connection are also different.

Load redistribution begins immediately at the time when the critical connection T2-B7 reaches is yield load of 1.45kN. After this point in time, the load required to withdraw the nails further also decreases. Load redistribution occurs for as long as the load at the critical connection exceeds its yield threshold.
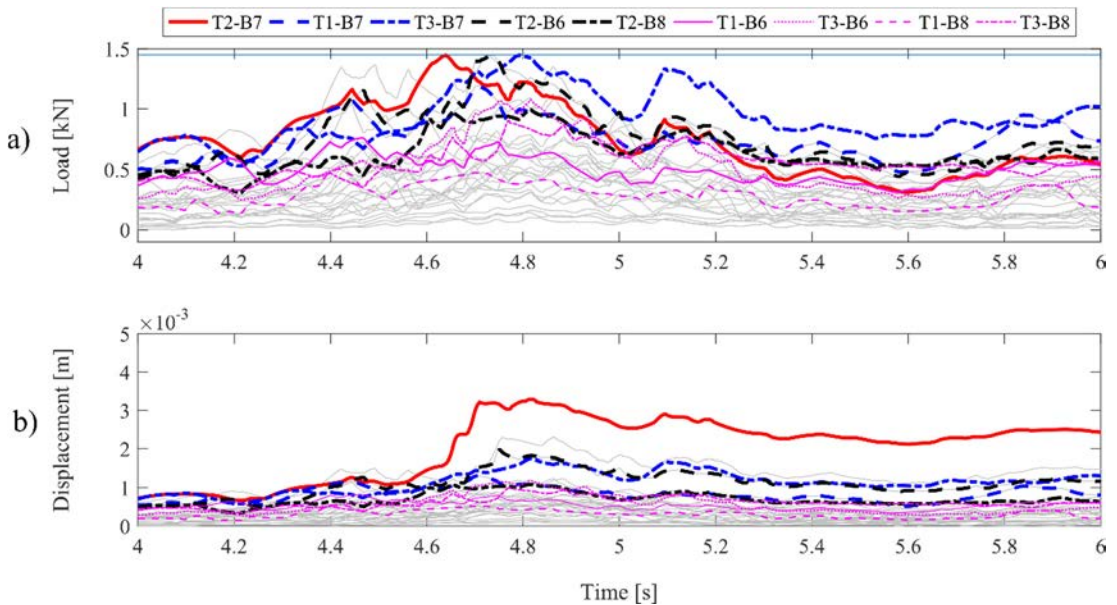
Figure 6.15 Detail of Load redistribution during a' peak-event' for wind direction 210° at 28.4m/s

It is difficult to see when the connections are yielding when studying the reaction forces alone. However, the displacement plots indicate connection T2-B7 begins to yield between about 4.6 and 4.8s, just before the apex of the peak event that occurs at about 4.65s. It appears as though the nail slip continues even when T2-B7 is no longer at 1.45kN. This is expected, as the yield threshold is lower for each connection after they yield. Additionally, yielded connections attract compression loads when unloaded as now the nails are being pushed back in place by the stiffness of the surrounding structure. Due to the small scale fluctuations within the peak event it is difficult to see when and where loads are redistributed *to* when T2-B7 is yielding.

Figure 6.16 shows the connection response during the same peak, with the same time scaling but at a lower magnitude that causes no damage to the connections. Spatial and temporal fluctuations can still be seen, however, no permanent deformation occurs during the peak event. Comparison of Figure 6.15 and Figure 6.16 shows that loads at connection T2-B6 do not increase to the same levels as when nail slip occurs, indicating the absence of load redistribution.
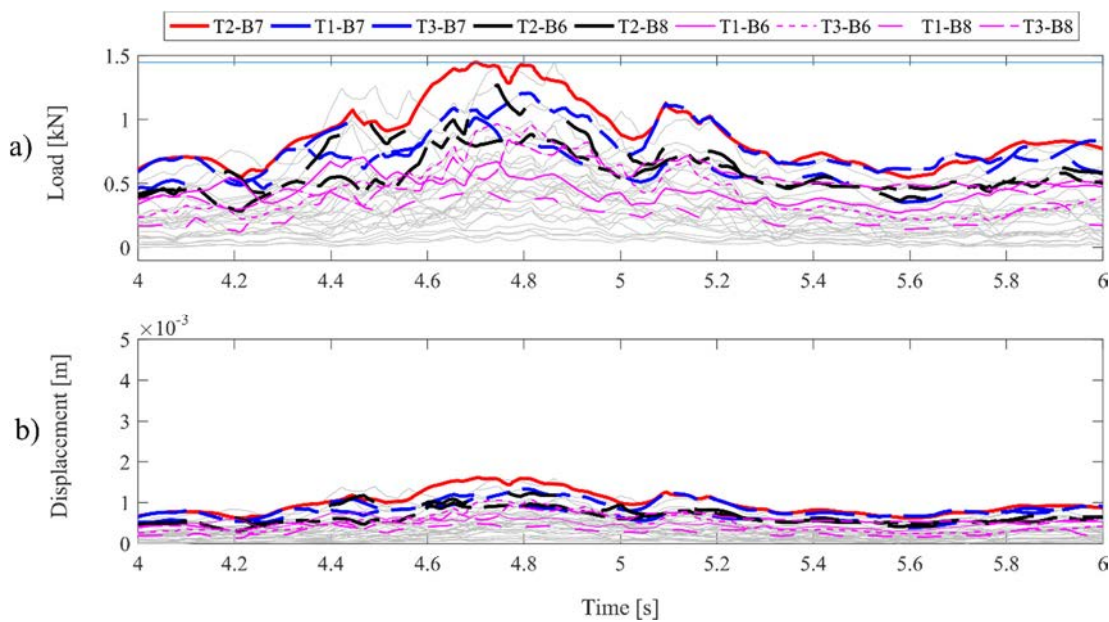
Figure 6.16 Detail of 'peak-event' for wind direction 210° at 27.6m/s, showing no damage.

Load redistribution will occur for a duration of time that the connection exceeds its yield threshold. This duration of time depends on the time history of the applied wind pressures and the current state of the connections i.e. how close they are to their yield threshold.

Lead or lag times between the maximum loads at different connections are of similar duration to the time that loads are redistributed for during peak events. Therefore, the correlations of peak events from neighbouring connections may affect load sharing and redistribution and hence progressive failure. Large lag times may still exacerbate cascading failure as some connections may reach their peak load at the time which they have loads redistributed to them. However, from the analysis results shown here, this effect seems to be limited.

As it is still difficult to examine the load redistribution behaviour during a peak event. An analysis using a synthetic peak event with a triangle shaped waveform is presented in the next section.

6.5.2 Triangular Peak Load Simulation

Objective:

1. Determine load redistribution behaviour under a simulated perfectly temporally correlated peak event

Modelling Parameters:

- Analysis Method: FNA
- Timestep size: 0.0001s
- Number of modes: 100
- Initial conditions: Dead Load
- Damping – Modal Damping 5%

To get a better understanding of the load redistribution during a peak event, the 'peak event' pressure distribution for wind direction 210° used in Section 6.3 was increased and decreased dynamically in a triangular waveform to simulate the loading rate of a 'peak event'. This analysis shows the structural response under a perfectly correlated dynamic load, i.e., loads increase and decrease at all connections at the same time and the shape of the pressure distribution across the roof surface remains constant.

Figure 6.17 shows the connection response during a perfectly temporally correlated synthetic peak event for the critical wind direction 210° at a magnitude that causes no damage to the structure. Loads and displacements at connections increase and decrease over the one-second 'peak event' and no permanent deformation occurs.
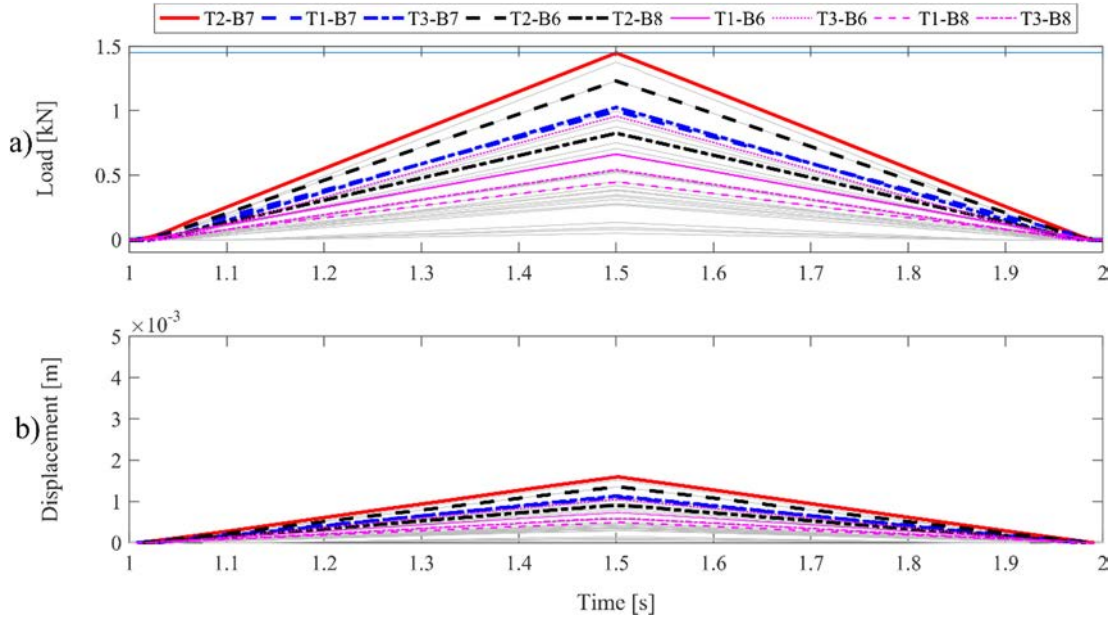
Figure 6.17 Perfectly correlated triangular peak event, representing a wind speed of 27.6m/s at 210° causing no damage to the structure.

Figure 6.18 shows the connection response under a peak event that causes partial damage to the structure where load redistribution and permanent deformation occurs. At approximately 1.45s connection T2-B7 reaches its yield load. Connection T2-B7 begins to yield and continues to do so until the maxima of the peak event, at which time the applied loads begin to decrease. The critical connection reaches its yield load slightly before the peak in applied loads. While the critical connection is yielding, loads at other connections increase. There is again a seamless transition to when load redistribution occurs.
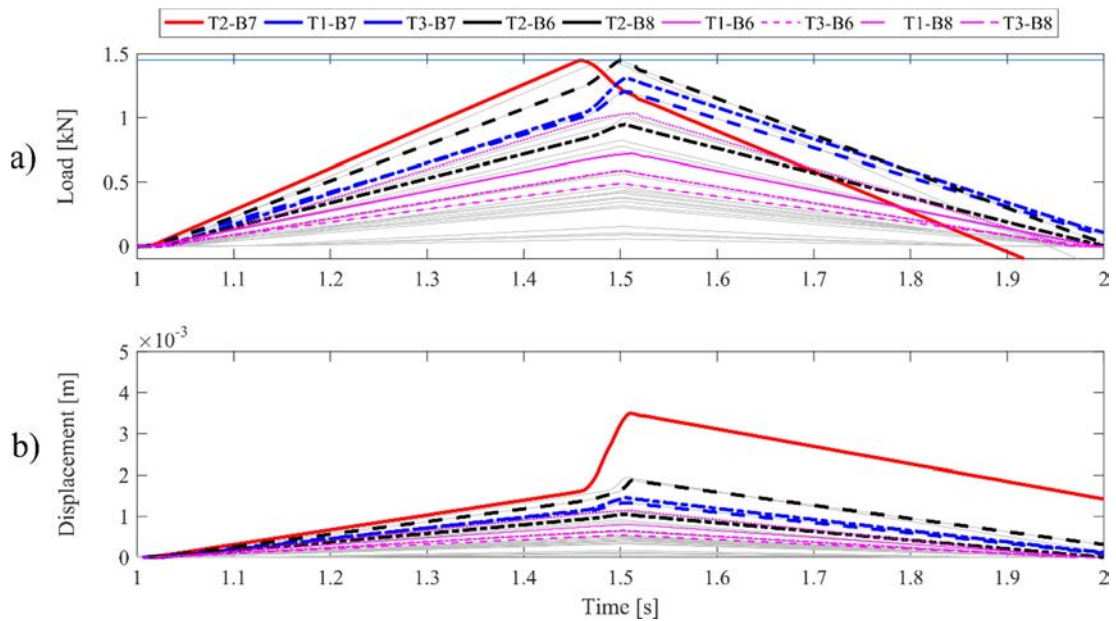
Figure 6.18 Triangular 'peak-event' representing a wind speed of 28.8m/s at 210°
Showing load redistribution during a perfectly correlated peak event.

Connections where load has been redistributed *to* reach their maximum load at the time when the maximum applied load occurs. As connection T2-B7 begins to yield, loads at neighbouring connections simultaneously increase as loads are redistributed to them in a seamless fashion. Reaction forces at these connections continue to increase until the maxima of the simulated peak event at 1.5s when loads at all connections decrease. At this particular magnitude 'peak event', it is only connection T2-B7 that is damaged.

Loads decrease during the ramp down of the simulated peak event, however, the critical connection that was damaged is subject to compressive loads after the structure is unloaded. This simulates the nails of the connection being pushed back into the rafter by the stiffness of the surrounding structure.

Load redistribution will occur regardless of whether neighbouring connections are also experiencing peak loads at the same time. Whether neighbouring connections yield may be influenced by lead or lag times and therefore the correlation wind pressures. However, it is expected that under real wind loads these lead or lag times will only have a minor effect.

The effects of increasing the magnitude of load even further are shown in Figure 6.19. Loads are increased in magnitude to represent a mean wind speed at mid roof height of 30.3m/s. However, time scaling is the same as the previous analyses so they can be readily compared to each other. At about 1.41 s T2-B7 has reached is yield load, applied loads continue to increase until 1.5 s at which time the damage to T2-B7 has caused it to fail completely.
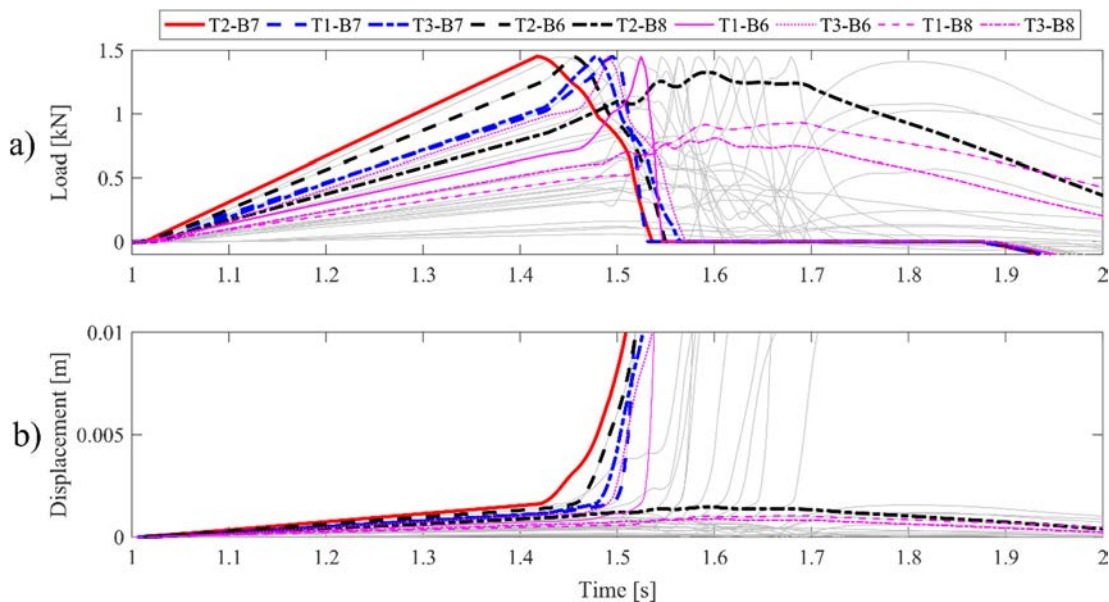
Figure 6.19 Triangular 'peak-event' representing a wind speed of 30.3m/s at 210º showing a partial failure cascade during a perfectly correlated peak event.

Neighbouring connections increase in load when T2-B7 begins to yield as shown in the previous figure. However, these connections also yield and fail one after another within 1.5s. By this time, a cascading failure has commenced and several other connections fail in rapid succession, even as applied loads decrease. However, in this case, a few connections remain intact at the end of the ramp down of the peak event.

For loads greater than the cascade threshold, load redistribution begins when the critical connection yields. Neighbouring connections then yield and fail in succession during the peak event as long as the applied pressure causes loads at connections to exceed their current yield threshold. In the case shown in Figure 6.19, loads are not high, for long enough for all connections to fail and the failure cascade is only partly complete.

6.5.3 Comments on the Effect of Load Duration

As noted from the previous analyses, transfer of load from one connection to the next occurs effectively instantly. However, the displacement of the connection in response to the load is time dependent, and is influenced by the mass, stiffness and damping of the structural system. Therefore, when subjected to a given load above the connection's yield load, the resulting connection displacement is dependent on the duration for which the load is applied.

Previous research has shown that the load rates of wind load do not affect nailed connection response. In fact, load rate cannot affect connection response in the computer model due to the way that nail behaviour is idealised as nonlinear links. However, the duration that load exceeds a connection's yield threshold affects the overall structural response as there is a time dependence for connections to displace in response to the loads they experience.

The time duration for connections to displace are similar duration to peak events, therefore connections can experience several peak events before a cascading failure takes place, as shown in Figure 6.11. Further displacement of a connection can result in further load redistribution to other connections. Thus, a 'balancing out' takes place, which occurs for about one second in the structure.

6.6 Ten-Minute Time History Analysis

Objectives:

1. Study structural response under realistic time history wind loads
2. Determine the effects of damage due to peak events of different magnitudes

Modelling Parameters:

- Analysis Method: FNA
- Timestep size: 0.01s
- Number of modes: 100
- Initial conditions: Dead Load
- Damping- Modal Damping 5%

Fluctuating wind pressures from the wind tunnel study across the entire study area were used to run a time history analysis for a ten-minute duration in full scale. This analysis is able to account for spatial and temporal variations in pressures as well as loading rate and dynamic effects. Using the FNA method the analysis takes about 30 minutes to complete using a personal computer.

The wind direction selected was the critical wind direction 210º for the entire ten-minute duration. The mean wind speed remains constant during the analysis. Results from two mean wind speeds are presented in the following sections: the onset-damage wind speed and an intermediate wind speed in between onset and cascading-damage thresholds.

6.6.1 Time History Analysis at Onset Damage Wind Speed (27.6m/s):

Connection responses are shown in Figure 6.20 for a 10-minute (600 s) duration under spatial and temporal pressure fluctuations representing a mean wind speed of 27.6m/s from wind direction 210°. Displacements of the connections, shown in Figure 6.20 b) indicates that an increasing amount of permanent deformation for only certain connections occur at this wind speed.
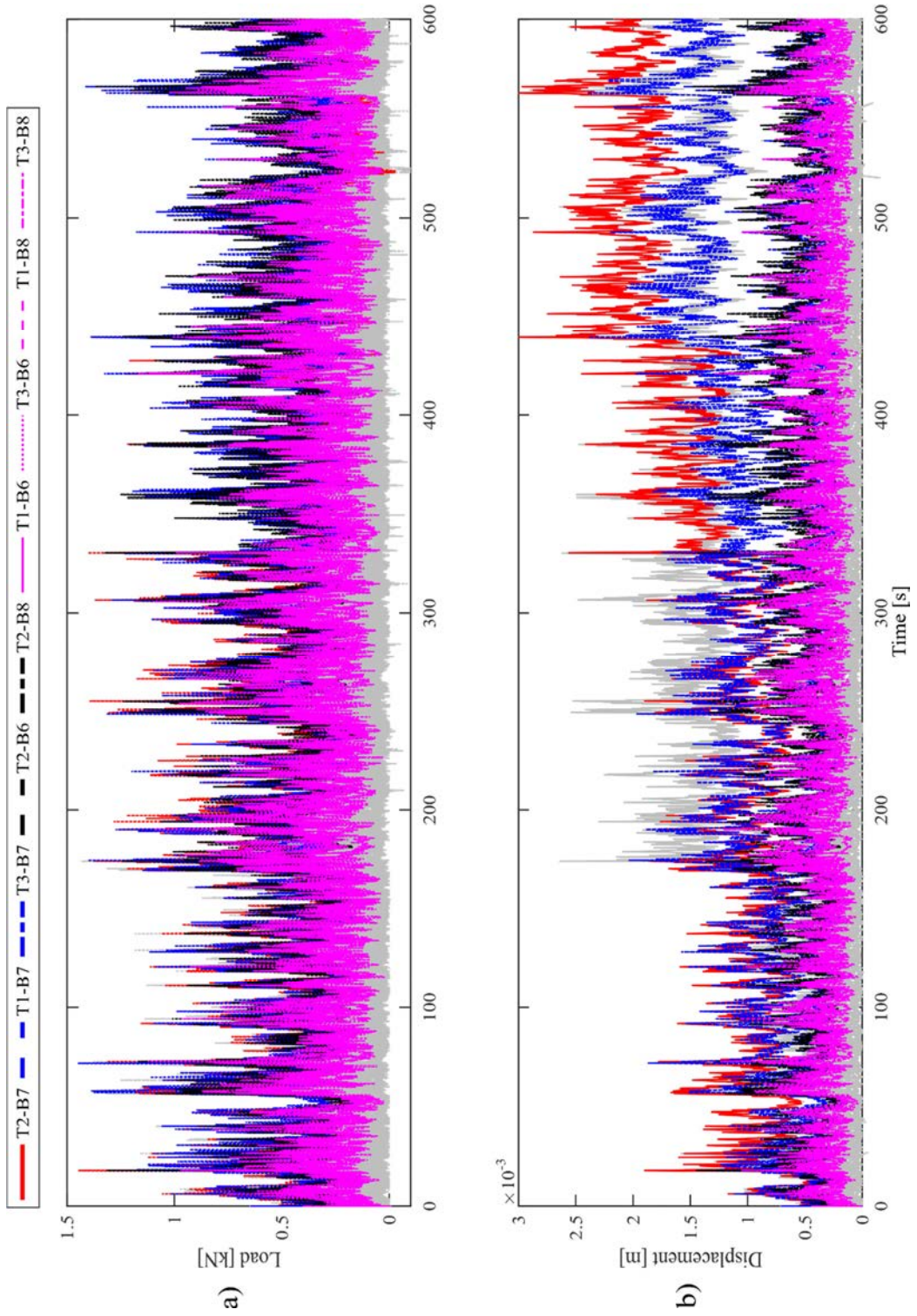
Figure 6.20 Structural response over 600s at 27.6m/s from wind direction 210° - a) reaction forces at connections, b) connection dispalcements

As shown in the previous analyses, damage to connections only occurs during peak events, and lower level pressure fluctuations do not cause permanent deformation. During this time, the connections in the study area are subject to several peak events of different magnitude. Due to the shape of the load displacement curves, once a connection yields due to a peak event, it can be damaged by lower magnitude peak events that may occur during a real wind loading trace. Unexpectedly, during the first peak event of this time history trace it was not connection T2-B7, but connection T2-B5 that experiences damage first. This demonstrates that there can be variability in the critical connections for each peak event even at the same wind direction.

The structural system experiences some damage during this time history analysis but does not fail completely by the end of the 10 minutes. This analysis has shown that the method can run efficiently to study a longer duration of realistic wind loading. To study failure of the roof system the wind speed was increased above the onset-damage wind speed and results are presented in the next section.

6.6.2 Time History Analysis at Intermediate Damage Wind Speed (28.4m/s)

The magnitude and time scaling of the pressure traces were adjusted to represent a mean wind speed of 28.4m/s in order to study the structural response at higher levels of damage. This wind speed was selected as it was in between the onset and cascading damage thresholds introduced in Section 6.4.4, and was expected to cause failure after a few peak events.

Figure 6.21 shows the connection response during the first 200s of the analysis. The structure fails at about 170s after 4 peak events of differing magnitudes. The incremental permanent deformation can be seen in Figure 6.21 b) that shows the displacement of connections over time.

As seen in previous analyses, the energy plots in Figure 6.21 c) show cumulative energy dissipated by permanent deformation of connections as in distinct steps during nail slips. Potential energy within the structure rapidly fluctuates with load fluctuations. Finally, kinetic energy increases and fluctuates rapidly during and after the failure cascade, indicating that the structure 'flaps' about after the failure of the roof as loads are continued to be applied to the surface of the cladding shell elements.
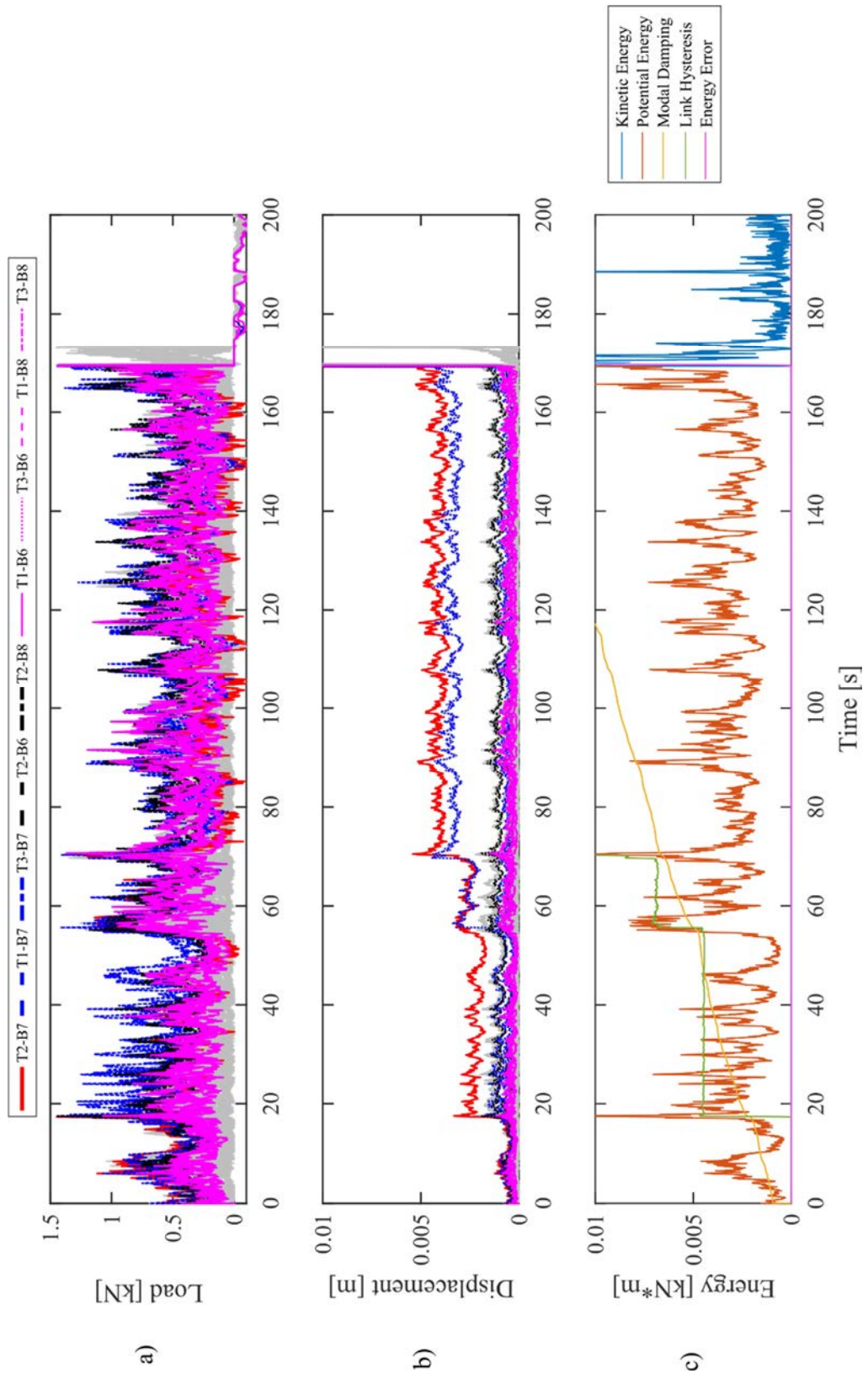
Figure 6.21 Structural response over 200s at 28.4m/s from wind direction 210° - a) reaction forces at connections, b) connection dispalcements, c) energy plots

Figure 6.22 to Figure 6.24 show the response of individual connections during this analysis. Force-displacement curves exhibit multiple slip bands, connection reaction forces show directions and times of load redistribution and connection displacements show incremental damage over time

The critical connections and the path of the failure cascade under realistic time history loads is similar to that found in the quasi static analyses. This similarity can be seen in Figure 6.25, indicating the pull up analyses presented previously can be used as an efficient method to determine where failures initiate and how they propagate across the roof. However, if the structure has been subject to high wind pressures from different directions previously, damage at different connections caused by this past loading history may alter the path of, or the point of initiation of the cascade.
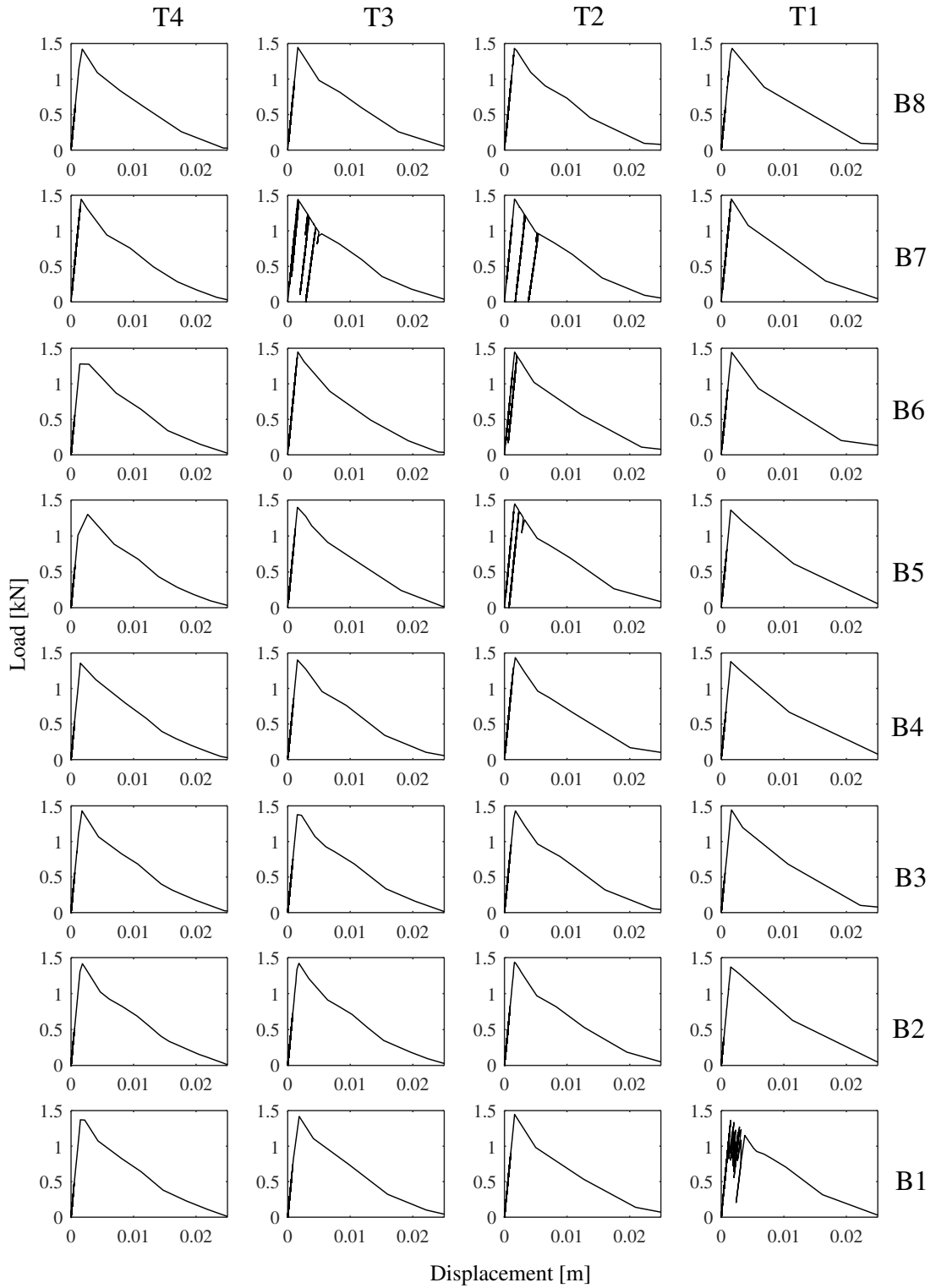
Figure 6.22 Force-displacement plots of the 32 connections in the study area showing diagonal bands from the incremental nail slips (wind speed 28.4m/s, wind direction 210°)
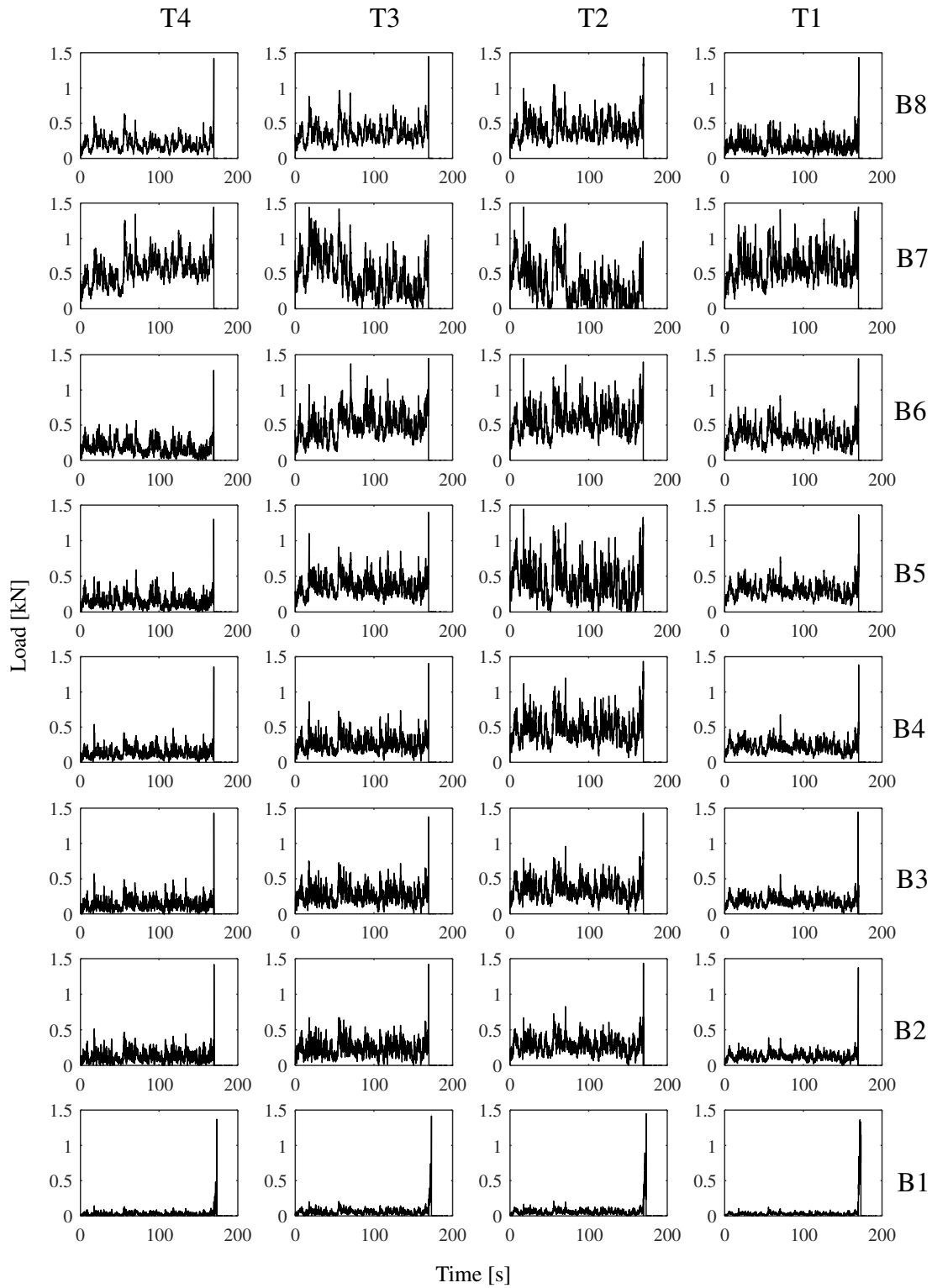
Figure 6.23 Reaction forces at connection over time showing load redistribution (wind speed 28.4m/s, wind direction 210°)
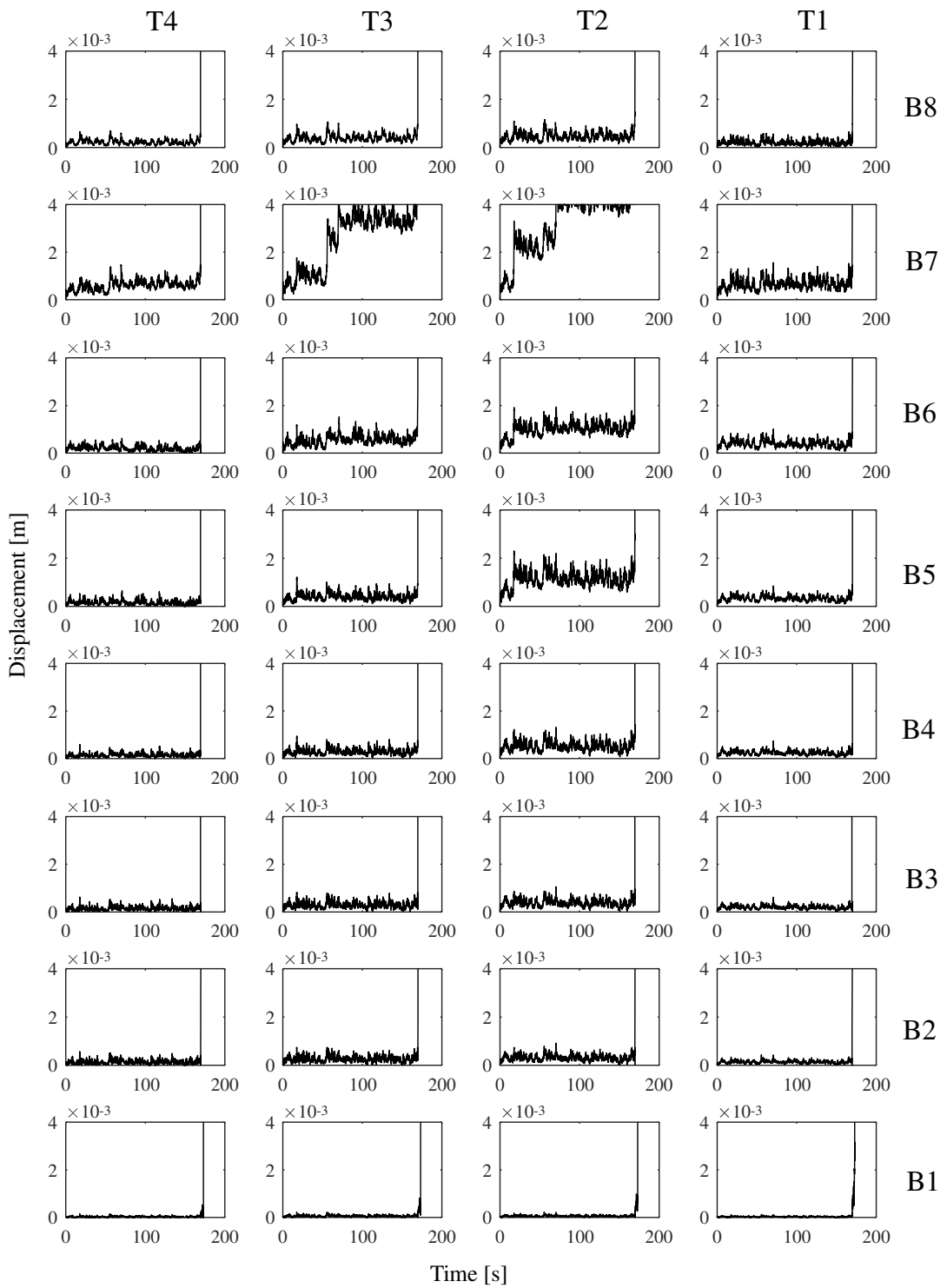
Figure 6.24 Displacement of connections over time showing jumps in displacement when nails slip (wind speed 28.4m/s, wind direction 210°)
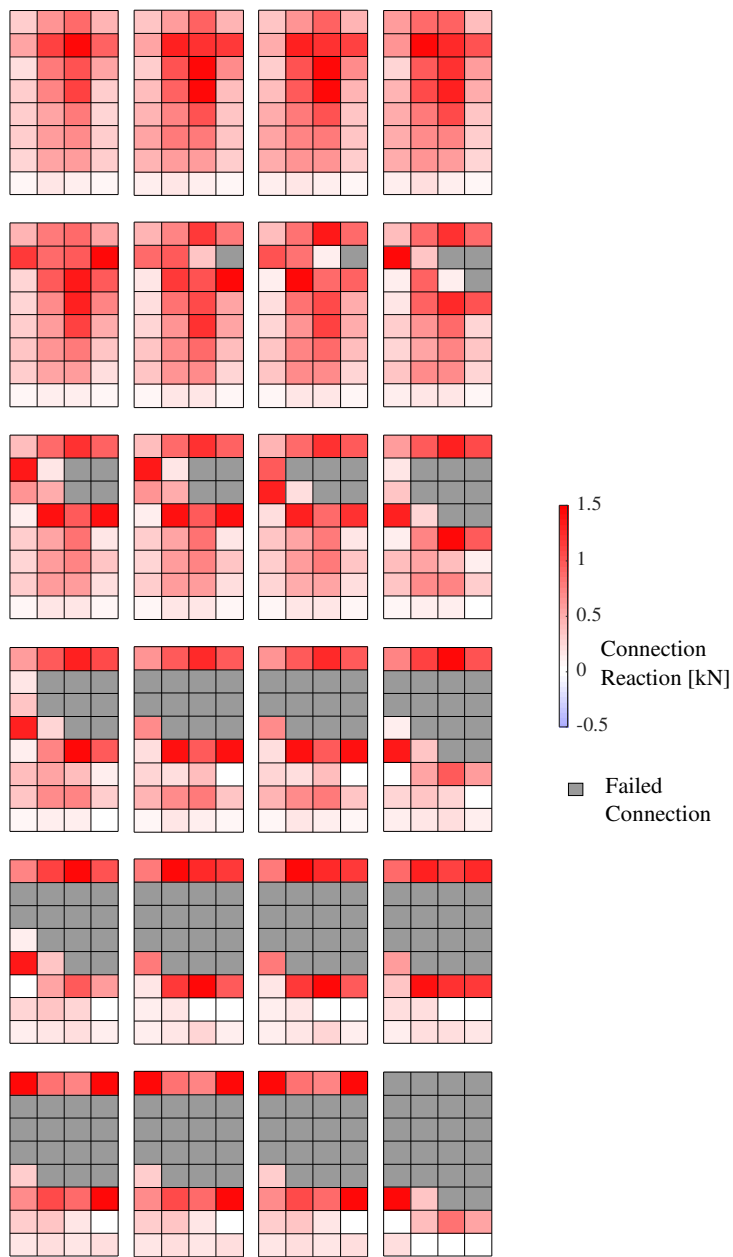
Figure 6.25 Colour-scale diagram showing sequence of connection failures during the time-history analysis (wind speed 28.4 m/s, wind direction 210°), bearing a close resemblance to the results from the pull-up analyses.

6.7 Summary of Dynamic Analyses

6.7.1 Repeated Peak Events

An approximately 2s duration of time history with a 'peak event' was applied to the structural system repeatedly. The magnitude and the time scaling of the pressure traces were modified appropriately based on the wind speed specified.

- No damage occurred below the onset damage wind speed determined from quasi-static analyses. A cascading failure would initiate at the first peak event if the wind speed was at or exceeding the cascade-damage wind speed from the quasi-static tests.
- For wind speeds in between the damage onset and cascading failure wind speed the structural system is able to withstand a varying number of peak events before a cascading failure.
- Depending on wind direction, the number of peaks the system can withstand is very sensitive to small changes in wind speed.
- As the yield threshold of a connection reduces after the first yield point, the loads that are required to cause nail slip reduce further. Therefore, peak events of lower magnitude will be able to cause damage to the structure after any initial damage occurs.

6.7.2 Load redistribution During a Peak Event

Connection and system response were examined in detail during a peak event causing incremental damage to the structure. Structural response was compared with a case with a slightly lower wind speed where no damage occurs. The time-steps where nails slip, and load redistribution occurs can be identified by the points when displacement of the connection increases.

- This load redistribution is a seamless process, there is no distinct point at which loads suddenly increase at neighbouring connections.
- Loads are redistributed to neighbouring connections regardless of whether there is a lead or lag time between the peak pressures influencing that particular connection. However, the time durations of load redistribution and the lead and lag times between peak applied loads are of similar magnitude. Therefore, correlations of loads to connections can have an effect on the spread of damage.
- Such lead or lag times may have an adverse or beneficial effect on the spread of failure. However, these effects appear to be marginal.

6.7.3 Triangular Peak Event

This analysis showed the structural response under a perfectly correlated dynamic load. i.e. loads increase and decrease at all connections at the same time and the pressure distribution across the roof surface remains constant.

- At a wind speeds less than the onset damage threshold no damage is observed. Additionally, all connections experience their peak loads at exactly the same time.
- When a peak event of greater magnitude than the onset damage threshold is applied, loads at the critical connection decrease immediately after the connection has reached its yield load.
- The critical connection reaches its yield load slightly before the peak in applied loads. While the critical connection is yielding, loads at other connections increase. There is again a seamless transition to when load redistribution occurs.

6.7.4 Ten-Minute Time History analysis

This penultimate analysis detailed the structural response under spatially and temporally varying wind loads for a duration of up to 10 minutes for a constant wind direction. Nails slip only during peak events, after initial damage occurs; lower magnitude peak events can then cause further damage. Additionally, as there is variation in the pressure distributions for each peak event there can also be variation in the critical connection that is damaged first. The sequence of connection failures is similar to that of the pull-up analyses showing that pull-up analysis can be an efficient way to study how failure may propagate through the structure.

6.8 Chapter Summary

Load redistribution and load paths change continuously as connections weaken and fail; this is especially evident from the 'pull-up' analyses performed. However, for less brittle connections, load redistribution occurs in stages with distinct load redistribution events when certain connections fail.

Load redistribution depends on several factors, these include:

1) The stiffness of the structural system in both directions. This in turn depends on: The cladding profile, batten size, Rafter and Batten spacing
2) Wind direction that influences where failure initiates and in which direction loads are transferred.
3) Ductility and elastic stiffness of individual connections and the overall shape of the force extension curve of the connections.
4) The distribution of weak and strong connections in the grid of batten to rafter connections.

This Chapter presented a series of computational experiments to study load redistribution and progressive failure behaviour of a system of batten to rafter connections. These studies increased in complexity from quasi static to realistic wind loads. Incremental failure of connections, changing load paths and cascading failures could be simulated using the FNA analysis method on the finite element model-successfully achieving the aims of this study. However, the analyses presented thus far are for an idealised situation where all batten to rafter connections have the same strength. The next Chapter will present preliminary studies using randomised connection properties.

7 APPLICATIONS

This Chapter presents exploratory studies to estimate the vulnerability of batten to rafter connections accounting for typical variability of connections and wind pressures. The preliminary fragility analyses and survival functions presented here highlight the potential applications of the overall procedure presented in this thesis.

Incorporating the connection variabilities determined in Chapter 4, the effects of a random distribution of connection strengths was investigated. The results of these analyses were used to develop simplistic fragility relationships. Finally, a sample of twelve roof structures with random connection properties were subjected to different time histories of pressures to determine the variability in performance of a structure under spatially and temporally varying wind loads.

Analyses that will be presented include:

1. An estimation of the variability in the thresholds of onset and cascading damage
2. Determination of survival functions for the onset and an intermediate damage wind speed from wind direction 210°. These survival functions estimate probabilities of failure while accounting for the effects of storm duration.
3. A preliminary retrofitting study

7.1 Fragility Analysis with Quasi-static Loads

Objectives

1. Determine effects of connection variability on thresholds of onset and cascading damage.

Modelling Parameters:

- Analysis Method: FNA
- Timestep size: 0.001s
- Number of modes: 100
- Initial conditions: Dead Load
- Damping – Modal Damping 5%

A lognormal distribution was fitted to connection strengths determined from connection testing and the idealised force-displacement curve of the computer model scaled in the y-axis to achieve the desired connection strength. As an example, 32 random connection properties are shown in Figure 7.1. All connections thus have the same overall shape for their force-displacement curves, a reasonable assumption based on the static connection tests.
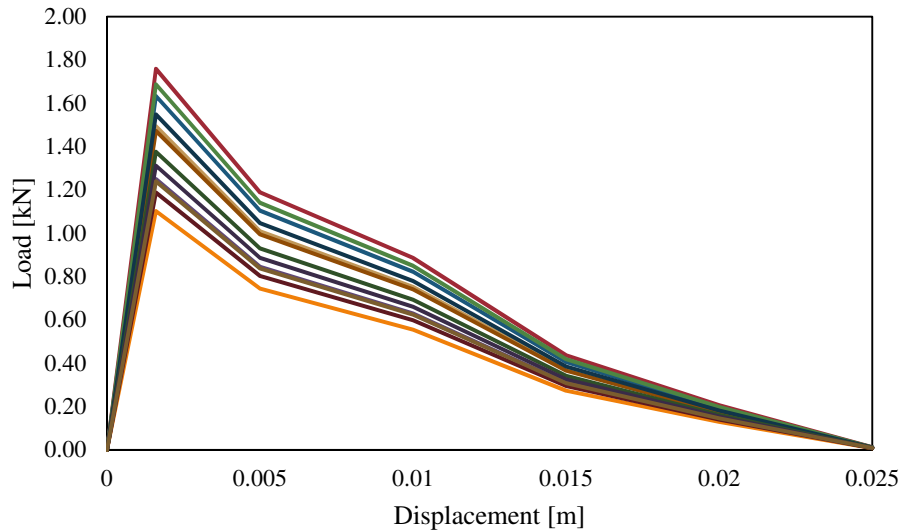
Figure 7.1 Force-displacement relationships of a set of 10 randomised connection properties

Twelve roof structure models were created, each with a random set of 32 connection strengths in the study area. Figure 7.2 shows twelve randomly generated connection sets used for the following probabilistic analyses.

Figure 7.2 Strengths of twelve randomised connection sets [kN], based on a probability distribution determined from connection testing.

A peak pressure pull up analysis using the 'peak event' pressure distribution for direction 210° was performed on all the twelve connection sets. Figure 7.3 shows the different onset and cascading damage wind speeds of the twelve structures. The fragility line of the system with uniform connection properties lies in the middle of the ranges. It is also apparent that the range of variability in cascade damage wind speeds is slightly lower than that of onset damage. Therefore, as indicated by the shaded region in the figure, the fragility of a system of batten to rafter connections is defined by a range, the extent of which is determined by the variability of the individual connections.
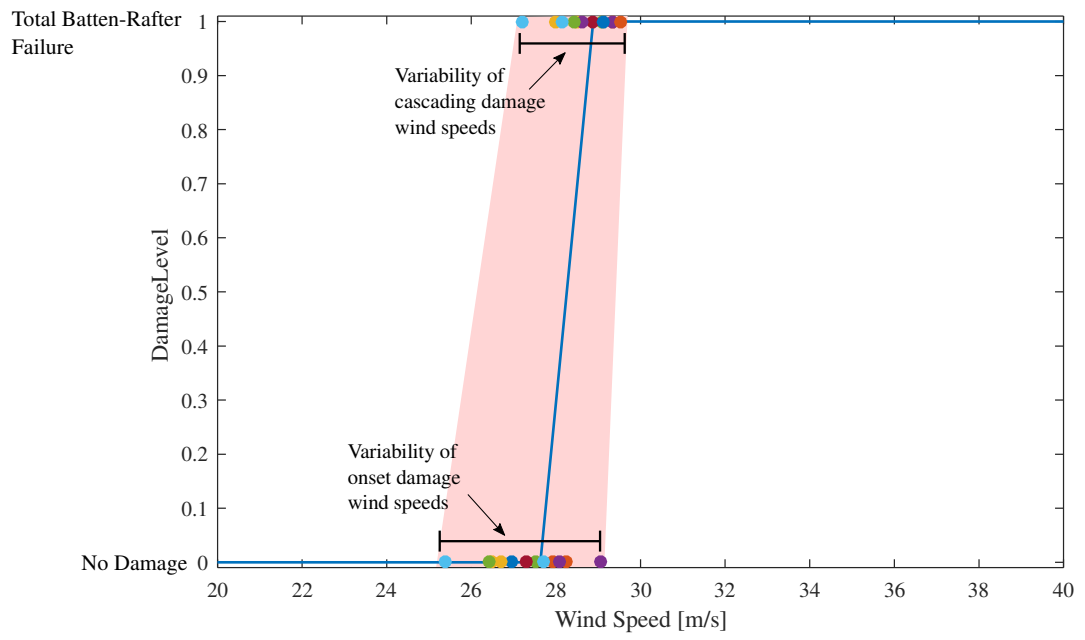
Figure 7.3 Batten-rafter fragility for wind direction 210° showing the expected range of onset and cascading damage wind speed accounting for variability of connections.

7.2 Probabilistic Analysis under Realistic Wind Loading

Objectives:

1. Assess performance accounting for variability of connections and variability in wind loads
2. Determine differences in fragility based on quasi static approach compared to a real wind load time history.

Modelling Parameters:

- Analysis Method: FNA
- Timestep size: 0.01s
- Number of modes: 100
- Initial conditions: Dead Load
- Damping – Modal Damping 5%

The ten-minute time history analysis presented in Section 6.6 was performed on the twelve analysis models, each with random connection properties, shown in Figure 7.2, with twelve different wind pressure time histories of ten minutes duration at wind direction 210°. The fluctuating component of pressure above the critical connection (T2-B7) is shown in Figure 7.4 for each of the twelve time histories. Varying numbers of peak events of different magnitudes occur during each 600s record.

Mean wind speed is again kept constant over the ten-minute duration. Two wind speeds are selected: onset damage (27.6m/s) and an intermediate wind speed within the onset-to-cascading damage range (28.4m/s).

At the onset-damage wind speed, ten of the twelve structures fail completely during the ten-minute analysis. Some of the structures survive several peak events and one fails at the first peak event, as shown in Figure 7.5. Once the onset of damage begins, the structures become vulnerable to peak events of increasingly lower magnitude. Thus, the fragility curves shown earlier move further to the left whenever the structure is subject to incremental damage.

All twelve structures fail at the intermediate damage wind speed, shown in Figure 7.6. This suggests that a fragility curve for batten rafter failures under time history wind loads may be steeper than the straight line shown in Figure 7.3
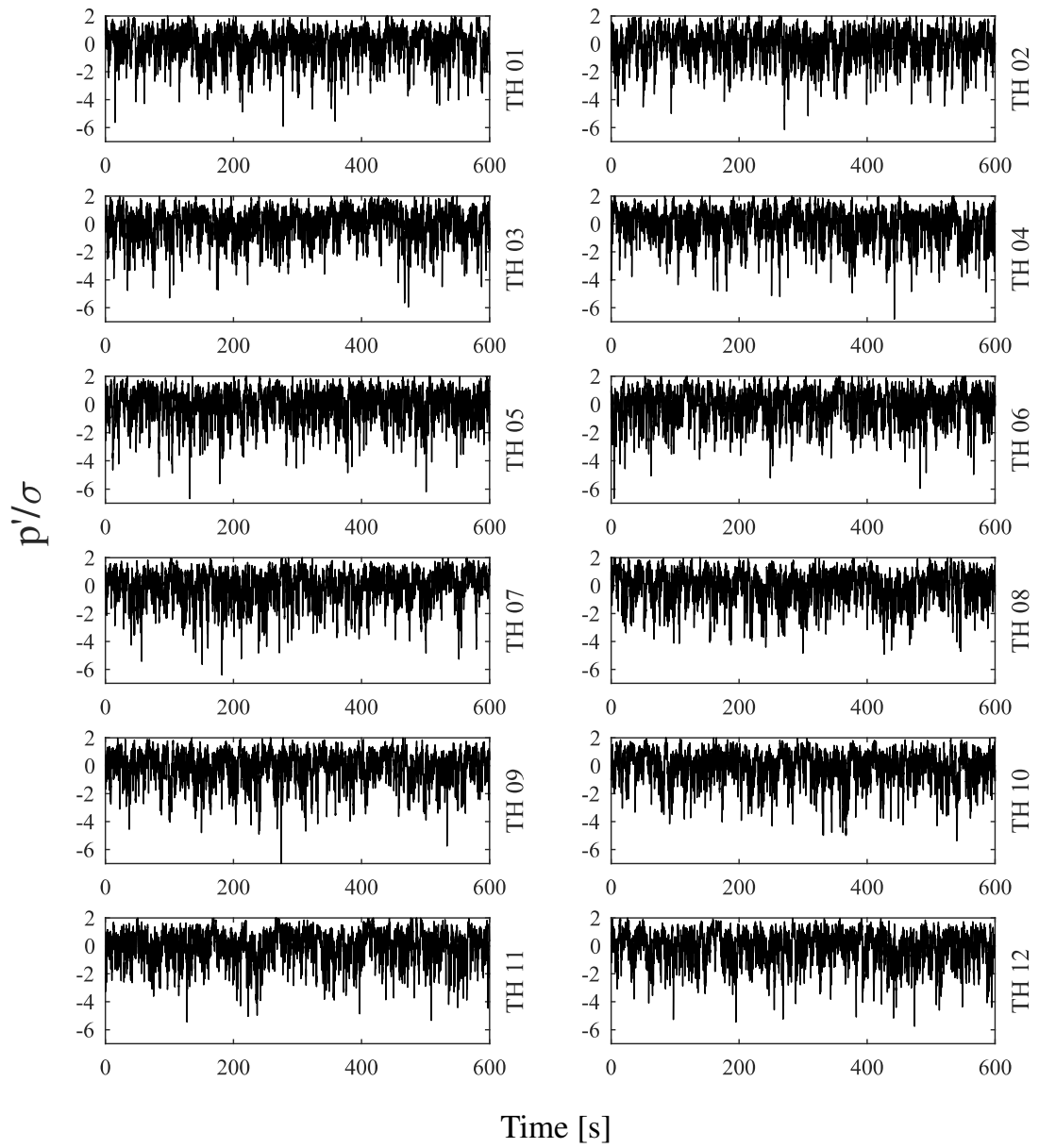
Figure 7.4 The twelve different wind time histories used for the analysis. Pressures only above connection T2-B7 are shown.
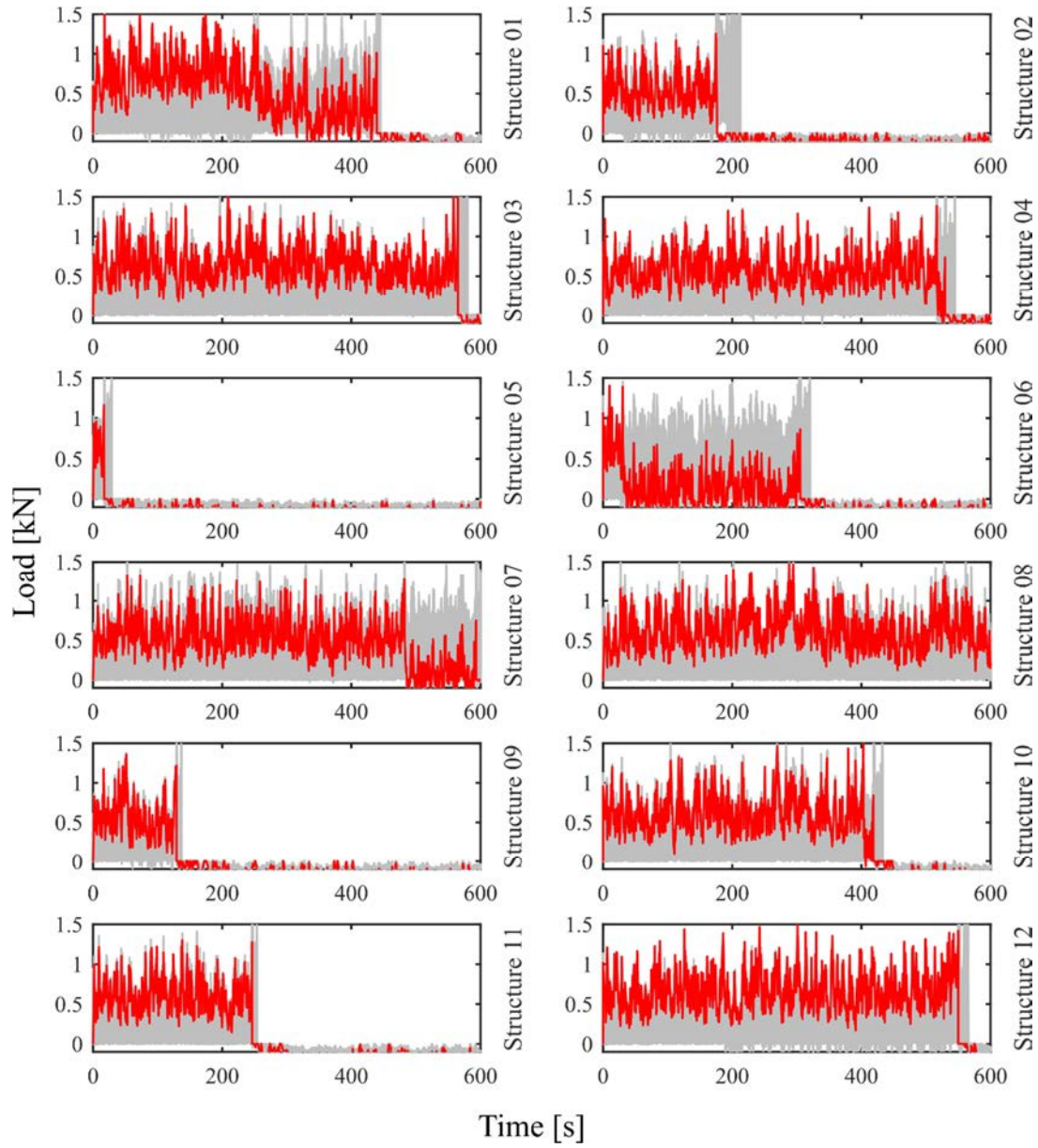
Figure 7.5 Ten-minute time histories of connection reactions at the onset damage wind speed (27.6m/s). Connection T2-B7 shown in red and all other connections shown in grey.
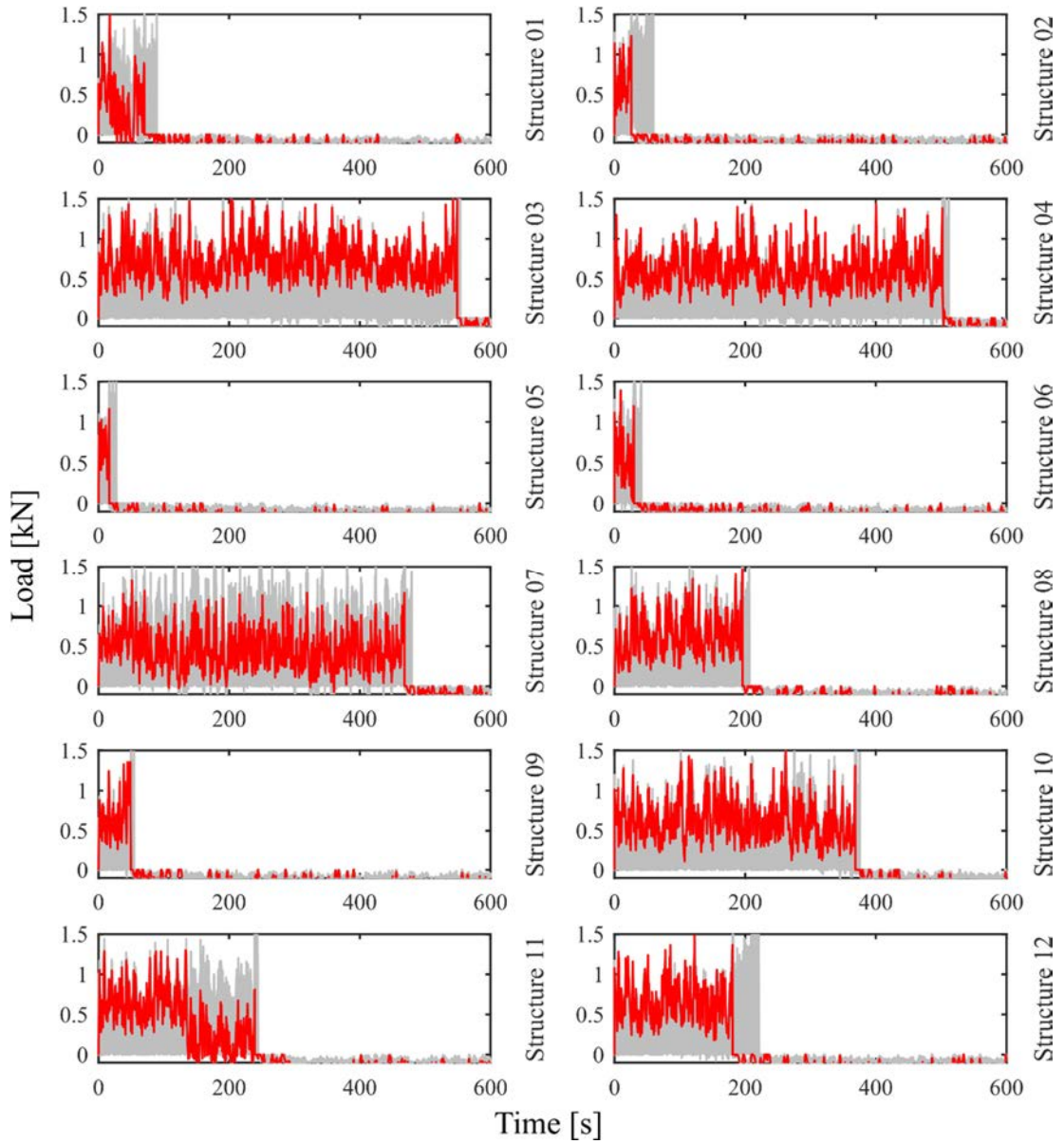
Figure 7.6 Ten-minute time histories of connection reactions at an intermediate damage wind speed (28.4m/s). Connection T2-B7 shown in red and all other connections shown in grey.

7.3 Survival Functions

Previous studies in wind engineering have not been able to define failures in probabilistic terms when accounting for storm duration effects as the complexities of failure mechanisms have not been studied in detail. Vulnerability models usually relate level of damage or cost of damage to a wind speed. However, the duration that these wind speed are sustained for is unknown. This Section presents a novel method of assessing vulnerability while accounting for wind speed as well as storm duration.

Survival analysis is a technique commonly used in the medical sciences for measuring effectiveness of treatments in improving life expectancy for patients suffering from a particular disease (Collett 2015, Newman 2003). These survival analysis techniques have also been used by engineers to estimate the working life of structures, effectiveness of retrofitting and most cost effective times for replacement. Beng and Matsumoto (2012) present a study for evaluating performance of bridges and infrastructure in Japan.

The efficient FNA analysis method is ideally suited for running multiple instances of the nonlinear time history analysis with different connection properties and different wind time histories to provide estimates of the probability of a cascading failure occurring. Results from the time history analyses presented in the previous section are used to determine probabilities of survival over the ten-minute duration as shown in Table 7.1 and Table 7.2

Table 7.1 Survival of structures at Mean wind Speed (mrh) = 27.6m/s (Onset Damage) for 210°

Time	Surviving Structures	Probability of Survival
0	12	1.00
100	11	0.92
200	10	0.83
300	8	0.67
400	7	0.58
500	5	0.42
600	2	0.17

Table 7.2 Survival of structures at Mean wind Speed (mrh) = 28.8m/s (Intermediate Damage) for 210°

Time	Surviving Structures	Probability of Survival
0	12	1.00
100	7	0.58
200	7	0.58
300	4	0.33
400	3	0.25
500	2	0.17
600	0	0.00

The probability of survival, which is also the inverse of the probability of a progressive failure occuring can be plotted with respect to duration of loading to produce survival functions, as shown in Figure 7.7. Such survival functions show how propability of survival decreases as for longer durations of wind loading for a particualr wind direction. For increasing wind speeds the probability of survival decreases more abruptly with increasing load duration. Examining the shapes of the curves, additional functions (shown in grey) indicate the estimated survival behaviour for other wind speeds.
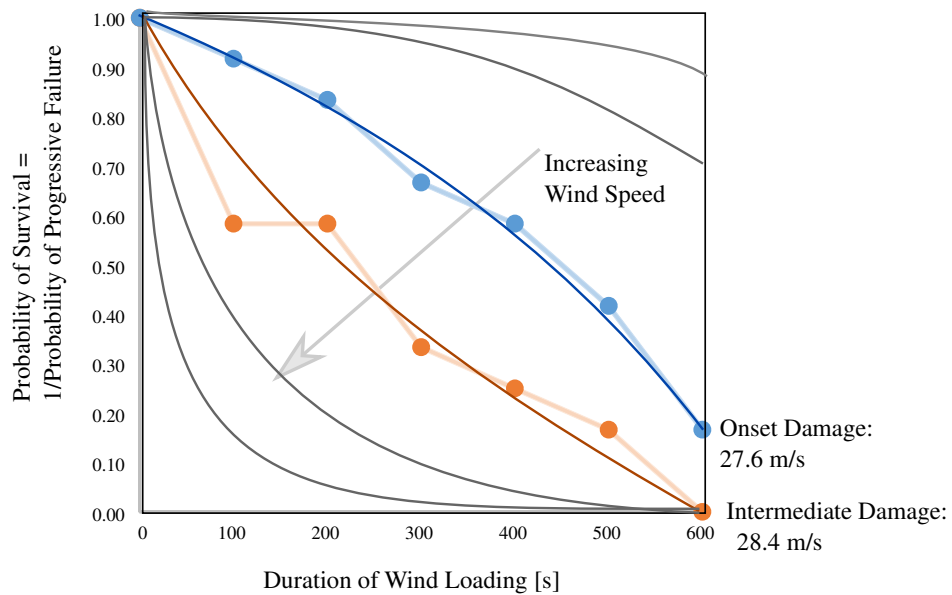
Figure 7.7 Survival functions for a range of wind speeds at wind direction 210°

Survival functions can also be determined for other wind directions. The shapes of the functions are expected to look similar to that shown in Figure 7.7, however the wind speeds causing damage will be different.

To estimate probabilities of failure during real wind events, the probabilities of failure for various segments of time duration and changing wind direction can be integrated. Finite Element time-history analysis may not be required for further analyses once a suite of survival functions have been determined. However, damage to the structure caused by a different wind direction cannot be accounted for when considering the probability of failure of a new wind direction.

7.4 Predictions of Performance During a Cyclone Event

During a cyclonic event of five hours, wind speed and wind direction vary constantly and running time history analyses for these durations would be computationally expensive. Furthermore, there is variability in the path of a cyclone, resulting in variability in wind directions at which the house would be subject to maximum loads. However, the understanding developed from the analyses presented in previous sections allows reasonable predictions to be made of the performance of batten to rafter connections during a cyclone event.

Peak events can cause incremental damage to a system of batten to rafter connections at the onset-damage wind speed, with each instance of damage leading the system to be vulnerable to peak events of lower magnitude. Thus, as shown in Section 6.6.2, a progressive failure is inevitable if wind speeds and direction remain similar for about ten minutes duration for wind speeds above the onset damage level. For wind directions that have a larger onset-to-cascade range this duration may be longer.

Under cyclone conditions, it is expected that a house would experience no damage to batten to rafter connections during times when the wind speed is below the onset-damage wind speed. The time at which onset damage would begin to occur will depend on the wind direction caused by the passage of the cyclone as well. After the onset of damage begins, a progressive failure is very likely to occur within the next ten minutes due to the slow rate of change in wind direction.

If the onset of damage does begin for an orthogonal wind direction such as 270° with a large onset-to-cascade range, a progressive failure may not occur before wind direction changes. However, a progressive failure is very likely to occur in the following minutes, as the wind direction would change to a cornering direction producing higher uplift pressures on the roof surface.

It is likely that a house may survive a cyclone with some accumulated damage only if onset of damage occurs at the time of peak wind speeds during the storm, as wind speed will begin to reduce after this point. Any accumulated damage from one storm will cause the house to be especially vulnerable to future wind events as its onset damage wind speed becomes reduced.

Additionally, a change in internal pressures can cause a change to the net (external - internal) pressures acting on the roof. A positive internal pressure resulting from a large opening such as a window on a windward wall will increase the loads on the roof and is a critical design condition. Internal pressure inside the building will cause onset damage to begin at lower wind speeds, shifting the fragility curves to the left. It is expected that during a cyclone event, the sudden internal pressurisation from the formation of a large opening could result in onset damage occurring immediately at the time of pressurisation. Depending on the external pressures at the time, a cascading failure may occur immediately or when the next peak event occurs.

7.5 Preliminary Retrofitting Study

Quasi-static pull up analysis with a 'peak-event' pressure distribution was performed on a structure with retrofitted connections to quantify improvements in performance. Batten to rafter connections on the first two rafters from the gable end are retrofitted with a self-drilling screw providing a strength of 3kN with a brittle failure mode as shown in Figure 7.8 and Figure 7.9.
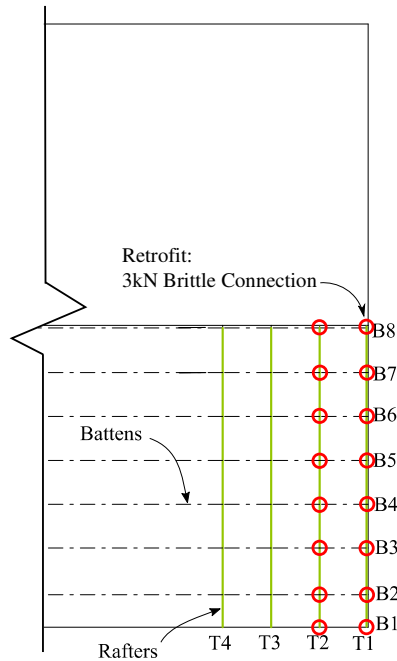
Figure 7.8 Locations of retrofitted connections
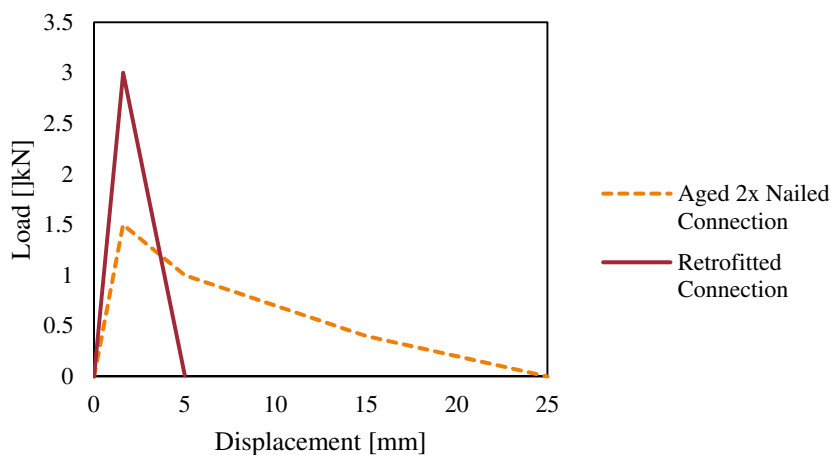
Figure 7.9 Connection properties of existing aged connections and retrofitted connections

A pressure distribution occurring during a peak event at wind direction 210°, shown in Figure 6.6 b) was increased in magnitude until failure. Reaction forces at connections surrounding connection T2-B7 are shown in Figure 7.10 for the as-built structure and with the retrofitted connections. Approximately 20% higher wind speeds are required for the onset of damage and cascading damage for the retrofitted structure.

Onset and cascading damage wind speeds can be used to plot fragility functions as shown in Figure 7.11. The retrofitting strategy used increases the mean onset damage wind speeds at mid roof height from 27.6 m/s to 33.4 m/s, corresponding to 0.2s gust wind speed at 10m height of 73.5 m/s to 88.9 m/s in Terrain Category 2.

This preliminary study has shown how the efficacy of retrofitting measures can be quantified while accounting for load redistribution and progressive failure. Further work can optimise the locations of retrofitted connections and check the effects of multiple wind directions and time history loads.
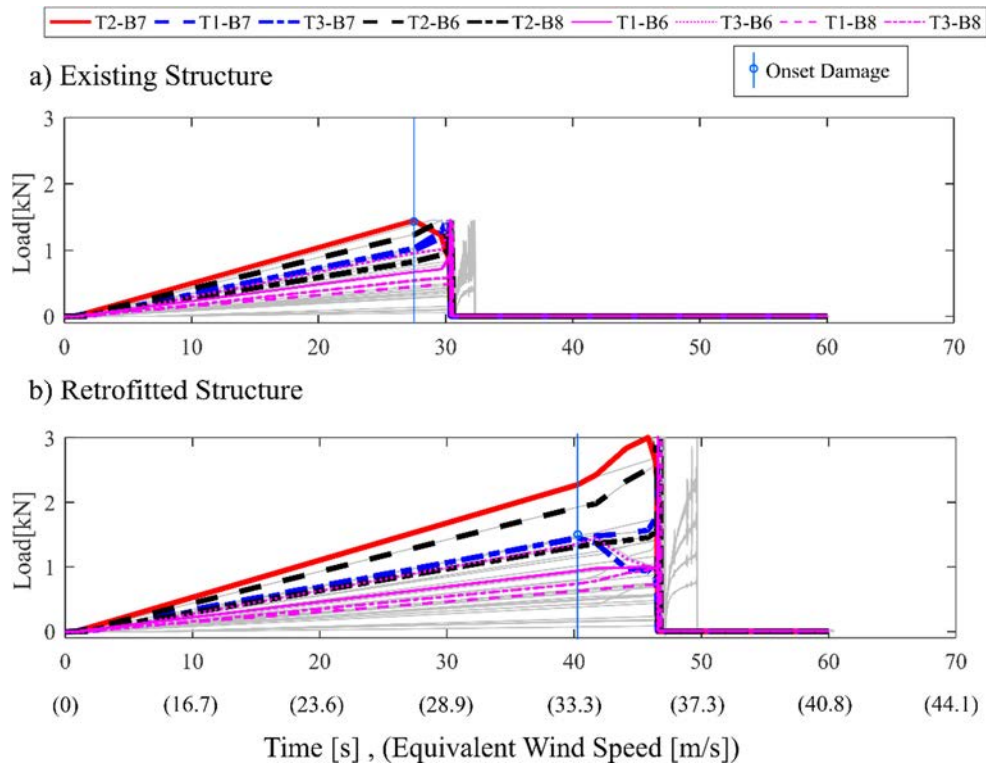
Figure 7.10 Reaction forces during the pull up analysis of connections during pull up analysis for a) the existing structure and b) the retrofitted structure
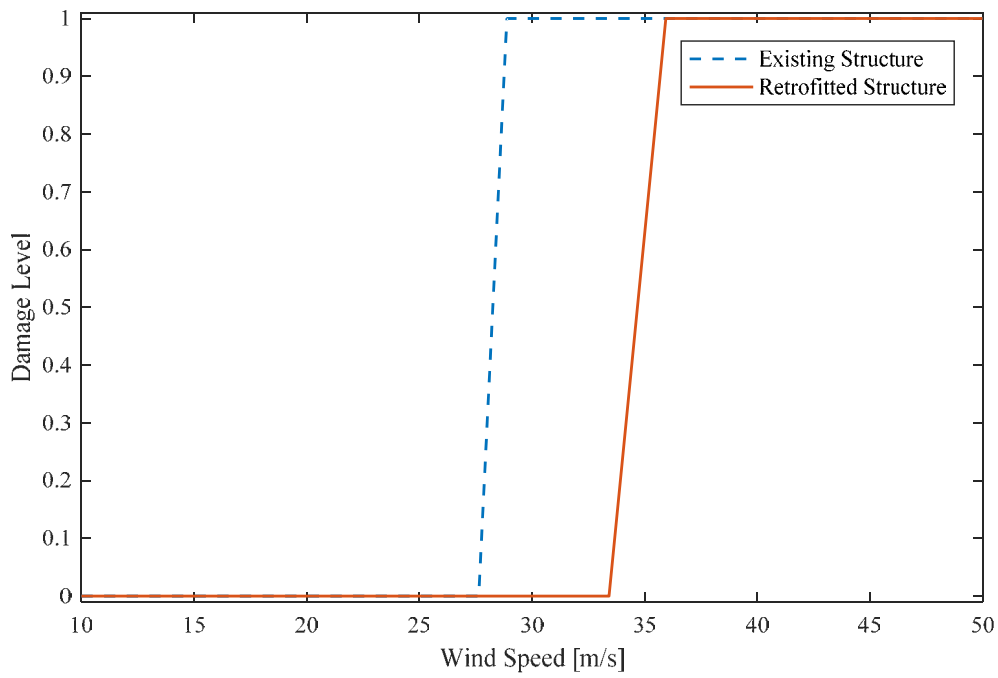
Figure 7.11 Fragility relationships for the existing and retrofitted structure showing increase in wind speeds required for the onset of damage and cascading damage for the retrofitted structure

8 CONCLUSIONS AND RECOMMENDATIONS

This thesis has presented a method for studying the progressive failure mechanisms of roof structures in a traditional Australian house under fluctuating wind loads. The study used spatial and temporal pressure data from wind tunnel tests, force-displacement curves derived from connection testing and a nonlinear finite element method model to simulate failures of batten to rafter connections. The methods used in this thesis could also be used for studying other roofing connections or other structural systems under severe wind loads. The analyses performed were used to determine basic fragility curves that account for progressive failures. Additionally survival functions that indicate probabilities of a progressive failure occurring as a function of the duration of wind loads were also determined using the methods presented.

8.1 Conclusions

Batten to Rafter connections in light framed timber houses are vulnerable to progressive failures under wind loading. The structural system, loading process and the structural response are complex and capturing progressive failure behaviour has been a challenge in wind engineering of light framed structures. This thesis has studied progressive failures of batten to rafter connections by using wind tunnel testing, dynamic connection testing and nonlinear structural analysis

The primary objective of this thesis was to determine *the load redistribution and progressive failure behaviour of batten to rafter connections under spatially and temporally varying wind pressures.* These complex failure modes can be described as follows:

- Progressive failures of batten to rafter connections are a complex process influenced by the pressure fluctuations on the roof surface, the response of individual connections and the behaviour of the structural system as a whole.

- Wind tunnel testing showed that external surface pressures are highly fluctuating, with flow separation and building induced turbulence causing intermittent 'peak events' that subject connections to especially high loads. These peak events move across the roof causing high loads to occur at different connections with slight lead or lag times.

- As noted by previous researchers, 'peak events' for a given wind direction are caused by distinct aerodynamic mechanisms. The locations of these 'peak events' are usually in the same part of the roof for a given wind direction. As the simultaneous loading of neighbouring connections produces more damage the extent of the flow separation regions on the roof surface can influence the initiation of damage.

- Dynamic connection testing showed that connections are damaged during 'peak events', with nails slipping incrementally with successive 'peak events'. These nailed connections are also highly variable in their performance and dynamic nail slip behaviour is bounded by the quasi-static force-displacement curves. Additionally, the loading rates caused by wind loads do not affect connection performance.

- Nonlinear Finite Element Analysis showed that load paths and load sharing to and between batten to rafter connections are determined by the stiffness of the cladding and the battens and the ductility of connections.

- Load redistribution for semi-ductile (realistic) connections is a continuous process, where loads at connections increase as soon as any adjacent connection begins to yield. Load redistribution continues until a certain number of neighbouring connections also yield and then a cascading failure begins where all connections fail in rapid succession.

- Wind direction affects where peak events occur, and therefore the locations on the roof where damage initiates. The structure has varying amount of redundancy depending on the location on the roof where this first damage occurs due to the amount of load sharing possible by the surrounding structure. Therefore, depending on wind direction, varying increases of wind speed are required to cause a cascading failure after any initial damage. However, after the onset of damage, 'peak-events' of smaller magnitude than the first may cause further nail withdrawal.

- Correlations of pressure fluctuations may have a slight effect on the spread of damage as the lead and lag times of pressure fluctuations are of similar duration as times when load is being redistributed.

- Analyses showed that load duration of 'peak events' affects the displacements of nailed connections and thus the damage sustained by the structure. Therefore, for wind speeds in between the onset and cascading damage thresholds, a structure can withstand several peak events before a cascading failure takes place.

- The winds speeds causing onset and cascading damage can give a measure of fragility of batten to rafter connections. Randomising connections and wind time histories gives a probabilistic assessment of the vulnerability of batten to rafter connections.

- A progressive failure of a large section of batten to rafter connections will most likely occur during a wind event when the onset damage level is reached and high wind speeds occur at a critical wind direction.

8.2 Recommendations for Further Research

The following recommendations address the limitations of this study and propose suggestions for further research.

8.2.1 Full Scale Testing

The computer simulations show behaviour closely resembling the connection response observed during laboratory testing, and the overall structural behavior resembled the failures documented in damage surveys. However, this study was not able to verify whether the load redistribution behavior was affected by the simplifications used in the computer analysis model such as the use of gap elements, full rotational fixity of the connections and full fixity of the cladding to the battens.

Full scale testing of a grid of batten rafter connections is recommended to verify load redistribution behaviour. Challenges involved with such tests include instrumenting connections and applying spatial and temporal fluctuating pressures using loading actuators. Furthermore, several structures may need to be destructively tested to draw reliable conclusions due to the variability of connections.

8.2.2 Changes in Aerodynamics and Internal Pressurization

Later stages of damage including the failure may be influenced by changes in aerodynamics due to the damage geometry i.e. the cladding and battens being peeled away. Resulting variations in external and internal pressure fluctuations would likely exacerbate the cascading failure. Simulations using CFD or a Multiphysics finite element program may be used to study the effects of changes in Aerodynamics and fluid-structure interaction. Alternatively, wind tunnel testing with a model with removable sections may be used to determine changes in pressures with changes in geometry, similar to the studies by Thampi et al. (2011).

8.2.3 Extension of Survival Analysis

The survival analysis presented in Section 7.3 shows promise as a useful method of visualizing and describing the vulnerability of a structural system under time history loads. Time history analyses with randomized connection strengths and wind loads as presented in Section 7.2 may be repeated for multiple wind directions and for increasing wind speeds.

8.2.4 Time-history Analysis Using a Design Cyclone Event

This study presents preliminary fragility and survival analyses that can be used to estimate the vulnerability of batten to rafter connections. However, there is still uncertainty in the behavior of a structure during a cyclonic event that may affect the structure for several hours over a range of wind directions. Using methods by Jancauskas et al. (1994) the structural analysis model may be subject to a 'design cyclone event'. Running several of these time-history analyses would be computationally expensive due to the long time duration of the cyclone. Therefore it is recommended that the survival or fragility methods presented in this study be used to determine a worst case cyclone event to be simulated.

8.2.5 The Study of Other Roofing Connections

This study has developed a method to study progressive failures in batten to rafter connections, and non-linear behavior was restricted to occur only at the nonlinear links in the model. Other connections such as roof to wall connections can also be studied using the method developed in this study to determine their fragility and survival functions. Although rarely seen in damage surveys, failures that involve damage of more than one connection type can also be explored by modelling nonlinear behaviour in several connection types in the analysis model.

8.3 Concluding Statement

This thesis has presented a method for effectively simulating progressive failures of batten to rafter connections in traditional Australian housing. This method also has the ability to study other roofing connections and other structural systems.

The procedure is the first of its kind that is able to account for:

1) Spatial and temporal fluctuations in pressures
2) Non-linear behaviour of connections
3) Storm duration effects and accumulated damage through time
4) Load redistribution through the structure.

As such, this research addresses key knowledge gaps in wind engineering as the structural response due to the above mentioned factors have not been accounted for in previous studies.

The study has been able to achieve its aims in gaining a better understanding of a complex failure mechanism of roof structures of light framed houses. Furthermore, the exploratory studies presented in Chapter 7 have shown potential to improve current vulnerability models and develop codes and guidelines for retrofitting the roofs of older structures. Thereby providing a significant contribution to research in improving the resistance to wind damage of existing houses in Australia.

REFERENCES

Amzallag, C., J. P. Gerey, J. L. Robert, and J. Bahuaud. 1994. "Standardization of the rainflow counting method for fatigue analysis." *International journal of fatigue* 16 (4):287-293.

ASTM. 2006. Standard test methods for mechanical fasteners in wood. ASTM D1761. ASTM International West Conshohocken, Pennsylvania.

Beng, S. S., and T. Matsumoto. 2012. "Survival analysis on bridges for modeling bridge replacement and evaluating bridge performance." *Structure and Infrastructure Engineering* 8 (3):251-268.

Boughton, G. 1982. "Simulated Wind Tests on a House. Part 2. Results."

Boughton, G. 1983. "Testing of a full scale house with simulated wind loads." *Journal of wind engineering and industrial aerodynamics* 14 (1):103-112.

Boughton, G. 1988. "An investigation of the response of full scale timber framed houses to simulated cyclonic wind loads." Dissertation/Thesis, James Cook University.

Boughton, G., D. Falck, J. Ginger, D. Henderson, and N. Satheeskumar. 2014. "Stochastic Models For Performance of Timber Roof Connections Under Wind Forces." World Conference on Timber Engineering, Quebec City, Canada, August 2014.

Boughton, G., D. Falck, D. Henderson, D. Smith, K. Parackal, T. Kloetzke, M. Mason, R. Krupar, M. Humphreys, S. Navaratnam, G. Bodhinayake, S. Ingham, and J. Ginger. 2017. Tropical Cyclone Debbie: Damage to buildings in the Whitsunday Region, Cyclone Testing Station, JCU, Report TR63.

Boughton, G., D. Henderson, J. Ginger, J. Holmes, G. Walker, C. Leitch, L. Sommerville, U. Frye, N. Jayasinghe, and P. Kim. 2011. Tropical Cyclone Yasi: Structural damage to buildings, Cyclone Testing Station, JCU, Report TR57.

Boughton, G., and G. Reardon. 1982. "Simulated Wind Tests on a House. Part 1. Description."

Boughton, G., and G. Reardon. 1984. Structural Damage Caused by Cyclone Kathy at Borroloola NT, Cyclone Testing Station, JCU, Report TR21.

Carson, J. 1995. Light Framed Timber Construction.

Cermak, J. E. 1970. *Separation-induced pressure fluctuations on buildings*: Colorado State University.

Chopra, A. K. 2007. *Dynamics of structures: theory and applications to earthquake engineering. 2007*: Prentice-Hall.

Collett, D. 2015. *Modelling survival data in medical research*: CRC press.

Cramer, S. M., J. M. Drozdek, and R. W. Wolfe. 2000. "Load sharing effects in light-frame wood-truss assemblies." *Journal of Structural Engineering* 126 (12):1388-1394.

Cramer, S. M., and R. W. Wolfe. 1989. "Load-distribution model for light-frame wood roof assemblies." *Journal of Structural Engineering* 115 (10):2603-2616.

CSI. 2016. "CSi Analysis Reference Manual." *I: Berkeley (CA, USA): Computers and Structures INC.*

Datin, P. L. 2010. "Structural load paths in low-rise, wood-framed structures."PhD Thesis, University of Florida.

Datin, P. L., and D. O. Prevatt. 2007. "Wind uplift reactions at roof-to-wall connections of wood-framed gable roof assembly." 12th International Conference on Wind Engineering, Australasian Wind Engineering Society, Cairns, Australia.

Davenport, A. G. 1960. Rationale for determining design wind velocities. National Research Council of Canada Ottawa (Ontario) Div of Building Research.

Davenport, A. G. 1961a. "The application of statistical concepts to the wind loading of structures." *Proceedings of the Institution of Civil Engineers* 19 (4):449-472.

Davenport, A. G. 1961b. "The spectrum of horizontal gustiness near the ground in high winds." *Quarterly Journal of the Royal Meteorological Society* 87 (372):194-211.

Davenport, A. G., D. Surry, and T. Stathopoulos. 1977. "Wind Loads on Low-Rise Buildings: Final Report of Phases I and II, Parts 1 and 2." *BLWT Report SS8-1977The University of Western Ontario, London, Ontario, Canada (1977).*

Davenport, A. G., D. Surry, and T. Stathopoulos. 1978. "Wind Loads on Low-Rise Buildings: Final Report of Phase III,." *BLWT Report SS4-1978 The University of Western Ontario, London, Ontario, Canada (1978).*

Doudak, G. 2006. *Field determination and modeling of load paths in wood light-frame structures*. Vol. 68.

Eaton, K. J., and J. R. Mayne. 1975. "The measurement of wind pressures on two-storey houses at Aylesbury." *Journal of Wind Engineering and Industrial Aerodynamics* 1:67-109.

El-Tawil, S., H. Li, and S. Kunnath. 2013. "Computational simulation of gravity-induced progressive collapse of steel-frame buildings: Current trends and future research needs." *Journal of Structural Engineering.*

Ellingwood, B. R., D. V. Rosowsky, Y. Li, and J. H. Kim. 2004. "Fragility assessment of light-frame wood construction subjected to wind and earthquake hazards." *Journal of Structural Engineering* 130 (12):1921-1930.

Ellingwood, B. R., R. Smilowitz, D. O. Dusenberry, D. Duthinh, H. Lew, and N. J. Carino. 2007. *Best practices for reducing the potential for progressive collapse in buildings*: US Department of Commerce, National Institute of Standards and Technology.

Ellis, B. R., and A. J. Bougard. 2001. "Dynamic testing and stiffness evaluation of a six-storey timber framed building during construction." *Engineering Structures* 23 (10):1232-1242.

Foliente, G. C. 1998. "Design of timber structures subjected to extreme loads." *Progress in Structural Engineering and Materials* 1 (3):236-244.

Fowler, R. 2003. "Fatigue Damage to Metal Battens Subject to Simulated Wind Loads."Honours Thesis, Engineering and Physical Sciences, James Cook University.

Friedman, D. 1975. Computer simulation of natural hazard assessment. Boulder, CO, USA: University of Colorado.

Frye, U., J. Ginger, and C. Leitch. 2012. Response of metal cladding systems to windborne debris impact. Cyclone Testing Station, James Cook University.

Gavanski, E., K. R. Gurley, and G. A. Kopp. 2016. "Uncertainties in the estimation of local peak pressures on low-rise buildings by using the Gumbel distribution fitting approach." *Journal of Structural Engineering* 142 (11):04016106.

Ginger, J. 2001. "Characteristics of wind loads on roof cladding and fixings." *Wind and Structures* 4 (1):73-84.

Ginger, J., D. Henderson, M. Edwards, and J. Holmes. 2010. "Housing damage in windstorms and mitigation for Australia." 2010 APEC-WW and IG-WRDRR Joint Workshop: wind-related disaster risk reduction activities in Asia-Pacific Region and Cooperative Actions, Incheon, Korea.

Ginger, J., D. Henderson, C. Leitch, and G. Boughton. 2007. "Tropical Cyclone Larry: Estimation of wind field and assessment of building damage." *Australian Journal of Structural Engineering* 7 (3):209-224.

Ginger, J., and C. Letchford. 1993. "Characteristics of large pressures in regions of flow separation." *Journal of Wind Engineering and Industrial Aerodynamics* 49 (1):301-310.

Guha, T., and G. A. Kopp. 2014. "Storm duration effects on roof-to-wall-connection failures of a residential, wood-frame, gable roof." *Journal of Wind Engineering and Industrial Aerodynamics* 133:101-109.

Gupta, R. 2005. "System behaviour of wood truss assemblies." *Progress in Structural Engineering and Materials* 7 (4):183-193.

Gupta, R., and P. Limkatanyoo. 2008. "Practical approach to designing wood roof truss assemblies." *Practice Periodical on Structural Design and Construction* 13 (3):135-146.

Gupta, R., T. H. Miller, and D.-R. Dung. 2004. "Practical solution to wood truss assembly design problems." *Practice Periodical on Structural Design and Construction* 9 (1):54-60.

Hambric, S. A. 2006. "Structural acoustics tutorial—Part 1: vibrations in structures." *Acoustics Today* 2 (4):21-33.

He, J., F. Pan, C. Cai, A. Chowdhury, and F. Habte. 2018. "Progressive failure analysis of low-rise timber buildings under extreme wind events using a DAD approach." *Journal of Wind Engineering and Industrial Aerodynamics* 182:101-114.

He, J., F. Pan, C. Cai, F. Habte, and A. Chowdhury. 2018. "Finite-element modeling framework for predicting realistic responses of light-frame low-rise buildings under wind loads." *Engineering Structures* 164:53-69.

Henderson, D. 2010. "Response of pierced fixed metal roof cladding to fluctuating wind loads."PhD Thesis, James Cook University.

Henderson, D., and J. Ginger. 2007. "Vulnerability model of an Australian high-set house subjected to cyclonic wind loading." *Wind & Structures* 10:269-285.

Henderson, D., and J. Ginger. 2011. "Response of pierced fixed corrugated steel roofing systems subjected to wind loads." *Engineering Structures* 33 (12):3290-3298.

Henderson, D., J. Ginger, C. Leitch, G. Boughton, and D. Flack. 2006. Tropical Cyclone Larry: Damage to buildings in the Innisfail area, Cyclone Testing Station, JCU, Report TR51.

Henderson, D., J. Ginger, M. Morrison, and G. A. Kopp. 2009. "Simulated tropical cyclonic winds for low cycle fatigue loading of steel roofing." *Wind & Structures* 12:381-398.

Henderson, D., and B. Harper. 2003. Queensland climate change and community vulnerability to tropical cyclones : cyclone hazards assessment stage 4 report : development of a cyclone wind damage model for use in Cairns, Townsville and Mackay. In *Queensland climate change and community vulnerability to tropical cyclones*.

Henderson, D., C. Leitch, U. Frye, J. Ginger, P. Kim, and N. Jayasinghe. 2010a. Investigation of house and sheds in Proserpine, Midge Point and Airlie Beach, following Tropical Cyclone Unlui, Cyclone Testing Station, JCU, Report TR56.

Henderson, D., C. Leitch, U. Frye, J. Ginger, P. Kim, and N. Jayasinghe. 2010b. Investigation of Housing and Sheds in Procerpine, Midge point, and Airlie Beach, Following Tropical Cyclone Ului. Cyclone Testing Station, James Cook University, Townsville. TR 56.

Henderson, D., M. Morrison, and G. A. Kopp. 2013. "Response of toe-nailed, roof-to-wall connections to extreme wind loads in a full-scale, timber-framed, hip roof." *Engineering Structures* 56:1474-1483.

Holmes, J. D. 1982. Wind pressures on houses with high pitched roofs. Department of Civil and Systems Engineerings, James Cook University of North Queensland.

Holmes, J. D. 1985. "Wind loads and limit states design." *Institution of Engineers (Australia) Civ Eng Trans* (1).

Holmes, J. D. 1994. "Wind pressures on tropical housing." *Journal of wind engineering and industrial aerodynamics* 53 (1):105-123.

Holmes, J. D. 2001. *Wind loading of structures*: CRC Press.

Irving, R. 1985. *The History & Design of the Australian House*: Oxford University Press Melbourne.

ISO. 2009. "Wind Actions on Structures." *International Organization for Standardization* 1:68.

Jacklin, R. B. 2013. "Numerical and Experimental Analysis of Retrofit System for Light-Framed Wood Structures Under Wind Loading."Masters Thesis, University of Western Ontario.

Jancauskas, E. D., M. Mahendran, and G. R. Walker. 1994. "Computer simulation of the fatigue behaviour of roof cladding during the passage of a tropical cyclone." *Journal of Wind Engineering and Industrial Aerodynamics* 51 (2):215-227.

Jayasinghe, N. 2012. "The distribution of wind loads and vulnerability of metal clad roofing structures in contemporary Australian houses."PhD Thesis, James Cook University.

Jensen, M. 1958. "The model-law for phenomena in natural wind." *Ingenioren* 2 (2):121-128.

Judd, J., and F. Fonseca. 2012. "Hysteresis modeling for nailed sheating connections in wood shear walls and diaphragms." *Madeira: arquitetura e engenharia* 8 (20).

Judd, J. P., and F. S. Fonseca. 2005. "Analytical model for sheathing-to-framing connections in wood shear walls and diaphragms." *Journal of Structural Engineering* 131 (2):345-352.

Kawai, H. 2002. "Local peak pressure and conical vortex on building." *Journal of Wind engineering and Industrial aerodynamics* 90 (4):251-263.

Khan, M. 2012. "Load-Sharing of Toe-Nailed, Roof-to-Wall Connections under Extreme Wind Loads in Wood-Frame Houses."Masters Thesis, University of Western Ontario.

Kirkham, W. J., R. Gupta, and T. H. Miller. 2013. "State of the art: Seismic behavior of wood-frame residential structures." *Journal of Structural Engineering* 140 (4):04013097.

Labonnote, N. 2012. "Damping in timber structures."PhD Thesis, Norwegian University of Science and Technology

Leicester, R., and G. Reardon. 1976. "A statistical analysis of the structural damage by Cyclone Tracy." Annual Engineering Conference 1976: Engineering 1976-2001.

Levitan, M. L., K. C. Mehta, C. V. Chok, and D. L. Millsaps. 1990. "An overview of Texas Tech's wind engineering field research laboratory." *Journal of Wind Engineering and Industrial Aerodynamics* 36:1037-1046.

Li, Z. 1996. "A practical approach to model the behavior of a metal-plate-connected wood truss system."

Li, Z., R. Gupta, and T. H. Miller. 1998. "Practical approach to modeling of wood truss roof assemblies." *Practice periodical on structural design and construction* 3 (3):119-124.

Lovisa, A., D. Henderson, V. Wang, and J. Ginger. 2013. "Wind loading tributaries for pierced fixed roof cladding."

Lovisa, A. C., V. Z. Wang, D. J. Henderson, and J. D. Ginger. 2013. "Development and validation of a numerical model for steel roof cladding subject to static uplift loads." *Wind and Structures* 17 (5):495-513.

Mahendran, M. 1990. *Fatigue behaviour of corrugated roofing under cyclic wind loading*: James Cook University.

Mahendran, M. 1993. *Simulation of cyclonic wind forces on roof claddings by random block load testing*: Cyclone Structural Testing Station, James Cook University of North Queensland.

Mahendran, M. 2001. "Design of Steel Roof and Wall Cladding Systems for Pull-out Failures." *Steel Construction* 35 (1):14-27.

Mahendran, M., and D. Mahaarachchi. 2002. "Cyclic pull-out strength of screwed connections in steel roof and wall cladding systems using thin steel battens." *Journal of Structural Engineering* 128 (6):771-778.

Mani, S. 1997. *Influence functions for evaluating design loads on roof-truss to wall connections in low-rise buildings*.

Mason, M., and K. Haynes. 2010. Adaptation lessons from Cyclone Tracy. Gold Coast, Australia: National Climate Change Adaptation Facility.

Mason, M., and K. Parackal. 2015. Vulnerability of buildings and civil infrastructure to tropical cyclones: a preliminary review of modelling approaches and literature. Risk Frontiers.

Morrison, M., D. Henderson, and G. Kopp. 2012a. "The response of a wood-frame, gable roof to fluctuating wind loads." *Engineering Structures* 41:498-509.

Morrison, M. J., D. J. Henderson, and G. A. Kopp. 2012b. "The response of a wood-frame, gable roof to fluctuating wind loads." *Engineering Structures* 41:498-509.

Morrison, M. J., and G. A. Kopp. 2009. "Application of realistic wind loads to the roof of a full-scale, wood-frame house." Proc., 11th Americas Conf. on Wind Engineering.

Morrison, M. J., and G. A. Kopp. 2011. "Performance of toe-nail connections under realistic wind loading." *Engineering Structures* 33 (1):69-76.

Nair, R. S. 2004. "Progressive collapse basics." *Modern steel construction* 44 (3):37-44.

Newman, S. C. 2003. *Biostatistical methods in epidemiology*: John Wiley & Sons.

Newmark, N. M. 1982. "Earthquake spectra and design." *Earthquake Eng. Research Institute, Berkeley, CA*.

Ostrowski, J., R. Marshall, and J. Cermak. 1967. "Vortex formation and pressure fluctuations on buildings." Proceedings of International Seminar on Wind Effects on Buildings and Structures.

Paevere, P. J. 2002. "Full-scale testing, modelling and analysis of light-frame structures under lateral loading."

Parackal, K., M. Mason, D. Henderson, G. Stark, J. Ginger, L. Sommerville, B. Harper, D. Smith, and M. Humphreys. 2015. Investigation of Damage: Brisbane, 27 November 2014 Severe Storm Event, Cyclone Testing Station, JCU, Report TR60.

Pham, L., J. Holmes, and R. Leicester. 1984. "Safety indices for wind loading in Australia." In *Wind Engineering 1983, Part 3B*, 3-14. Elsevier.

Pita, G., J. Pinelli, K. Gurley, and S. Hamid. 2013. "Hurricane vulnerability modeling: Development and future trends." *Journal of Wind Engineering and Industrial Aerodynamics* 114 (0):96-105.

Pita, G., J. Pinelli, K. Gurley, and J. Mitrani-Reiser. 2015. "State of the Art of Hurricane Vulnerability Estimation Methods: A Review." *Natural Hazards Review* 0 (0):04014022.

Reardon, G., and D. Henderson. 1996. "Simulated wind loading of a two storey test house." Int. Wood Eng. Conf., New Orleans, USA, 1996.

Reardon, G., D. Henderson, and J. Ginger. 1999. A Structural Assessment of the Effects of Cyclone Vance on Houses in Exmouth WA, Cyclone Testing Station, JCU, Report TR48.

References

Reardon, G., G. Walker, and E. Jancauskas. 1986. Effects of Cyclone Winifred on Buildings, Cyclone Testing Station, JCU, Report TR27.

Reardon, G. F. 1979a. *The Strength of Batten-to-rafter Joints: Recommendations for High Wind Areas*: Cyclone Testing Station, Department of Civil & Systems Engineering, James Cook University of North Queensland.

Reardon, G. F. 1979b. *The Strength of Batten-to-rafter Joints: Test Results and Derivation of Design Loads*: Cyclone Testing Station, Department of Civil and Systems Engineering, James Cook University of North Queensland.

Reed, T., D. Rosowsky, and S. Schiff. 1997. "Uplift capacity of light-frame rafter to top plate connections." *Journal of architectural engineering* 3 (4):156-163.

Riley, M. A., and F. Sadek. 2003. *Experimental testing of roof to wall connections in wood frame houses*: US Department of Commerce, Technology Administration, National Institute of Standards and Technology.

Rosowsky, D. V., and T. A. Reinhold. 1999. "Rate-of-load and duration-of-load effects for wood fasteners." *Journal of Structural Engineering* 125 (7):719-724.

Saathoff, P., and W. Melbourne. 1989. "The generation of peak pressures in separated/reattaching flows." *Journal of Wind Engineering and Industrial Aerodynamics* 32 (1):121-134.

Saathoff, P., and W. Melbourne. 1997. "Effects of free-stream turbulence on surface pressure fluctuations in a separation bubble." *Journal of Fluid Mechanics* 337:1-24.

Satheeskumar, N., D. Henderson, J. Ginger, M. Humphreys, and C. Wang. 2016. "Load sharing and structural response of roof–wall system in a timber-framed house." *Engineering Structures* 122:310-322.

Shanmugam, B., B. G. Nielson, and D. O. Prevatt. 2009. "Statistical and analytical models for roof components in existing light-framed wood structures." *Engineering Structures* 31 (11):2607-2616.

Sherlock, R. 1947. "Gust factors for the design of buildings." *Intern. Assoc. Bridge Struct. Eng* 8:207-235.

Shivarudrappa, R., and B. G. Nielson. 2012. "Sensitivity of load distribution in light-framed wood roof systems due to typical modeling parameters." *Journal of Performance of Constructed Facilities* 27 (3):222-234.

Smith, D., D. Henderson, and J. Ginger. 2015. "Improving the wind resistance of Australian legacy housing." Proceedings of the 17th Australasian Wind Engineering Society Workshop.

Smith, D., M. Wehner, K. Parackal, D. Henderson, R. Ryu, J. Ginger, and M. Edwards. 2018. "Modelling vulnerability of Australian housing to severe wind events: past and present." *Natural Hazards Review*.

Standards Australia. 1999. HB132.2: Structural uprading of older houses - Cyclone areas. Sydney, Australia: Standards Australia.

Standards Australia. 2001. AS1649: Timber - Methods of test for mechanical fasteners and connections - Basic working loads and characteristic strengths. Sydney, Australia: Standards Australia.

Standards Australia. 2010a. AS1684.3 - Residential timber framed construction - Cyclonic Areas. Sydney, Australia.

Standards Australia. 2010b. AS1720.1 - Timber Structures - Design Methods. Sydney, Australia.

Standards Australia. 2011. AS/NZS1170.2 - Structural design actions Part 2: Wind actions. Sydney, Australia.

Standards Australia. 2012. AS4055: wind loads for housing. Sydney, Australia: Standards Australia.

Stanton, T. E. 1925. "Report on the Measurement of the Pressure of the Wind on Structures." Minutes of the Proceedings of the Institution of Civil Engineers.

Stevenson, S., G. Kopp, and E.-A. M. 2017. "Numerical assessment of partial hip roof failures during tornadoes." 13th Americas Conference on Wind Engineering, Gainesville, Florida, USA.

Stewart, M. G., P. C. Ryan, D. J. Henderson, and J. D. Ginger. 2016. "Fragility analysis of roof damage to industrial buildings subject to extreme wind loading in non-cyclonic regions." *Engineering Structures* 128:333-343.

Szyniszewski, S. 2009. "Dynamic energy based method for progressive collapse analysis." Structures Congress 2009: Don't Mess with Structural Engineers: Expanding Our Role.

Tan, L., and J. Hernandez. 2017. "Investigation of the Failure Progression of a 1-Story Gable-Roof Building Subjected to Sustained Wind Speeds." 9th Asia-Pacific Conference on Wind Engineering, Auckland, New Zealand.

Thampi, H., V. Dayal, and P. P. Sarkar. 2011. "Finite element analysis of interaction of tornados with a low-rise timber building." *Journal of Wind Engineering and Industrial Aerodynamics* 99 (4):369-377.

Vickery, P. J., P. F. Skerlj, J. Lin, L. A. Twisdale Jr, M. A. Young, and F. M. Lavelle. 2006. "HAZUS-MH hurricane model methodology. II: Damage and loss estimation." *Natural Hazards Review* 7 (2):94-103.

Walker, G. R. 1975. *Report on Cyclone" Tracy': Effect on Buildings, December 1974*: Department of Housing and Construction.

Walker, G. R. 1995. "Wind vulnerability curves for Queensland houses." *Alexander Howden Reinsurance Brokers (Australia) Ltd., Sydney*.

Walker, G. R. 2011. "Modelling the vulnerability of buildings to wind — a review " *Canadian Journal of Civil Engineering* 38 (9):1031-1039. doi: 10.1139/l11-047.

Wehner, M., C. Sandland, J. Holmes, P. Kim, N. Jayasinghe, and M. Edwards. 2010. "Development of a software tool for quantitative assessment of the vulnerability of Australian residential building stock to severe wind." 14th Australasian Wind Engineering Society Workshop.

Wilson, E. L. 2002. "Three-dimensional static and dynamic analysis of structures."

Wilson, E. L., M. W. Yuan, and J. M. Dickens. 1982. "Dynamic analysis by direct superposition of Ritz vectors." *Earthquake Engineering & Structural Dynamics* 10 (6):813-821.

Woldeyes, K., Y. Shifferaw, T. Birhane, and B. Bitsuamlak. 2017. "Structural Response of Lightweight Composite Wall Systems under Spatiotemporal Variation of Wind Pressure." 13th Americas Conference on Wind Engineering, Gainesville, Florida, USA.

Wolfe, R., and T. LaBissoniere. 1991a. *Structural Performance of Light-Frame Roof Assemblies*: US Department of Agriculture, Forest Service, Forest Products Laboratory.

Wolfe, R. W., and T. LaBissoniere. 1991b. *Structural Performance of Light-Frame Roof Assemblies*: US Department of Agriculture, Forest Service, Forest Products Laboratory.

Wolfe, R. W., and M. McCarthy. 1989. "Structural performance of light-frame roof assemblies. 1. Truss assemblies with high truss stiffness variability." *Research paper FPL RP-US Department of Agriculture, Forest Service, Forest Products Laboratory (USA)*.

Xu, Y. L. 1993. *Wind-induced fatigue loading on roof cladding of low-rise buildings*: Cyclone Testing Station, James Cook University of North Queensland.

Zisis, I., and T. Stathopoulos. 2009. "Wind-induced cladding and structural loads on low-wood building." *Journal of structural engineering* 135 (4):437-447.

Zisis, I., and T. Stathopoulos. 2012. "Wind load transfer mechanisms on a low wood building using full-scale load data." *Journal of Wind Engineering and Industrial Aerodynamics* 104:65-75.

References

172

APPENDICES

APPENDIX A – AS BUILT CONNECTION TESTING

Extraction of Connections

The Cyclone Testing Station surveyed a group of 1960's houses in Adelaide to record data for vulnerability modelling. The survey was conducted in the Bedford Park area of Adelaide in collaboration with the Department of Planning, Transport and Infrastructure (DPTI) and the University of Adelaide. Sixteen houses were surveyed and the structural systems and connection details of the roof and walls were recorded.

Most of the houses surveyed were built in the 1960's and were single storeyed with double brick walls and pitched frame hip and valley roofs. Batten to rafter connections from one of these houses were extracted (Figure A.1) and sent back to the James Cook University materials testing laboratory for testing

Figure A.1 Extraction of as built batten to rafter connections

Connections were securely braced before they were cut away from the roof structure so that they could be interlocked and transported safely via road freight (Figure A.2). Rafters and battens were named such that connections on the same rafter and the same batten could be identified.

Moisture contents were determined for the samples using oven drying that showed similar results to an electronic moisture meter that was used during testing conducted later. A comparison to moisture contents taken of samples inside the roof spaces of neighbouring houses with the same material indicated that the levels of moisture had not changed significantly during transit.

Timber species were identified by a specialist using appearance and microscopy of the cell structure, shown in Figure A.3. Hardwood rafters were identified as Karri (*Eucalyptus diversicolor*) and battens were Tasmanian Oak (*Eucalyptus obliqua*).

Figure A.2 Connections being prepared for extraction (left) and being packed for transit (right).
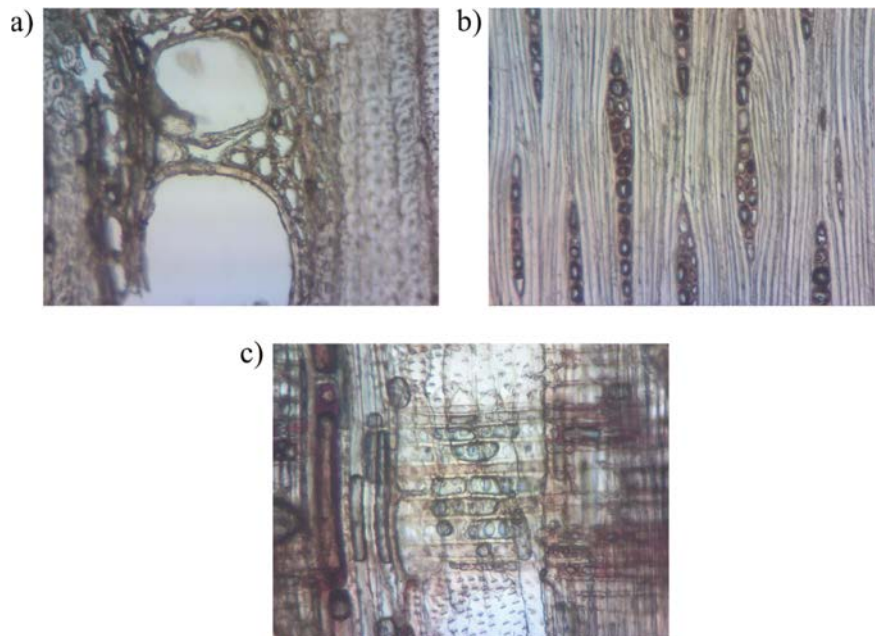
Figure A.3 Microscopy images of Karri (Eucalyptus diversicolor) rafters, 16μm thickness slides at 100× magnification: a) transverse section, b) tangential-longitudinal section, c) radial-longitudinal section.

Connection Samples

Laboratory tests were conducted on the hardwood batten to rafter connection specimens. The tests provided data on the performance of in-service nailed connections and enabled quantification of age-related deterioration. Tested samples consisted of:

- Approx. 300mm length Karri Harwood rafter 120 × 35 mm
- Approx. 300mm length Messmate batten 25 × 35 mm
- Single flat head plain shank nail 50 × 2.8 mm

The strength of nailed connections can be influenced by a number of factors; these were recorded for each specimen:
1) moisture content,
2) edge distances,
3) angle of nails,
4) initial gap between batten and rafter,
5) embedment depth of the nail,
6) ring size of rafter timber,
7) orientation of the rings of rafter timber,
8) condition of the nail,
9) splits in the timber.

Correlations between connection strengths and these factors were examined. Several of these showed that there were weak relationships between connection strength and the given property. However, it appears that the variability of the connection performance is so great that these properties have little overall effect.

Static Tests

Static pull out testing was conducted using a United Instruments 2kN universal testing machine for the as-built samples. Force-displacement relationships for these connections showed an initial elastic range with a constant slope followed by a reduction in stiffness before the maximum load or characteristic strength of the connection is achieved, shown in Figure A.4. Following this point the connections would show a plateau area of elastic perfectly plastic behaviour. Followed by a negative sloped region where the load required to cause plastic deformation was constantly decreasing.

Static tests showed similar initial force - displacement slopes (connection stiffness) among all samples. However, there was a significant variation in ultimate strengths. Some connections showed a very small elastic range with a very large plastic plateau area where the nail was pulled out continuously with no increase in load. Other connections showed a very high yield loads with little plastic region.

The samples were nailed back together with a new nail and re-tested. These connections with new nails were almost twice the strength of the aged connections, as shown in Table A.1.

Table A.1 Performance of as-built and newly nailed connections

	Sample Size	Mean Ult. Load (N)	Standard Deviation (N)	Cov
Hardwood	30	607.3	199.4	33%
Hardwood New Nail	20	1150.5	373.1	32%
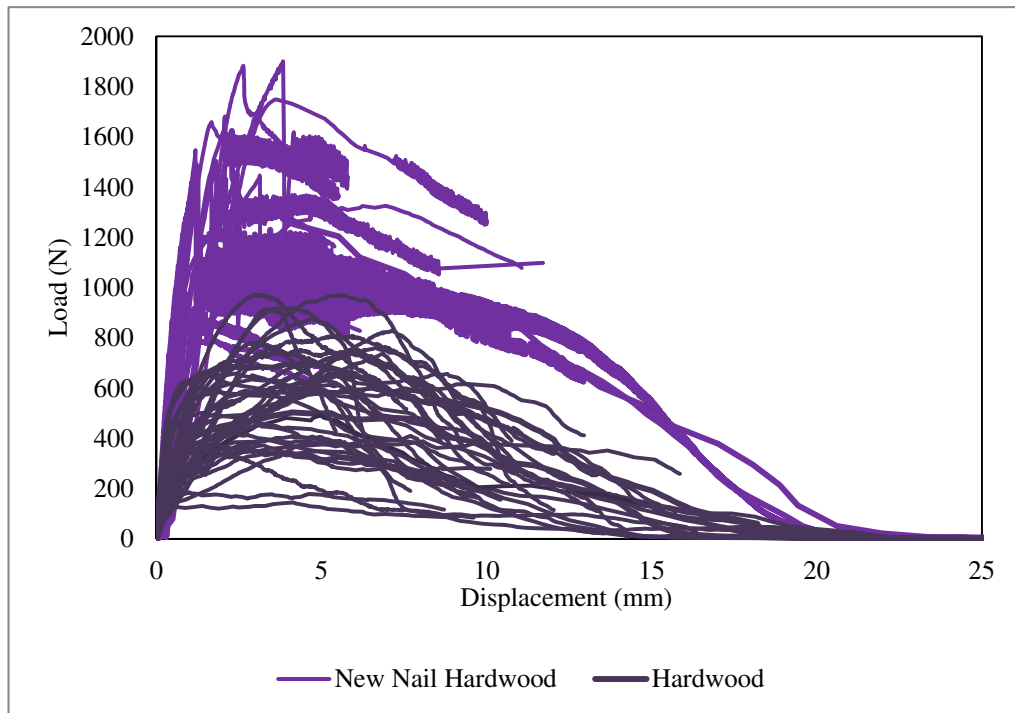
Figure A.4 Force-displacement behaviour of static pullout tests.

Dynamic testing

Dynamic tests of single batten to rafter connections were undertaken to characterize incremental failure of connections under fluctuating wind loads. Preliminary testing showed that the connection specimens experienced damage only during peak events with low-level fluctuations causing only elastic deformation of the connections. Additionally, the softwood connections were too weak to be tested using the Intsron under a load controlled test procedure and results of only the hardwood connections are presented in this Section.

Dynamic Testing – Stepped Synthetic Peaks

It was decided to create a 'synthetic' load trace consisting of several peak loads repeatedly. As it is still unknown what load level would cause damage to the connection, it was decided to test the connections in several load steps. To minimise the number of steps required for the test, these steps were based on the yield loads determined from static testing.

The yield loads of the static connections were found to be normally distributed. Thus a reasonable first loading step was set to be one standard deviation below the mean, the mean yield load, one standard deviation above the mean, and two standard deviations above the mean.

Each loading step consisted of 10 peak events, equivalent to about two hours of full scale time duration. Although it is highly unlikely that strong wind speeds and direction would remain constant over such a long duration, the repeated peaks still give valuable information of the incremental failure behaviour of the connections.

Figure A.5 shows an example of connection behaviour under stepped peak events. The vertical bands in this plot indicate the loading and unloading paths during low level load fluctuations between peak events. During peak events, the nail slips causing a permanent withdrawal of the nail. As the pressure fluctuations do not reverse the direction of the load on the nail, the connection deforms elastically resulting in another vertical band in the plot between each peak event. In this case, there was an increase in performance after a slight withdrawal of the nail as the magnitude of each slip decreased near the centre of the plot. After about 7mm of nail withdrawal, the connection rapidly lost strength and failed.
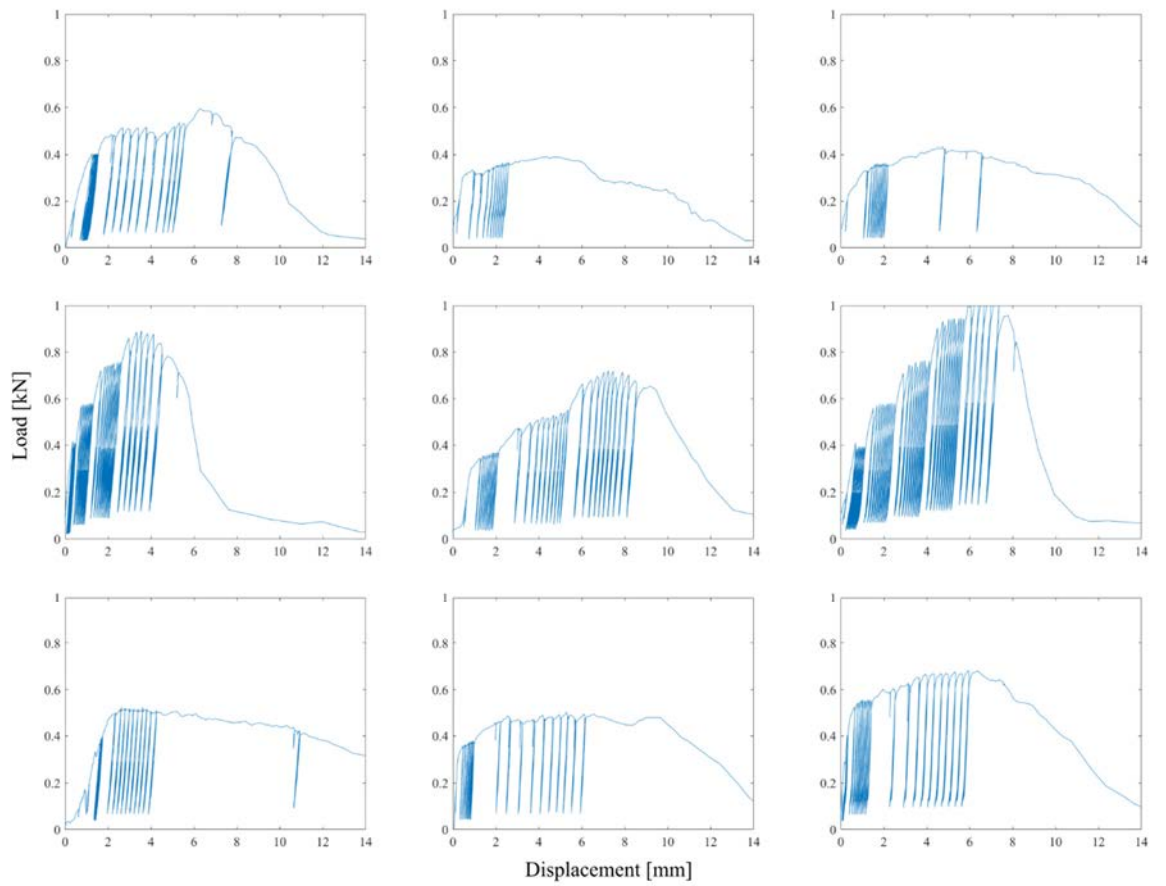
Figure A.5 Force - displacement behaviour under stepped peak events showing the eventual failure of connections at different magnitudes of loading.

The dynamic tests showed that a connection's elastic stiffness, indicated by the gradient of the loading and unloading paths, does not change with accumulated damage through successive peak events. This indicates that load redistribution to adjacent connections occurs when the load acting on that connection exceeds the yield load of that connection causing nail slip, rather than due to a decrease in elastic stiffness.

Dynamic Testing – Repeated Peaks to Failure

Another set of dynamic tests was conducted that involved subjecting the connections to a repeated peak load of the same magnitude until failure. From the previous stepped synthetic load trace it was found that most of the connections would show slip behaviour when subject to a peak magnitude equal to the mean connection strength from the static tests.

An issue with the stepped synthetic load trace is that the true performance of a connection during a particular loading step is unknown due to the effect of the previous loading history. For example, the amount of nail slip and the number of peaks the connection could withstand when subject to a peak event of magnitude two standard deviations higher than the mean would be significantly lower as the connection has already been subject to several peak events of one standard deviation below, the mean connection strength and one standard deviation above.

Figure A.6 shows the connection response of aged connections under repeated peak events at the mean connection strength load. Nail slip occurs with each peak event. In most cases, there was an improvement in performance similar to strain hardening behaviour in steel as the magnitude of each slip decreased near the centre of the plot. After the accumulated nail slip had reduced the depth of embedment to a critical level, the connection rapidly lost strength and failed as shown at the right hand side of the plot.

The results of repeated mean peak tests still showed large variability in connection performance, with some connections able to survive only 2 or 3 peaks and some able to survive more than 100 peaks. All showed some ductility, as they were able to sustain loads at deformations much higher than their elastic limit.
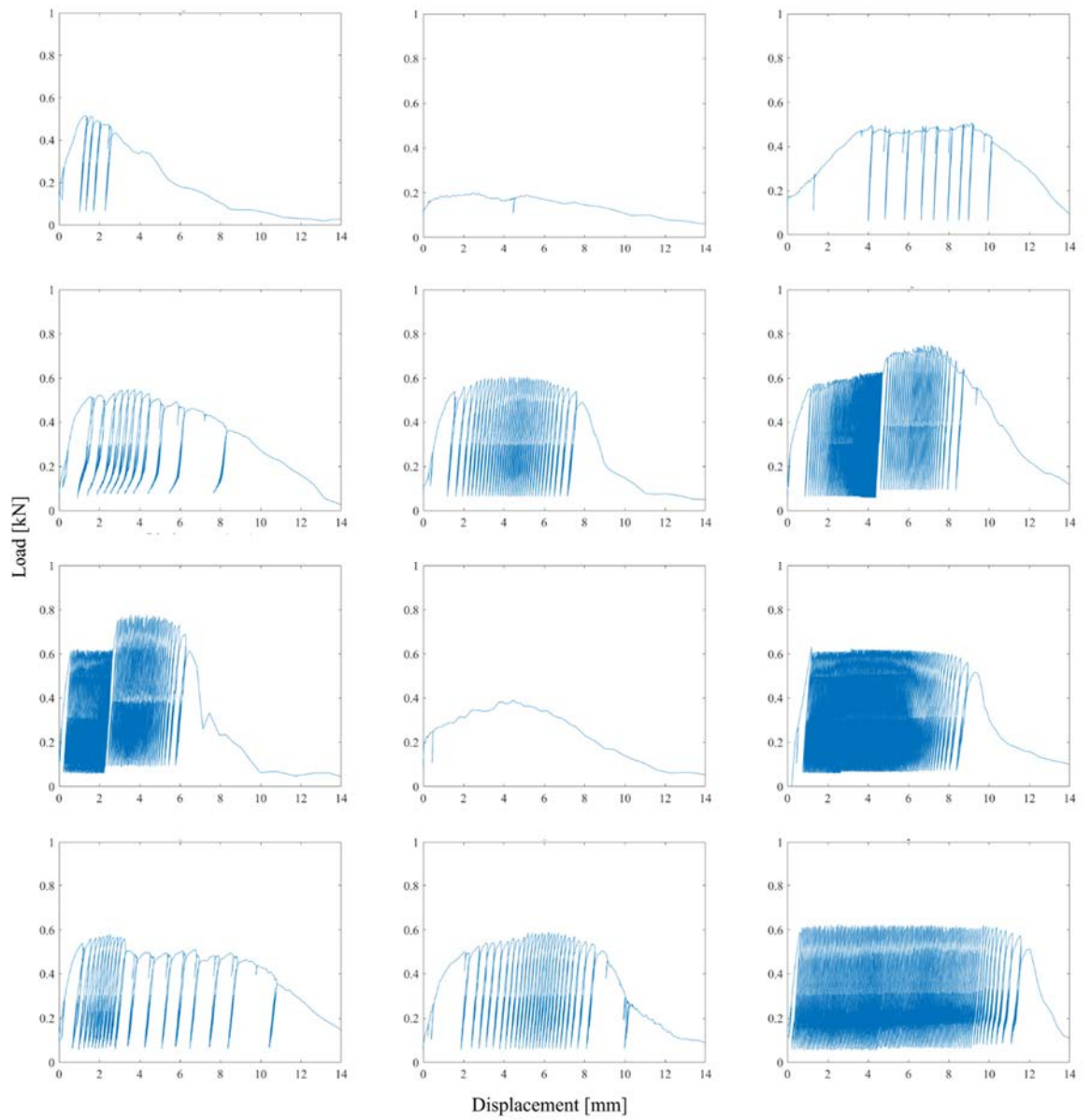
Figure A.6 Force vs. displacement behaviour of a hardwood batten to rafter connection under repeated peak events

Discussion – Performance of Aged Connections

Dynamic connection testing of connections showed that connections failed due to incremental nail slip during peak events with their elastic stiffness remaining the same throughout the loading process until failure. Both the staged load trace and the peaks to failure method showed loading and unload bands in between each peak load event. The slopes of these bands remain constant throughout the test until failure indicating that the connection stiffness remains constant. Additionally, the connections showed a large variability in performance.

Additionally, there was significant reserve plastic capacity after the connection had reached its yield load. Several peak events were required for the connection to fail. Thus, the ductility of connections afforded them some resistance beyond what is usually considered the 'strength' of connections. All aged connections sustained at least one peak at the mean static test strength. The results of the dynamic tests still showed large variability in connection performance, with some connections able to survive only two or three peak events and some able to survive more than 100 peaks.

APPENDIX B – REVERSE CYCLE LOADING OF CONNECTIONS

One of the dynamic tests presented Chapter 4 was aborted halfway through the test and could not be continued under the same test procedure. It was then decided to subject the connection to displacement controlled cyclic load. A triangular waveform was used to vary the displacement of the machine's crosshead to 25mm and back to 5mm repeatedly.

Figure B.1 shows the loading vs displacement path of the connection under reverse cyclic loading. The test begins with the nails at15mm displacement and load within the connection decreases as the nails a withdrawn until a displacement of 25mm. At this point, the machine reverses its direction and begins to push the nail back into the rafter material. The load-displacement path in compression mirrors that of it in tension showing the connection being subject to higher loads as the nails are pushed further into the rafter material. The direction is reversed again at 5mm, before zero displacement to avoid damaging the clamping apparatus.

Strength degradation is apparent with each loading cycle as lower loads are required to move the nails in and out of the rafter material with each loading cycle. This strength degradation may be due to the smoothening of the nail to rafter surface contact or due increase in temperature of the nail affecting the coefficient of friction. However, nails did not appear to be hot to the touch after the test. This strength degradation is not observed during dynamic loading under repeated peak events, where loading is in one direction only.
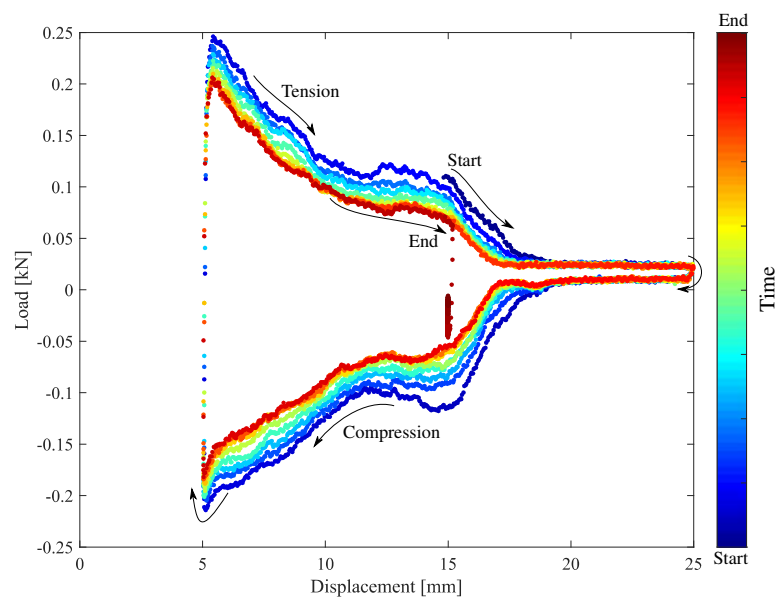
Figure B.1 Connection response under reverse cycle loading

Appendix C – Fast Non-Linear Analysis

Fast nonlinear analysis (FNA) is a method developed by Wilson et al. (1982) for seismic engineering purposes and can accurately perform non-linear time history analyses with significantly less computational effort than direct integration methods. FNA is a modal superposition time-history analysis using load dependent Ritz vectors. A key requirement of FNA is that nonlinear behaviour be localised at determined points that represent dampers, base isolators or predefined plastic hinge locations. This method is ideal for seismic engineering where structures are often designed to have localised energy dissipation devices.

In the case of light framed construction under wind loading, nonlinear behaviour is usually limited to connections as evidenced from damage surveys. Failure of members does occur but this usually takes place only in advanced stages of failure. The following section outlines the basic mathematical principles behind the FNA method originally presented in (Wilson 2002).

Modal Superposition Dynamic Analysis

Dynamic structural analysis involves solving the differential equation that represents the dynamic equilibrium of the structure.

$$M\ddot{u}(t) + C\dot{u}(t) + Ku(t) = F(t) \qquad Eq.C.1$$

Where M, C and K are the mass, damping and stiffness matrices of the structure and $\ddot{u}, \dot{u}, u$ are the acceleration, velocity and displacement of the structure. These arrays of simultaneous equations can be solved through computationally expensive direct integration methods. However, a more efficient approach to the solution is to uncouple these equations based on the deformed shapes of different modes of vibration.

The solution to (1) can be converted into the form:

$$u(t) = \Phi Y(t) \qquad Eq.C.2$$

Where Φ is an N_d by N matrix with N spatial vectors that are not a function of time. and Y(t) is a function of time. In order to uncouple the system of equation in (1), 'modal' mass, stiffness and damping matrices must be formed:

$$\Phi^T M \Phi = I$$

$$Eq.C.3$$

$$\Phi^T K \Phi = \Omega^2$$

$$Eq.C.4$$

$$\Phi^T C \Phi = \lambda$$

$$Eq.C.5$$

The terms of the diagonal matrix Ω^2 are ω^2 that may be but are not necessarily free vibration frequencies of the structure. In real structures, the modal damping matrix is not diagonal, therefore to uncouple the dynamic equilibrium equations (1) classical damping must be assumed where there is no coupling between the modes and d_{mn} are the diagonal terms of the damping matrix:

$$d_{mn} = 2\xi_n\,\omega_n \qquad\qquad\qquad Eq.C.6$$

Where ξ_n is the damping ratio of each mode of vibration. Therefore, an uncoupled modal equation for the nth mode can be written as:

$$\ddot{y}(t)_n + 2\xi_n\,\omega_n\,\dot{y(t)} + \omega_n^2 y(t) = \bar{f}(t)_n \qquad\qquad Eq.C.7$$

Such uncoupled equations can be solved exactly with significantly less computational effort than the system of equations in (1) The results of the uncoupled equations can be superimposed to determine the dynamic response of the whole structure. The method's accuracy depends on the generation of an adequate number of mode shapes for the structure and is less sensitive to the selection of the time step size.

Load Dependent Ritz Vectors

The dynamic response of a structure will be a function of the spatial distribution of the loading process that it is being subject to. The recursive equations used to calculate load dependent Ritz vectors (LDRs) is similar to the Lanczos algorithm used to calculate exact eigenvalues and eigenvectors. However, the starting load vectors are the static displacements caused by the spatial load distribution.

Unlike Eigenvectors that describe the free vibration shapes of a structure, Ritz vectors describe the vibration shapes that would be excited due to a particular loading. If frequencies and mode shapes that would be calculated using Eigenvalues and eigenvectors are missed during the Ritz vector analysis it is because the dynamic loading applied to the structure does not excite those particular natural frequencies.

The FNA method

In Fast Non-linear analysis, non-linear forces are treated as external loads and a set of LDRs are used to account for the effects of these forces.

$$M\ddot{u}(t) + C\dot{u}(t) + Ku(t) + R_{NL}(t) = R(t) \qquad\qquad Eq.C.8$$

Where $R(t)$ are the external applied loads and $R_{NL}(t)$ is a node force vector that is the sum of the forces from the nonlinear elements computed by iteration at each point in time. If the model is not stable without the presence of the non-linear link elements then 'effective elastic elements' can be placed at the location of the nonlinear elements of arbitrary stiffness K_e.

K_e can be added to both sides:

$$(K + K_{e)}u(t) = \bar{K}u(t) \qquad\qquad Eq.C.9$$

$$R(t) - R(t)_{NL} + K_e u(t) = \bar{R}(t) \qquad\qquad Eq.C.10$$

Therefore:

$$M\ddot{u}(t) + C\dot{u}(t) + \bar{K}u(t) = \bar{R}(t) \qquad\qquad Eq.C.11$$

Equation C.11 is then uncoupled using the matrix Φ of LDRs. Displacements are calculated using iteration within each time step, the equilibrium, compatibility and element force deformation equations are satisfied for each non-linear element. For a linear variation of force over a small time-step, the modal equations are solved exactly. Moreover, unlike direct integration methods numerical damping and integration errors from large time steps do not occur.